



This work supported in part by
U.S. DEPARTMENT OF
ENERGY



THE OHIO STATE
UNIVERSITY

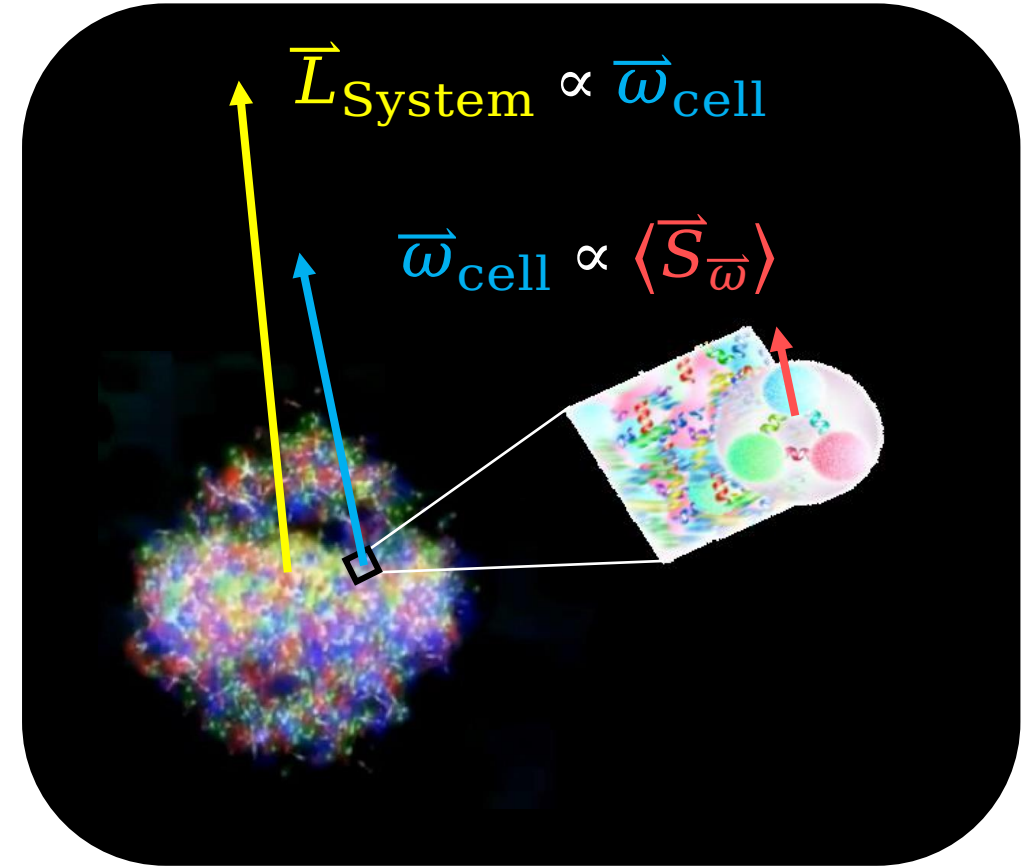
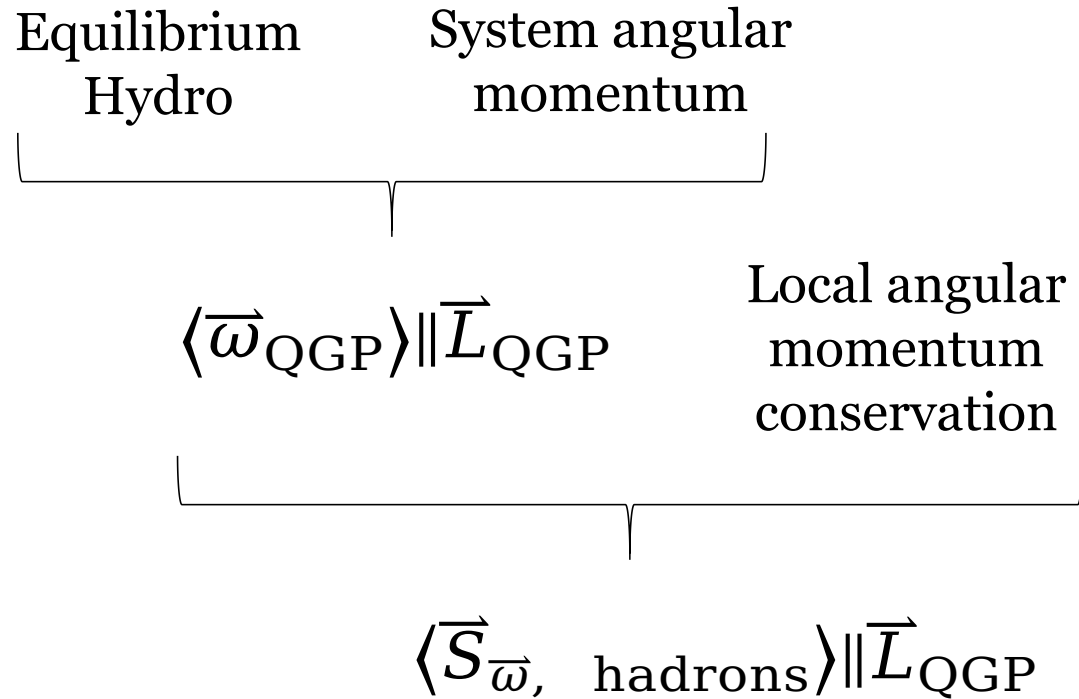
STAR results of hyperon polarization

Joey Adams, for the STAR Collaboration
Chirality, Vorticity and Magnetic Field in Heavy Ion Collisions
Stony Brook University
2 November 2021

STAR 

BROOKHAVEN
NATIONAL LABORATORY

Spin polarization of hadrons



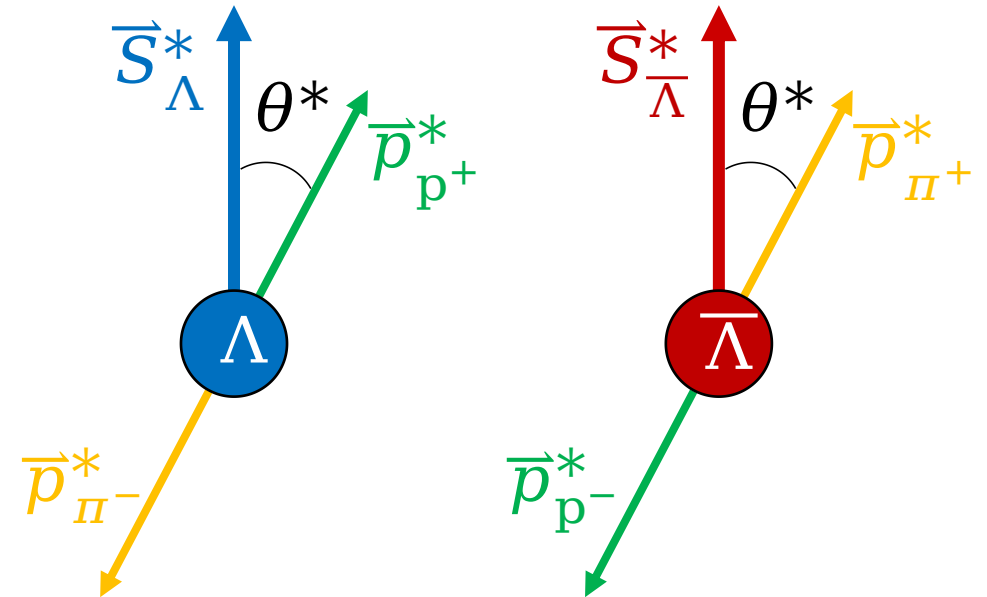
Spin polarization of Lambda hyperons

- Lambdas preferentially emit positively charged daughters along the direction of their spin

$$\frac{dN}{d\theta^*} = 1 + \alpha_\Lambda P_\Lambda \cos \theta^*$$

("*" indicates the Lambda rest frame)

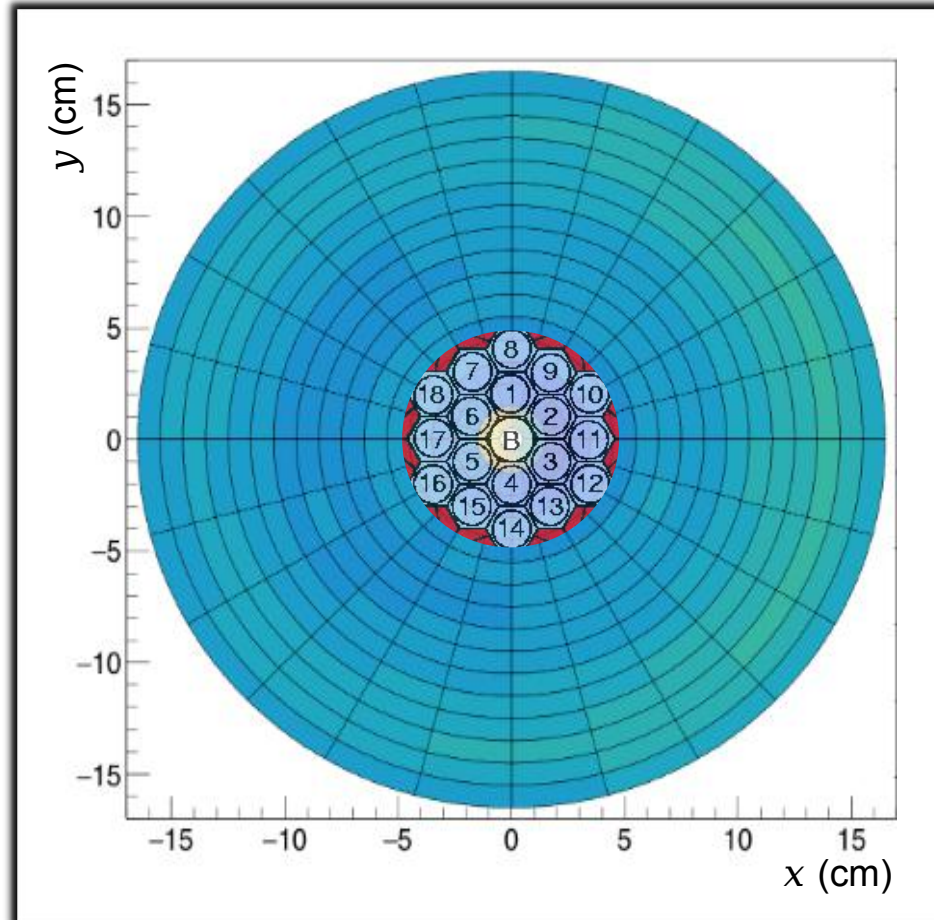
$$(\alpha_\Lambda = 0.732)$$



Measuring \widehat{L}_{QGP}

J. Adams *et al.*, Nucl. Instrum. Meth. A **968**, 163970 (2020), arXiv:1912.05243 [physics.ins-det].

- The EPD has far more coverage than the BBC



East EPD hits rotated by Ψ_1 , EPD West

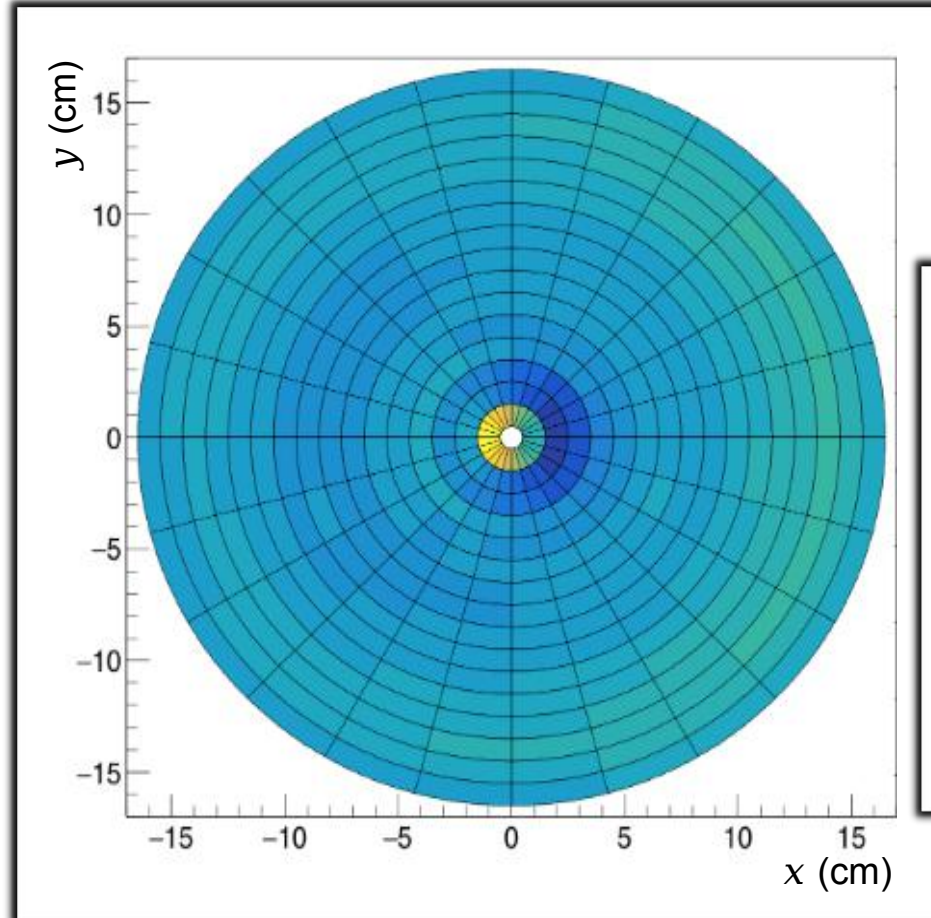
<https://drupal.star.bnl.gov/STAR/blog/lisa/subtle-flow-and-anti-flow-patterns-visible-epd-auau-27-gev>

Measuring \hat{L}_{QGP}

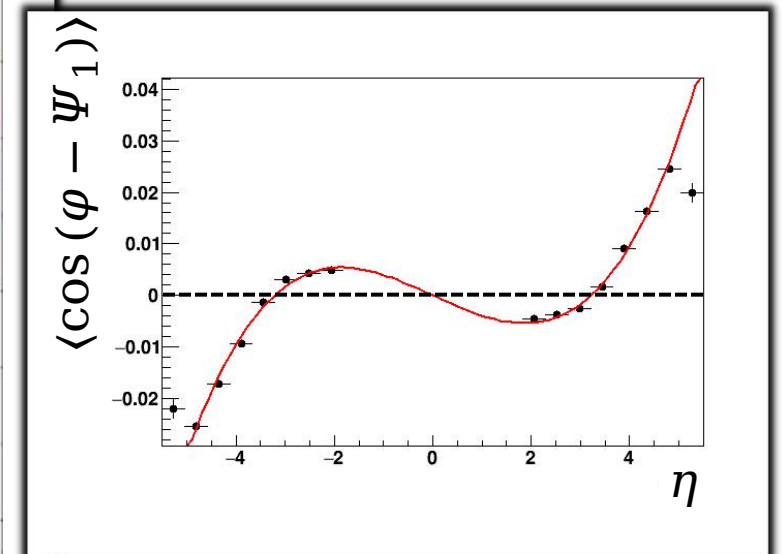
- The EPD has far more coverage than the BBC

East EPD hits rotated by Ψ_1 , EPD West

<https://drupal.star.bnl.gov/STAR/blog/lisa/subtle-flow-and-anti-flow-patterns-visible-epd-auau-27-gev>



$\sqrt{s_{NN}} = 27 \text{ GeV}$



Measuring Lambda Polarization

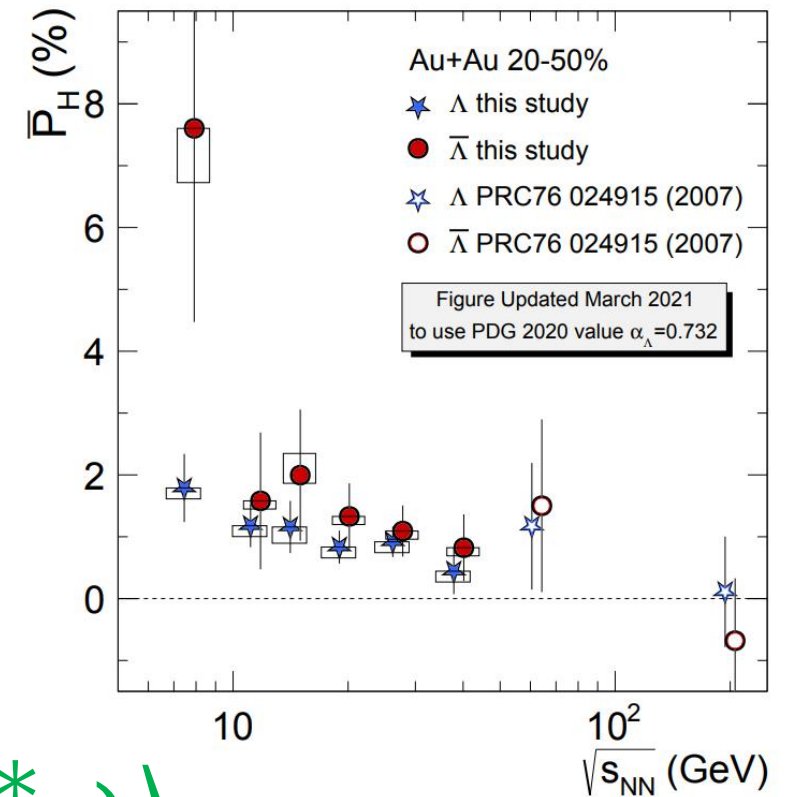
Nature 548, 62-65

The measured Ψ_1 differs from Ψ_{RP}

$$\overline{P}_{\Lambda/\overline{\Lambda}} = \frac{1}{\alpha} \frac{1}{R_{EP}^{(1)}} \langle \sin(\Psi_1 - \varphi_{p^+}^*) \rangle$$

Lambdas do not emit their positive daughters exactly along the direction of their spins

Correlates angular momentum of the system (\hat{J}_{sys}) with the orientation of the Lambda's spin



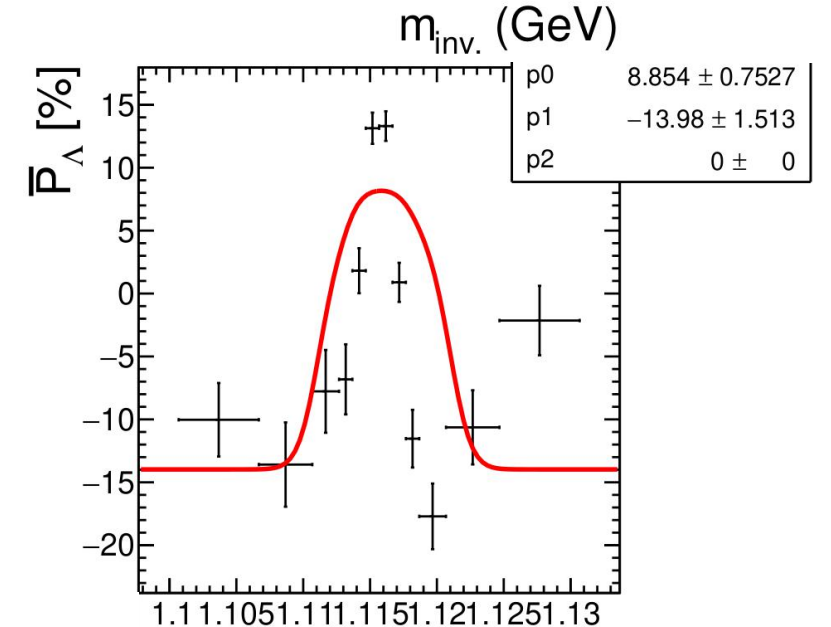
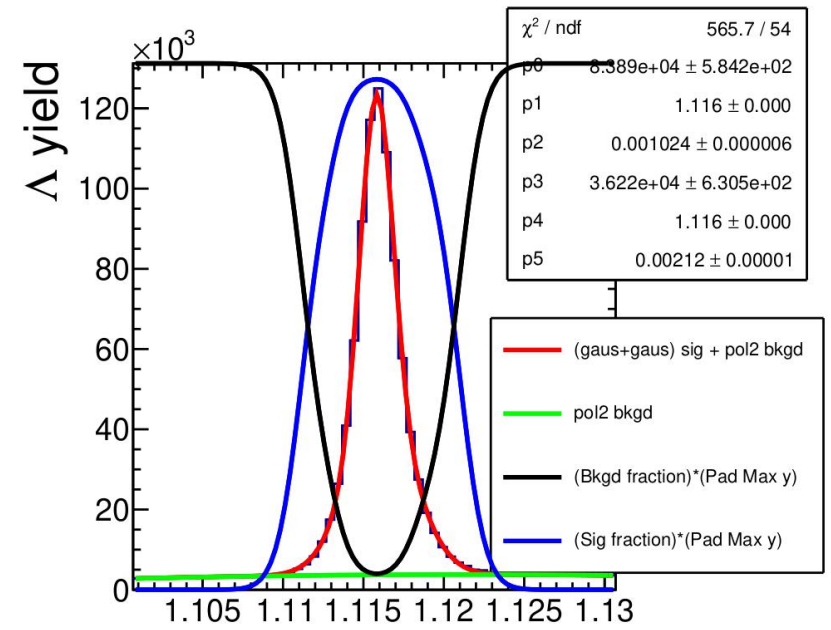
A new method for the fixed-target setup

- Observed polarization is expected to follow

$$\bar{P}_{\Lambda}^{obs}(m_{inv.}) = f^{bkgd}(m_{inv.})\bar{P}_{\Lambda}^{bkgd} + f^{sig}(m_{inv.})\bar{P}_{\Lambda}^{sig}$$

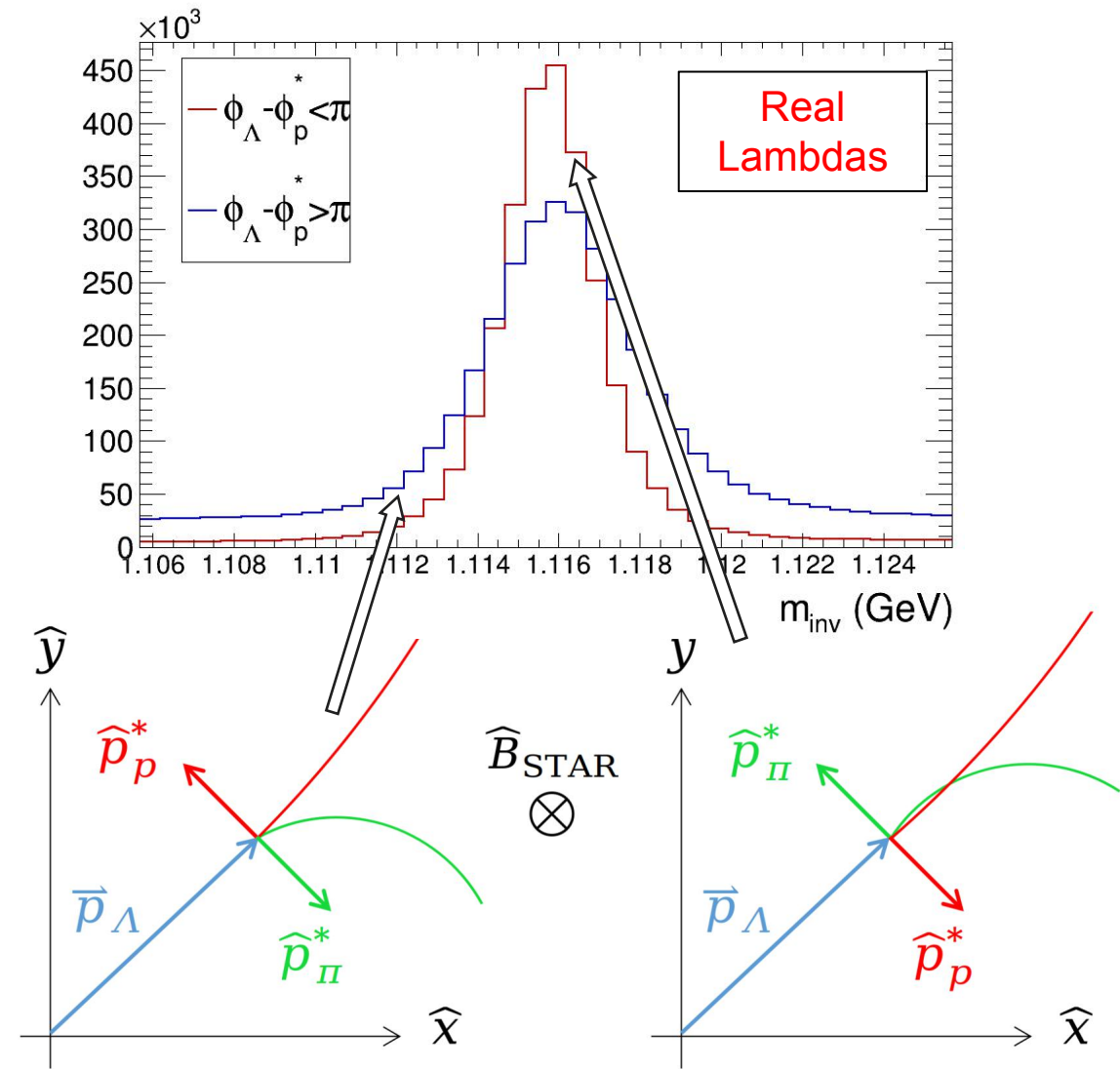
- In our case, due to very low background, this is dominated by \bar{P}_{Λ}^{sig}

- Instead, $\bar{P}_{\Lambda}^{obs}(m_{inv.})$ in *fixed target mode* is more sharply peaked near m_{Λ}^{PDG} and it dips on the sides mass peak



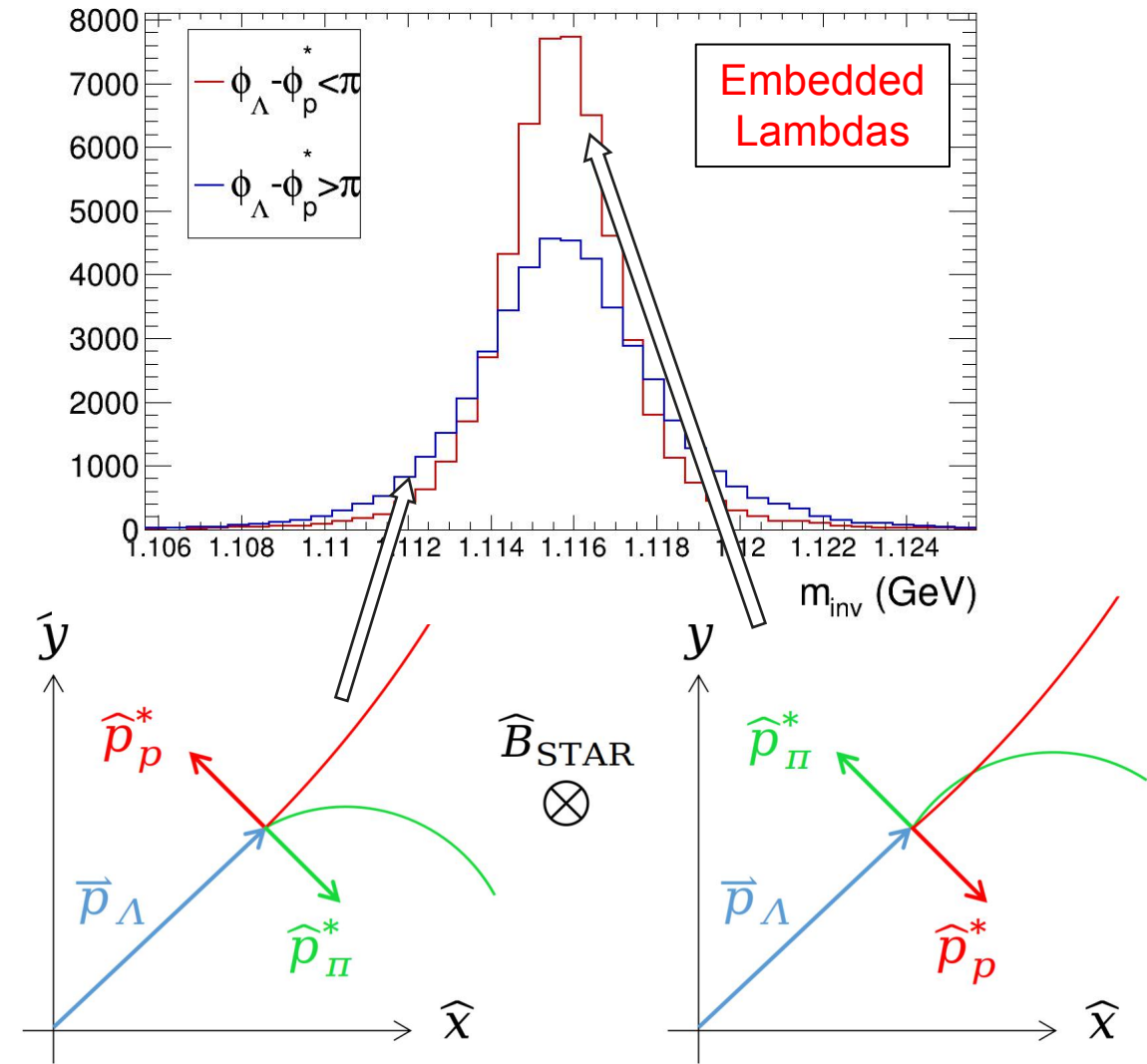
The cause

- The width of the m_{inv} distribution depends on the daughter's azimuthal emission angle relative to the Λ ($\varphi_\Lambda - \varphi_p^*$; "*" denotes Λ frame). We call this the "azimuthal emission efficiency" (AEE)
 - Let's first consider the two cases $\varphi_\Lambda - \varphi_p^* > \pi$ and $\varphi_\Lambda - \varphi_p^* < \pi$



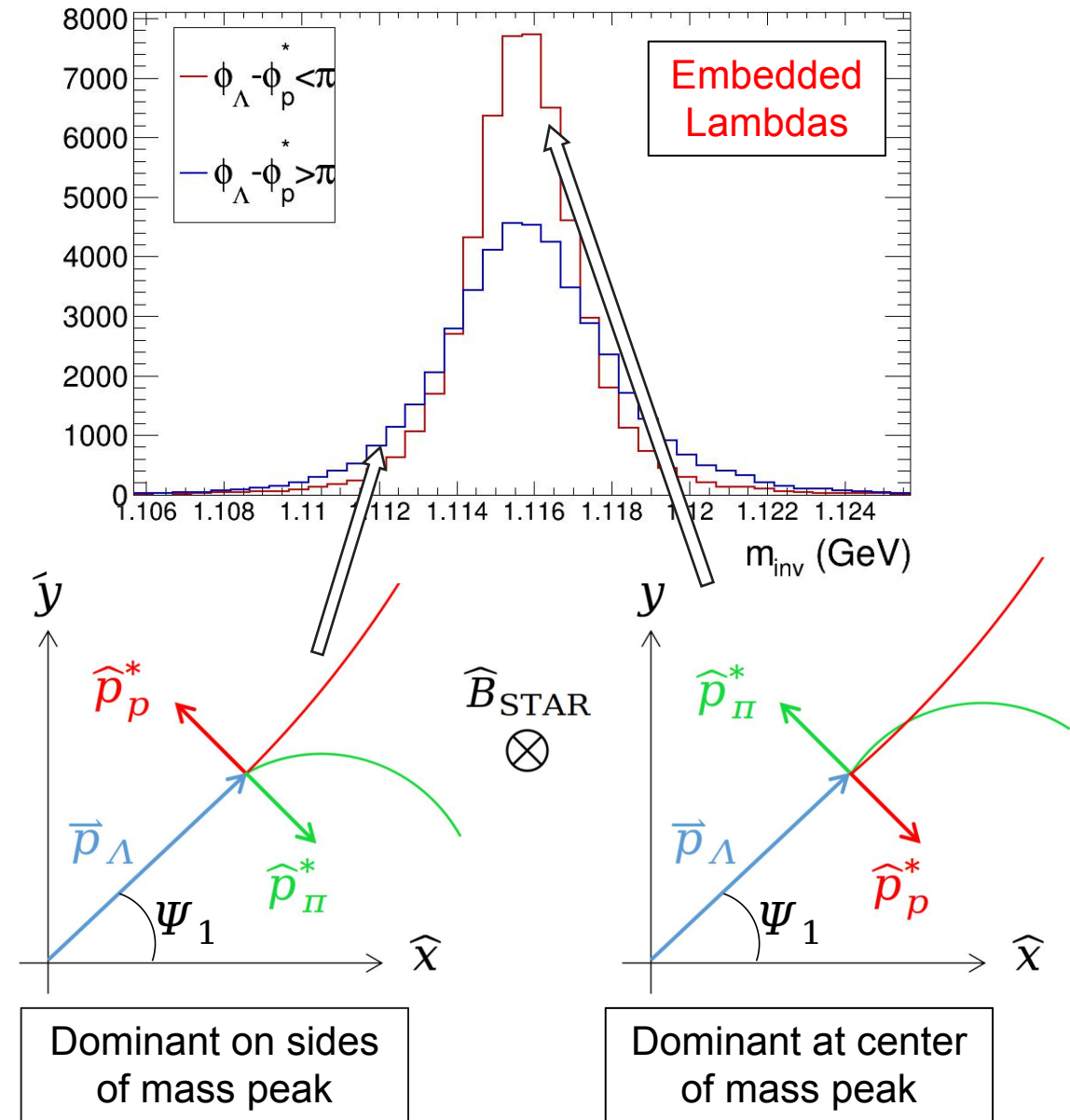
The cause

- The width of the m_{inv} distribution depends on the daughter's azimuthal emission angle relative to the Λ ($\varphi_\Lambda - \varphi_p^*$; "*" denotes Λ frame). We call this the "azimuthal emission efficiency" (AEE)
 - Let's first consider the two cases $\varphi_\Lambda - \varphi_p^* > \pi$ and $\varphi_\Lambda - \varphi_p^* < \pi$
- We see the same effect more clearly in embedded Λ s where there is no background; this is obviously a reconstruction effect
 - Data provided by Yue-Hang Leung



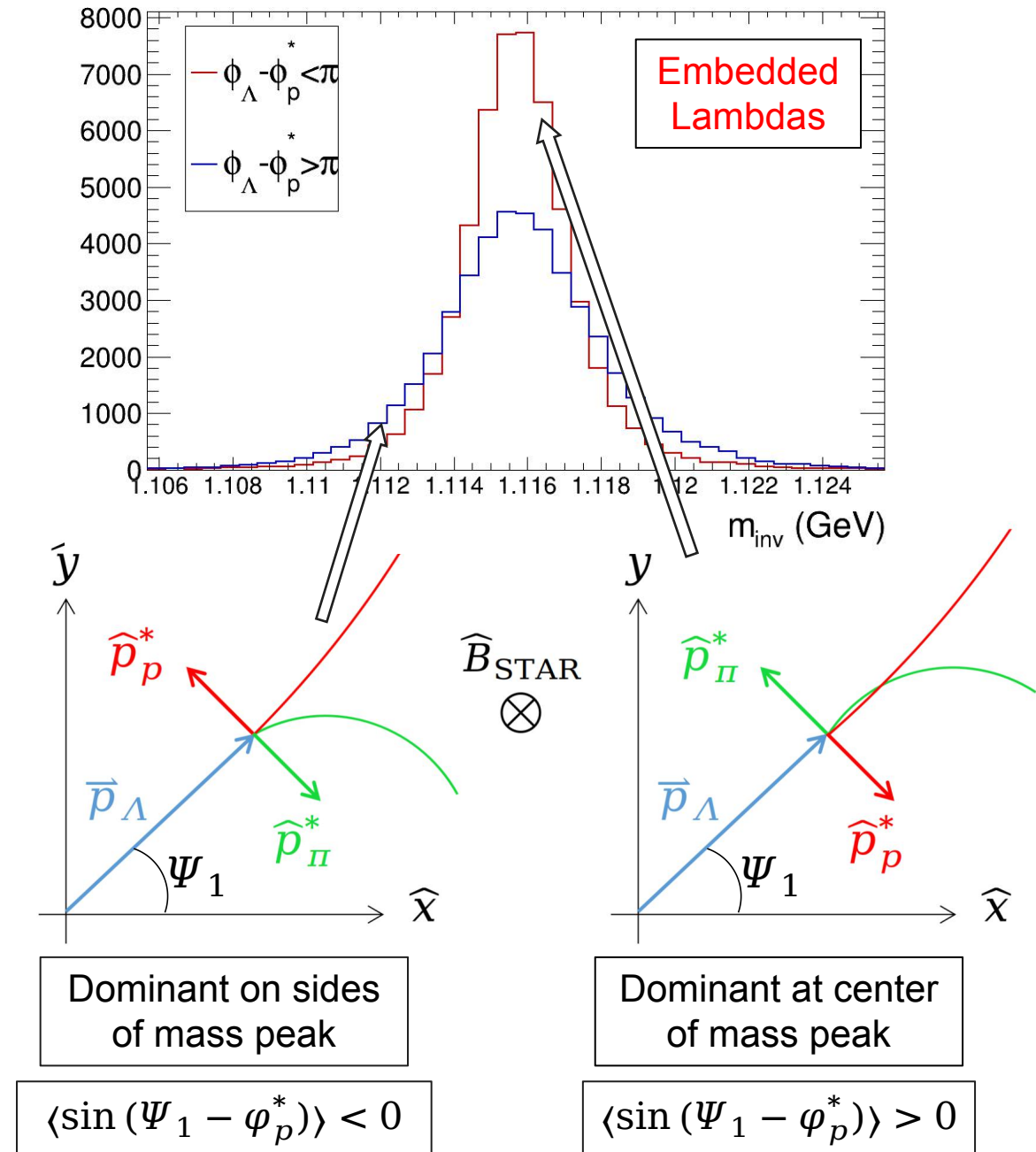
The cause

- The center of the mass peak is dominated by $\varphi_\Lambda - \varphi_p^* > \pi$ and sides are dominated by $\varphi_\Lambda - \varphi_p^* < \pi$



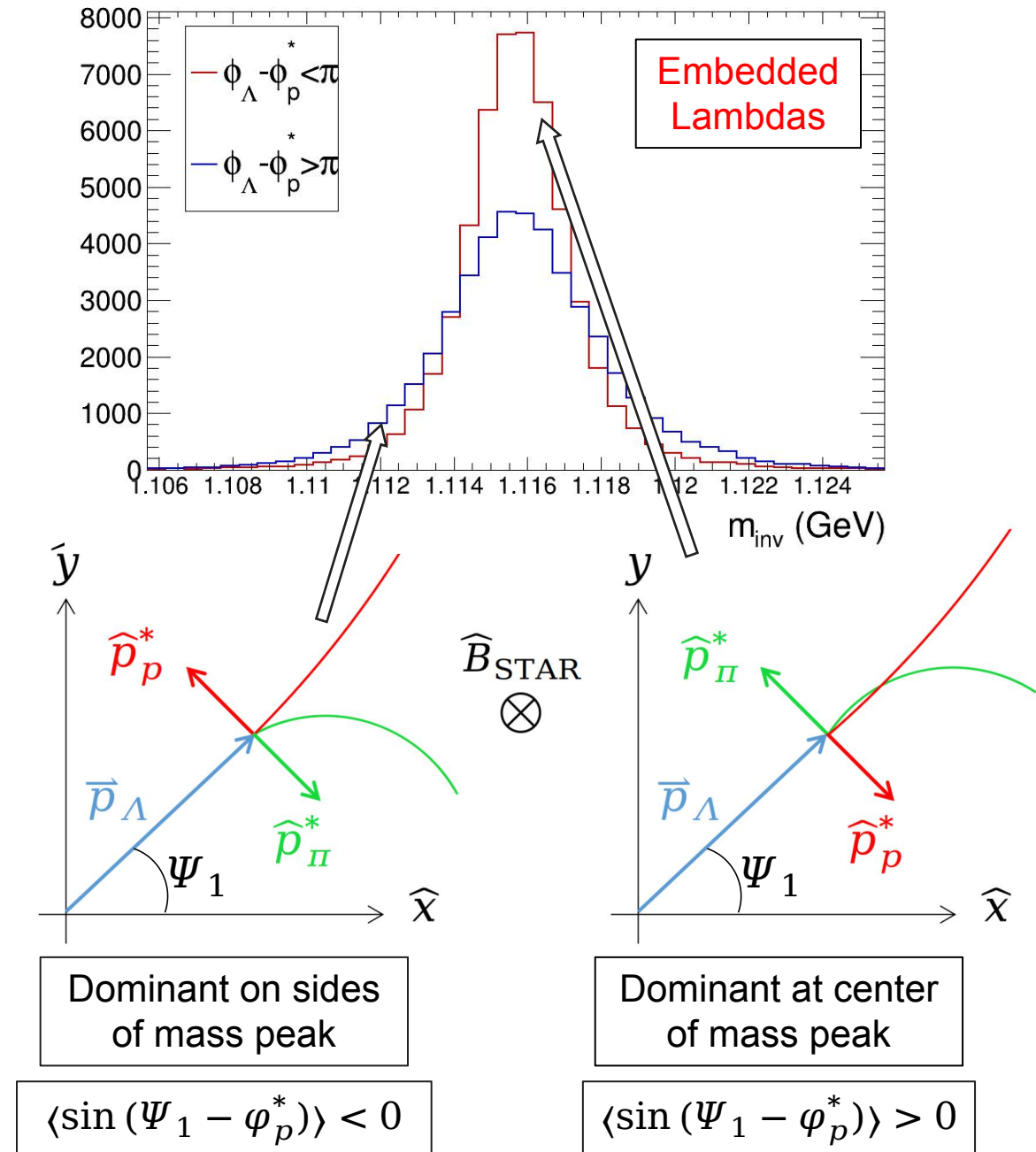
The cause

- The center of the mass peak is dominated by $\varphi_\Lambda - \varphi_p^* > \pi$ and sides are dominated by $\varphi_\Lambda - \varphi_p^* < \pi$
- Due to Λ directed flow, Ψ_1 and φ_Λ are correlated (in fixed-target mode, we are dominated by Λ s with $v_1 > 0$)



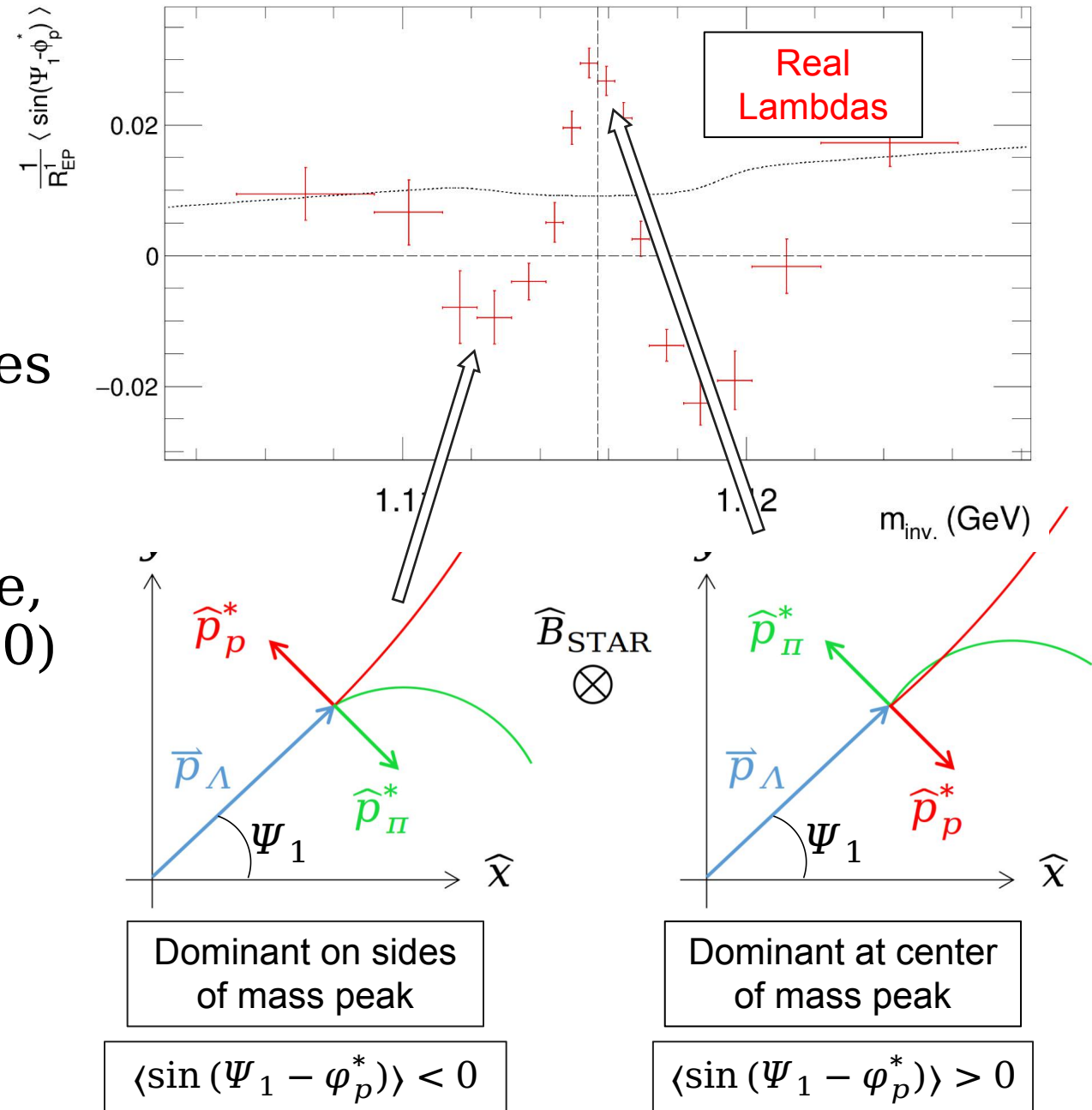
The cause

- The center of the mass peak is dominated by $\varphi_\Lambda - \varphi_p^* > \pi$ and sides are dominated by $\varphi_\Lambda - \varphi_p^* < \pi$
- Due to Λ directed flow, Ψ_1 and φ_Λ are correlated (in fixed-target mode, we are dominated by Λ s with $v_1 > 0$)
- \bar{P}_Λ measured using $\langle \sin(\Psi_1 - \varphi_p^*) \rangle$ will therefore depend on $\varphi_\Lambda - \varphi_p^*$



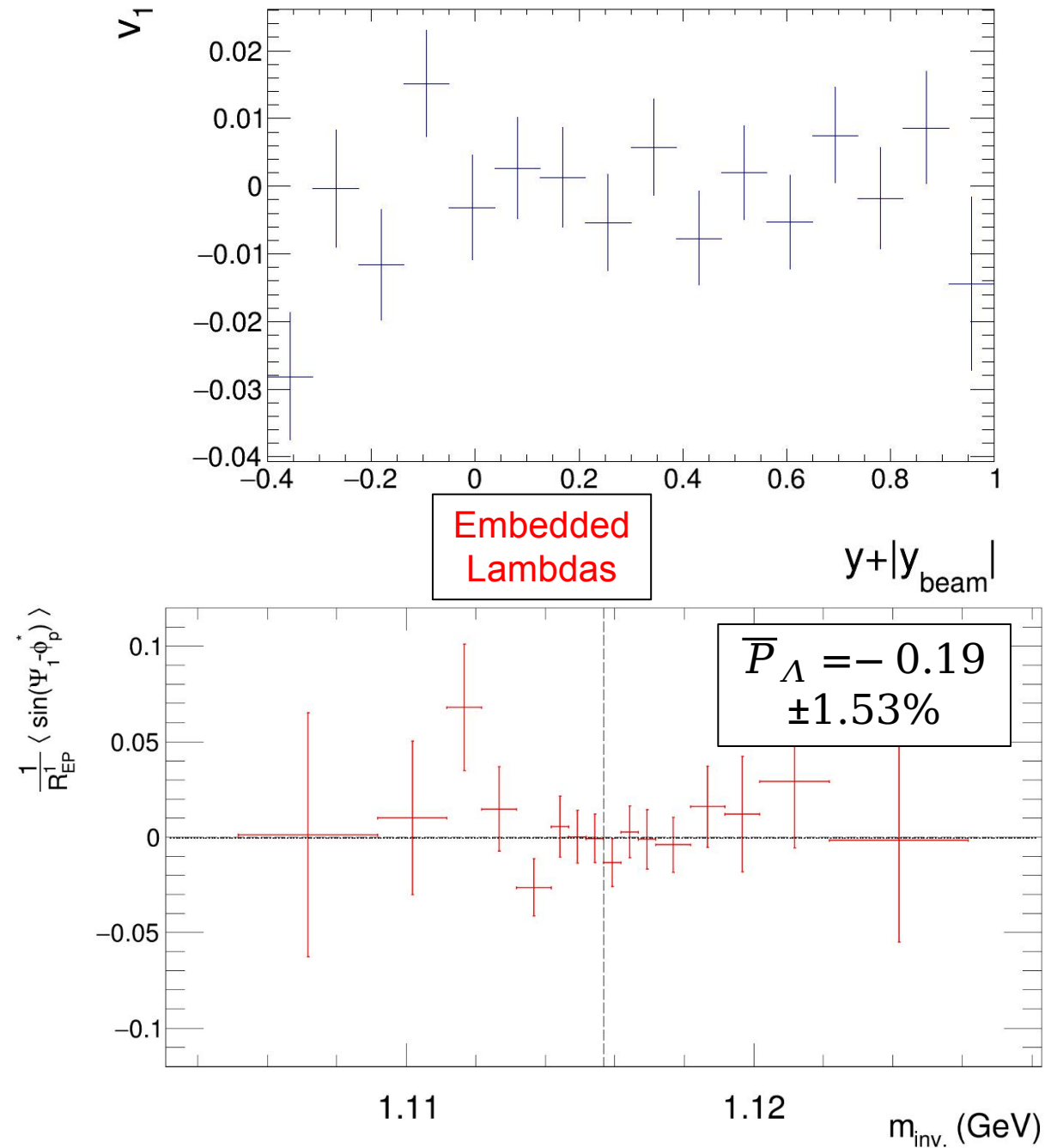
The cause

- The center of the mass peak is dominated by $\varphi_\Lambda - \varphi_p^* > \pi$ and sides are dominated by $\varphi_\Lambda - \varphi_p^* < \pi$
- Due to Λ directed flow, Ψ_1 and φ_Λ are correlated (in fixed-target mode, we are dominated by Λ s with $v_1 > 0$)
- \bar{P}_Λ measured using $\langle \sin(\Psi_1 - \varphi_p^*) \rangle$ will therefore depend on $\varphi_\Lambda - \varphi_p^*$ and is in turn enhanced near the center of the mass peak and suppressed on the sides



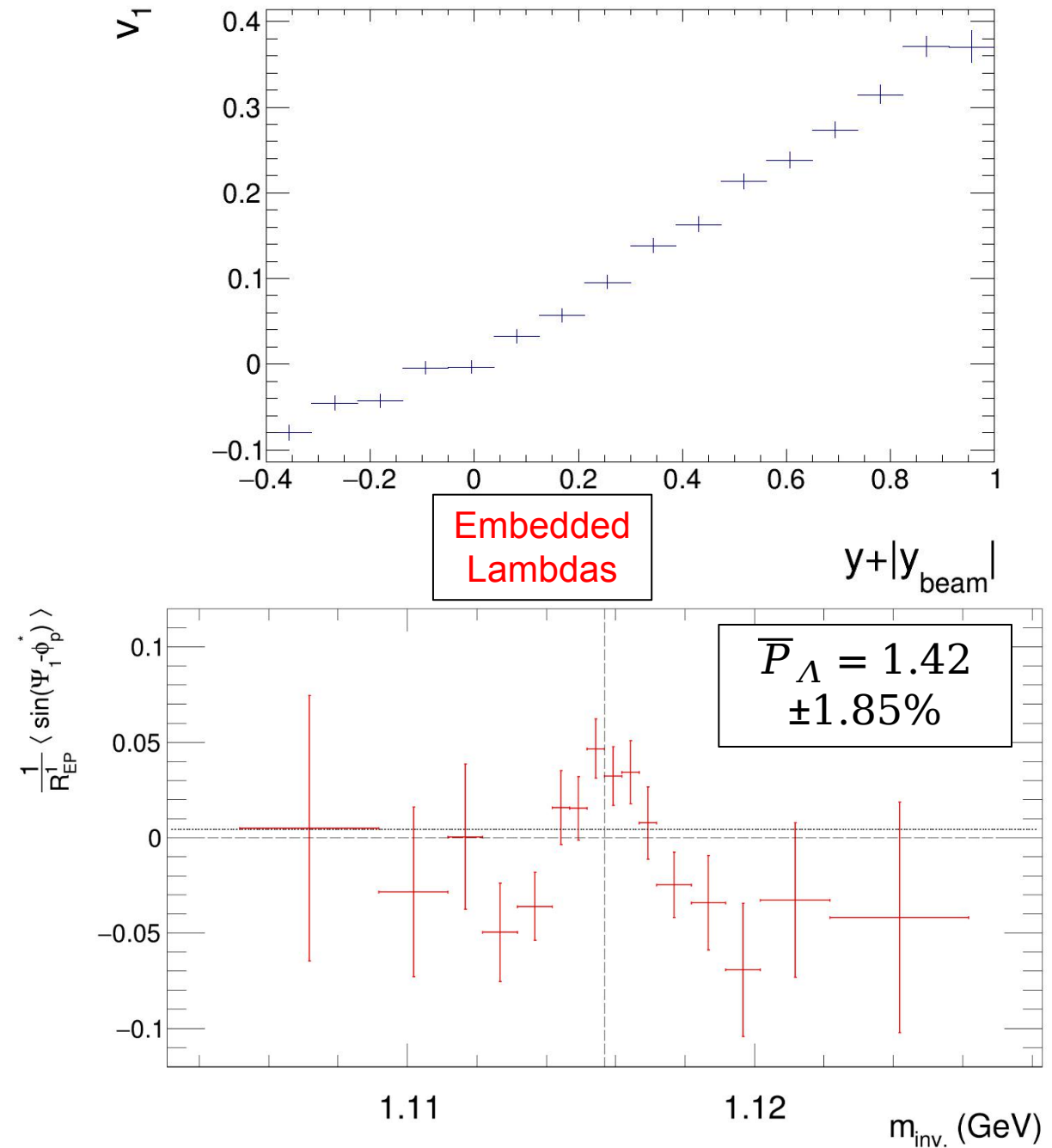
The cause

- Embedded Λ s have $\overline{P}_\Lambda = 0$ and $\nu_1 = 0$ by default



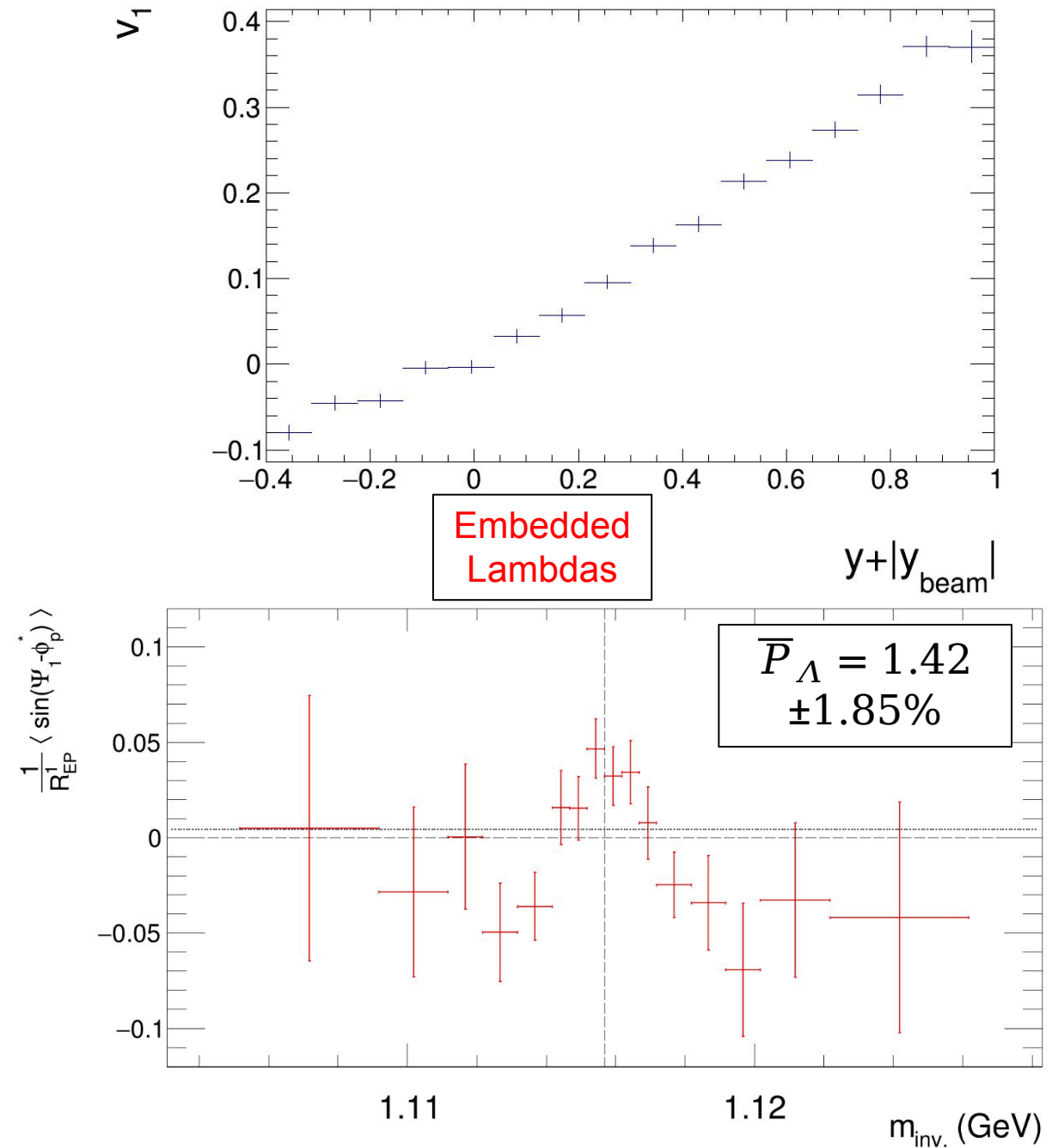
The cause

- Embedded Λ s have $\overline{P}_\Lambda = 0$ and $\nu_1 = 0$ by default
- When imposing a non-zero ν_1 , we see the same $m_{inv.}$ -dependent \overline{P}_Λ and we measure a false, non-zero \overline{P}_Λ



The cause

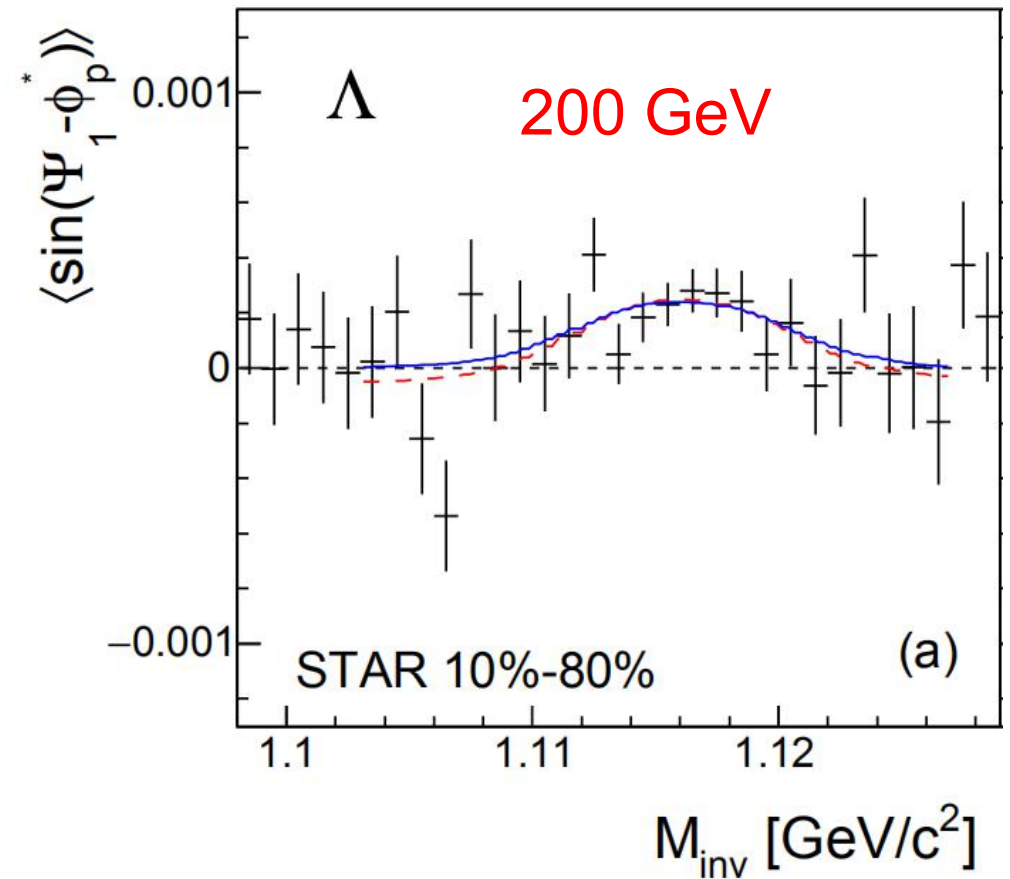
- Embedded Λ s have $\overline{P}_\Lambda = 0$ and $\nu_1 = 0$ by default
- When imposing a non-zero ν_1 , we see the same $m_{inv.}$ -dependent \overline{P}_Λ and we measure a false, non-zero \overline{P}_Λ
- The current method for measuring \overline{P}_Λ is invalid



The cause

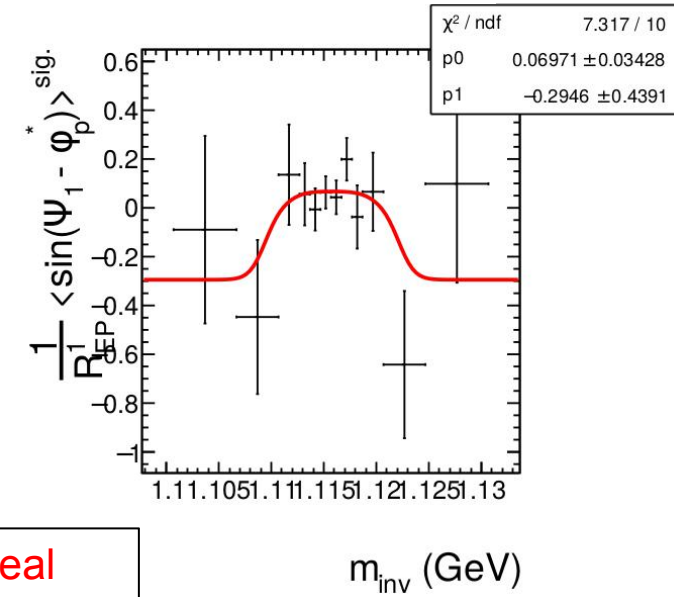
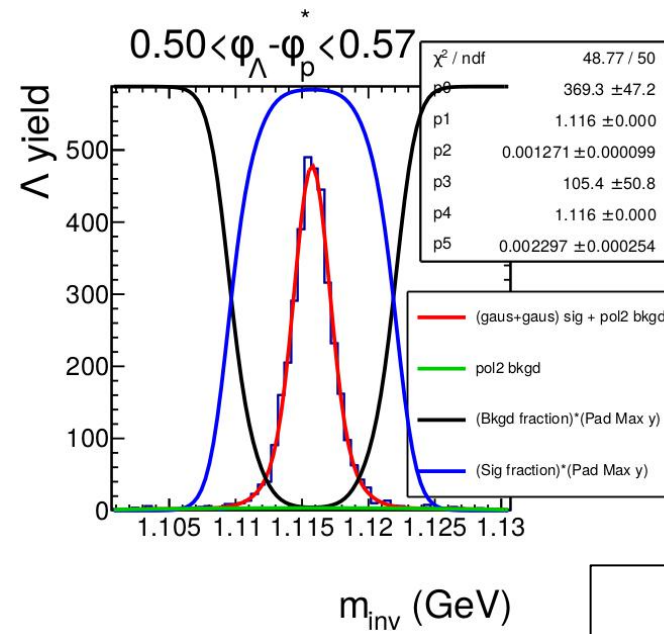
- Embedded Λ s have $\overline{P}_\Lambda = 0$ and $\nu_1 = 0$ by default
- When imposing a non-zero ν_1 , we see the same $m_{inv.}$ -dependent \overline{P}_Λ and we measure a false, non-zero \overline{P}_Λ
- **The current method for measuring \overline{P}_Λ is invalid**
 - This does not invalidate previous results in collider mode where ν_1 is small and acceptance is close to symmetric about mid rapidity

Phys. Rev. C 98, 014910 (2018)

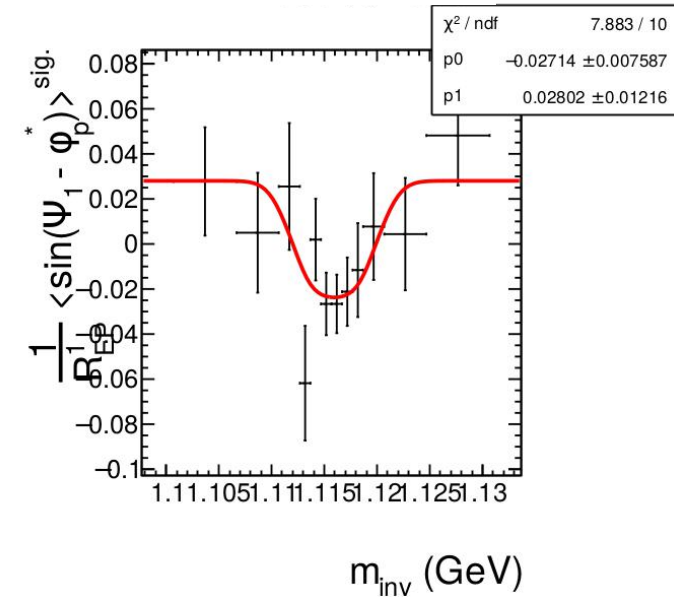
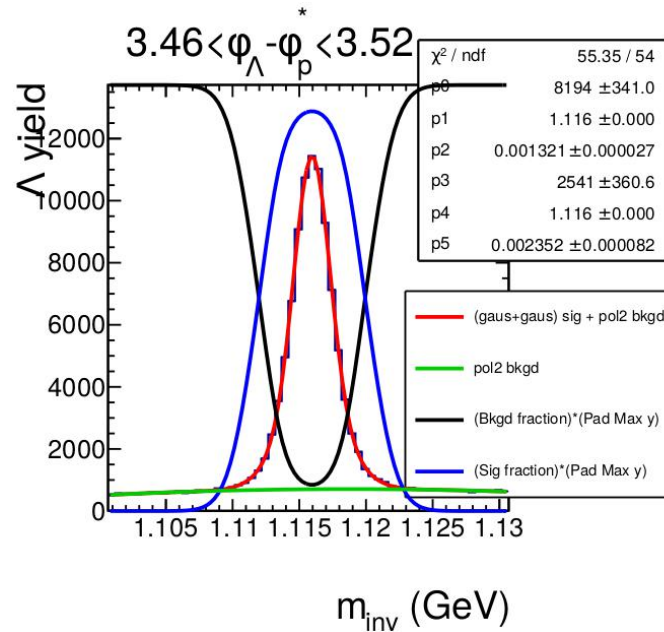


The solution

- Since this effect comes from the m_{inv} distribution's dependence on $\varphi_{\Lambda} - \varphi_p^*$, if we look at thin slices in $\varphi_{\Lambda} - \varphi_p^*$ the invariant-mass method works as expected

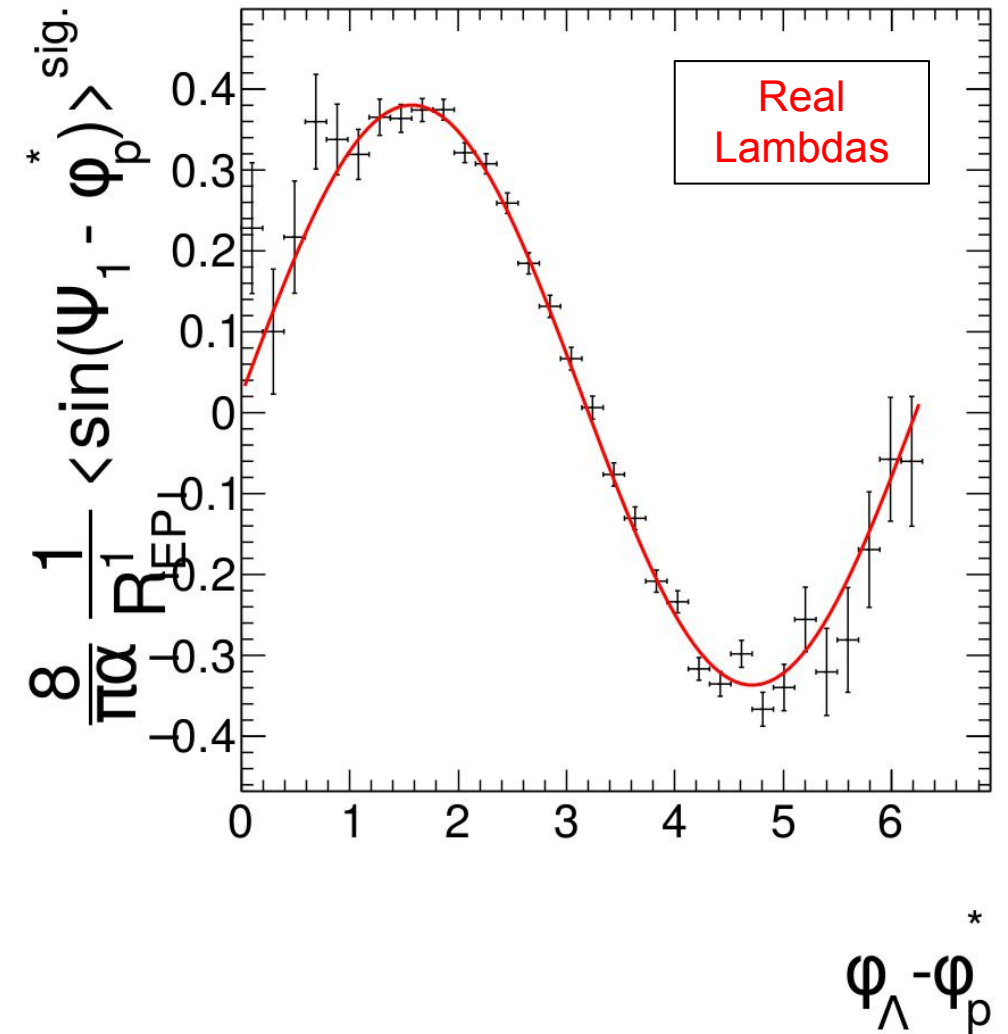


Real
Lambdas



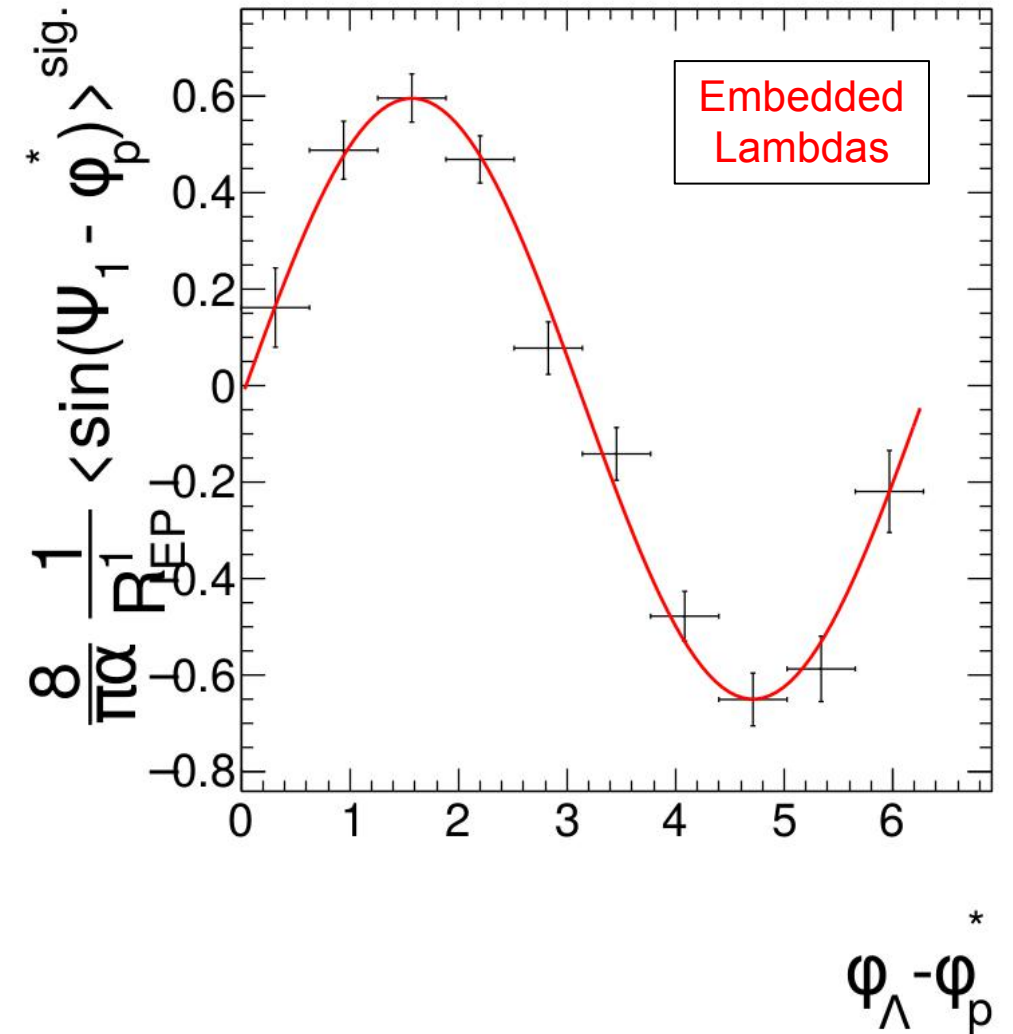
The solution

- Since this effect comes from the m_{inv} distribution's dependence on $\varphi_\Lambda - \varphi_p^*$, if we look at thin slices in $\varphi_\Lambda - \varphi_p^*$ the invariant-mass method works as expected
- The extracted signals are then plotted against $\varphi_\Lambda - \varphi_p^*$, and follow a sine curve
 - ν_1 drives the correlation between Ψ_1 and φ_Λ



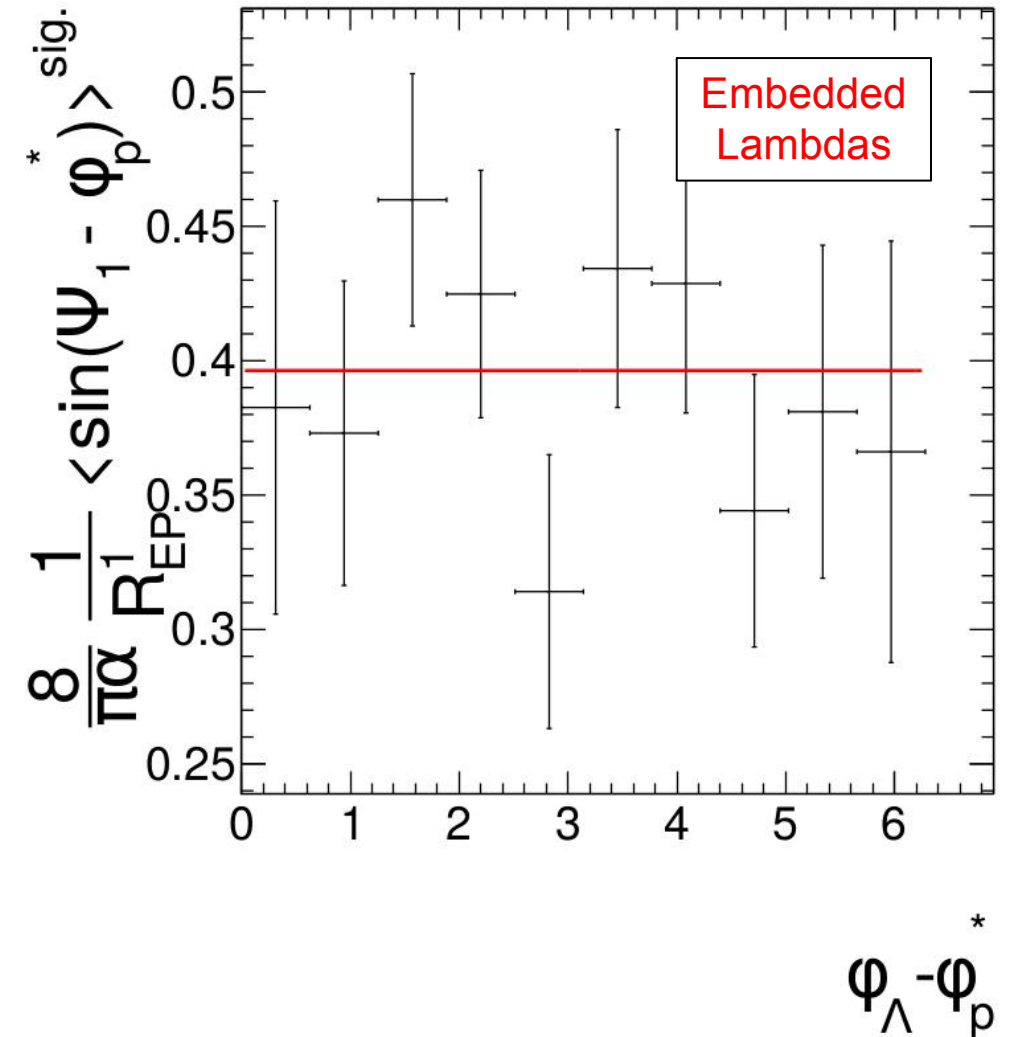
The solution

- Again using embedded Lambdas, imposing non-zero ν_1 but leaving $\overline{P}_\Lambda = 0$, we see the same sinusoidal behavior



The solution

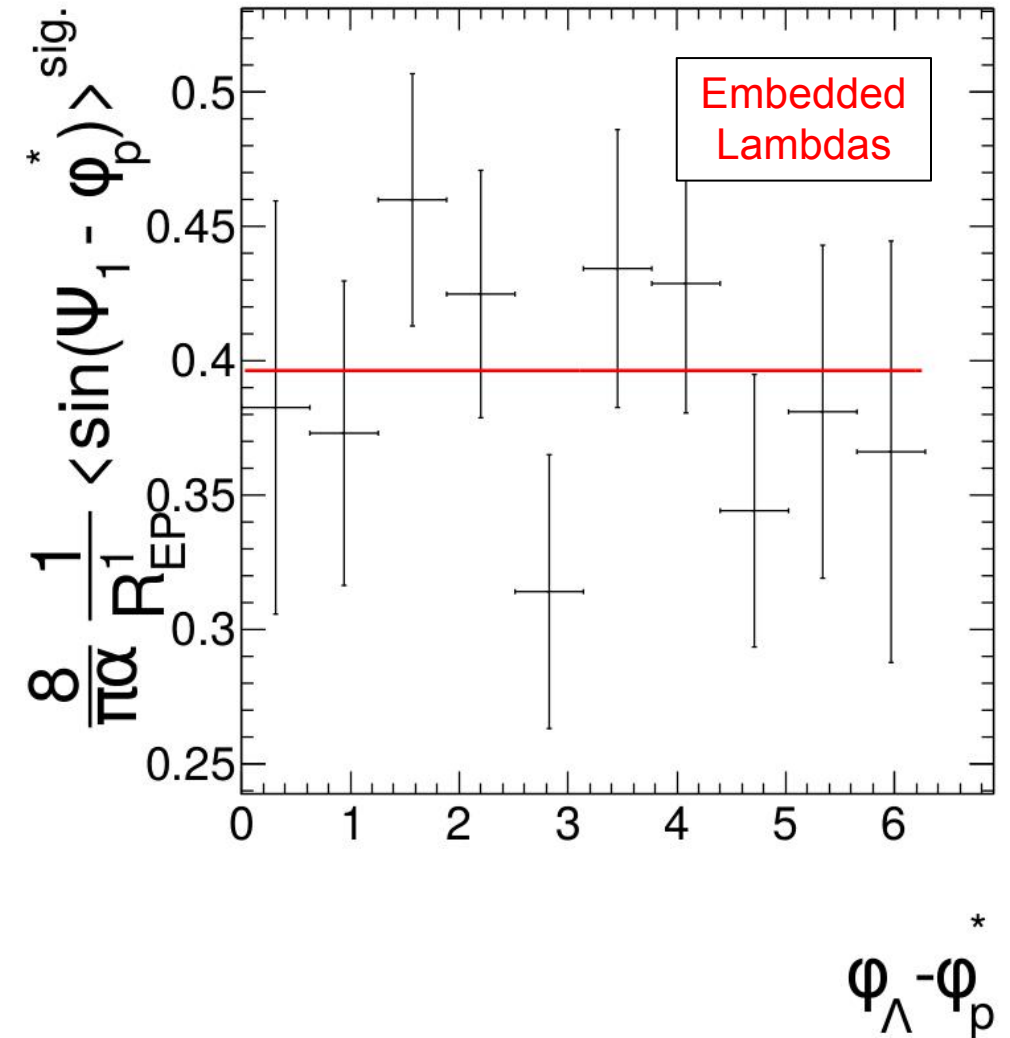
- Again using embedded Lambdas, imposing non-zero ν_1 but leaving $\bar{P}_\Lambda = 0$, we see the same sinusoidal behavior
- If we instead impose non-zero \bar{P}_Λ , but leave $\nu_1 = 0$, we see \bar{P}_Λ vs. $\varphi_\Lambda - \varphi_p^*$ consistent with flat



The solution

- We then assume true polarization of the form:

$$\frac{8}{\pi\alpha} \frac{1}{R_{EP}^1} \langle \sin(\Psi_1 - \varphi_p^*) \rangle^{\text{sig.}} = \bar{P}_\Lambda^{\text{true}} + c\nu_1 \sin(\varphi_\Lambda - \varphi_p^*)$$

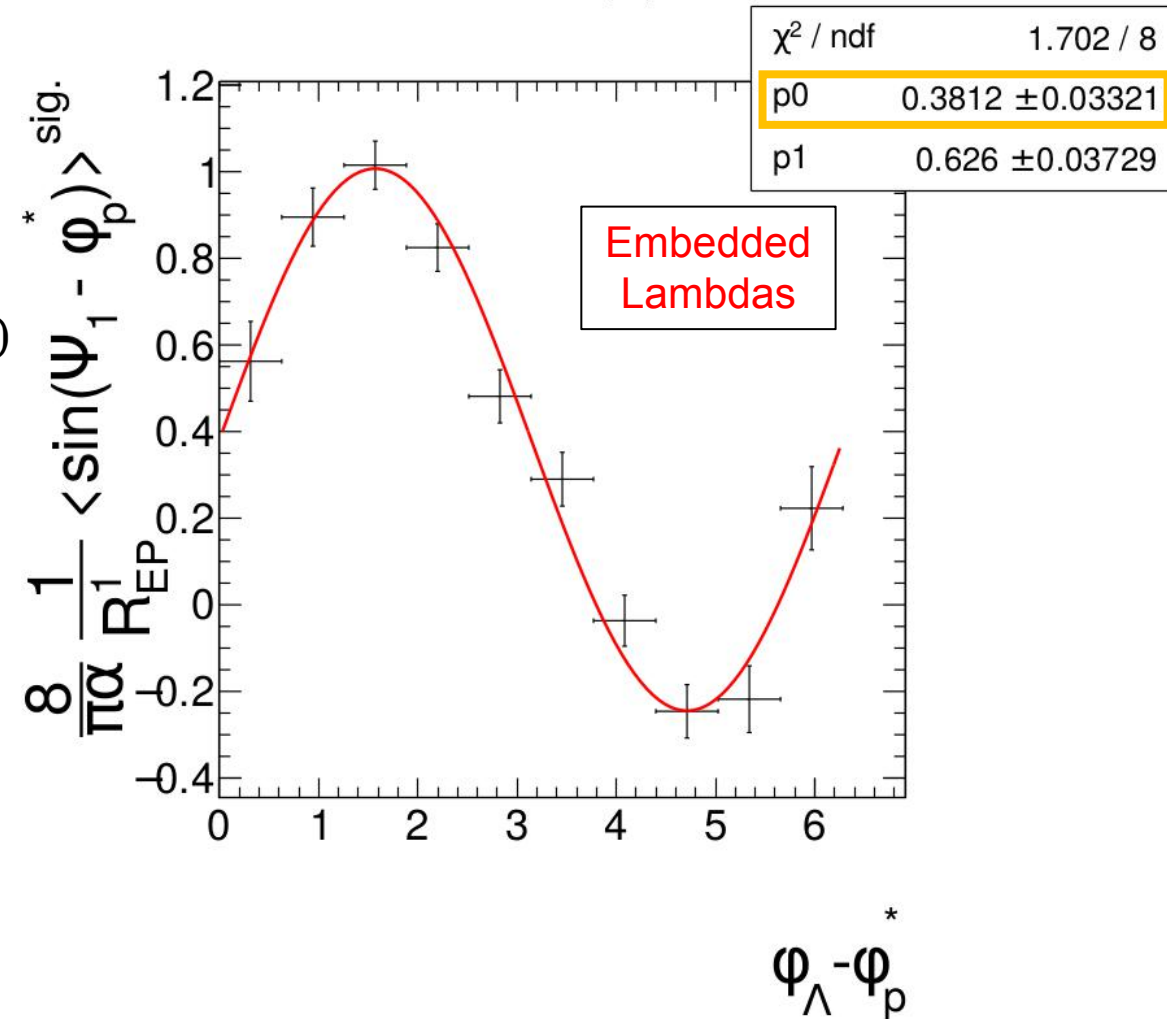


The solution

- We then assume true polarization of the form:

$$\frac{8}{\pi\alpha} \frac{1}{R_{EP}^1} \langle \sin(\Psi_1 - \varphi_p^*) \rangle^{\text{sig.}} = \bar{P}_\Lambda^{\text{true}} + c\nu_1 \sin(\varphi_\Lambda - \varphi_p^*)$$

- Now we impose ν_1 and $\bar{P}_\Lambda^{\text{true}} = 40\%$. Assuming the form above, we extract $\bar{P}_\Lambda^{\text{true}}$ and find it to be consistent with the input

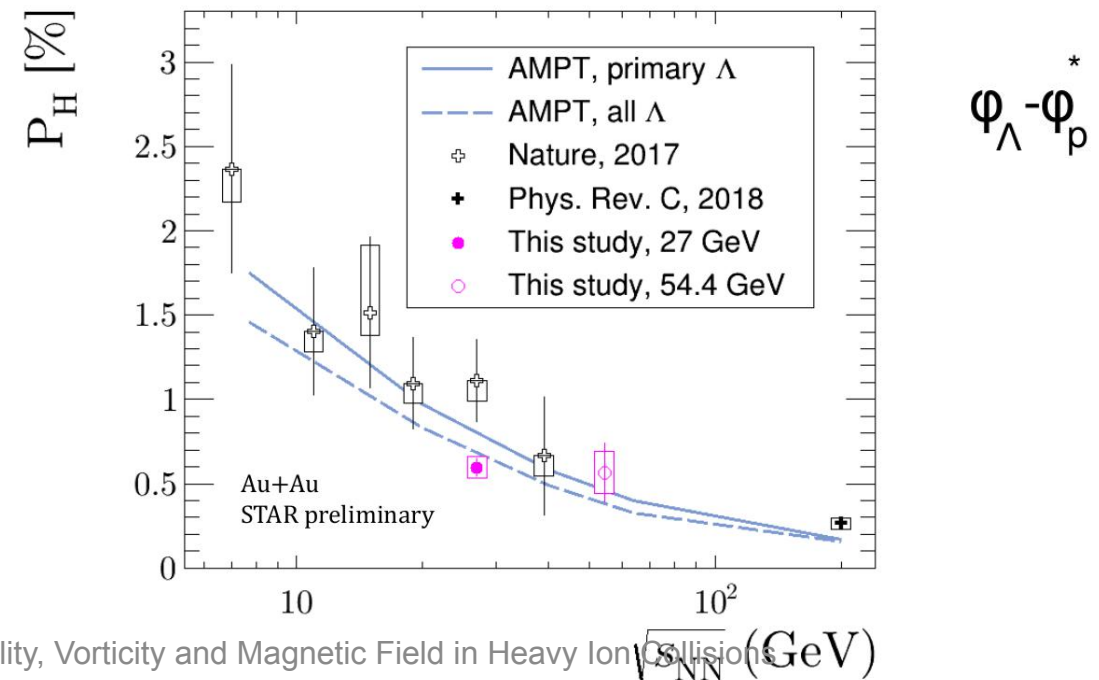
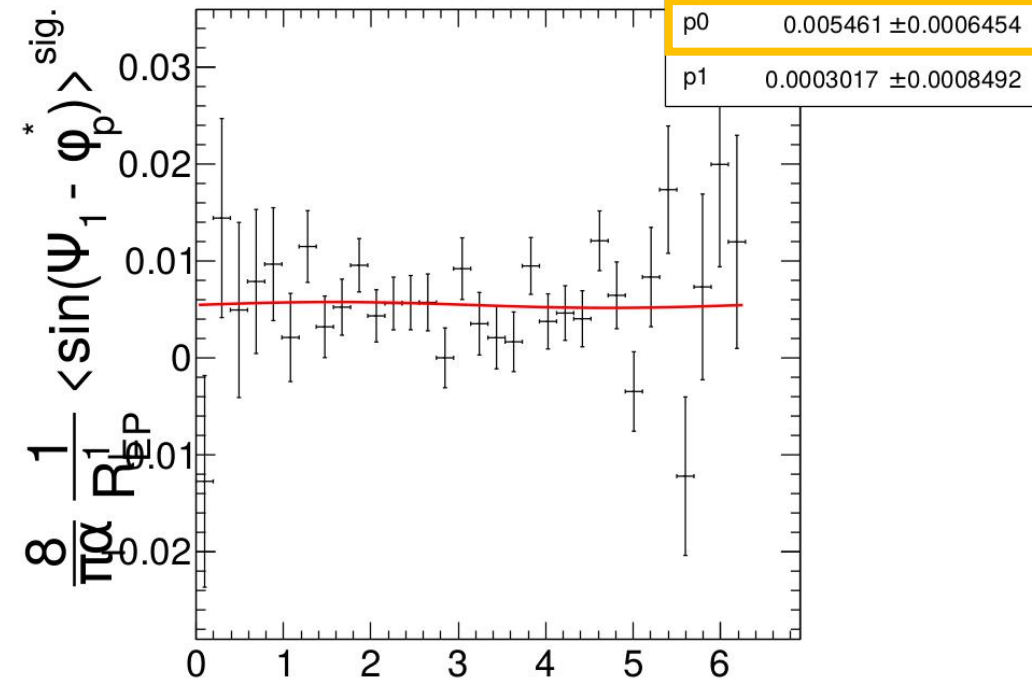


The solution

- We then assume true polarization of the form:

$$\frac{8}{\pi\alpha} \frac{1}{R_{EP}^1} \langle \sin(\Psi_1 - \varphi_p^*) \rangle^{\text{sig.}} = \bar{P}_\Lambda^{\text{true}} + c\nu_1 \sin(\varphi_\Lambda - \varphi_p^*)$$

- Now we impose ν_1 and $\bar{P}_\Lambda^{\text{true}} = 40\%$. Assuming the form above, we extract $\bar{P}_\Lambda^{\text{true}}$ and find it to be consistent with the input
- Using this method on 2018 27 GeV data set yields the same result as previously found and shown at Quark Matter



Further comments on this method

- This method is crucial for measuring \overline{P}_Λ when:
 - v_1 is non-negligible
 - acceptance is not symmetric about mid rapidity
 - comparing \overline{P}_Λ to $\overline{P}_{\overline{\Lambda}}$
 - measuring rapidity dependence of \overline{P}_Λ
- We will implement this method for measuring $\overline{P}_{\Lambda, \overline{\Lambda}}$ at $\sqrt{s_{\text{NN}}} = 19.6 \text{ GeV}$
- This method removes any contributions of production-plane polarization to the result; our result is entirely vorticity driven
 - This is actually desirable as it makes the comparison to theory curves (which don't include production-plane polarization) more meaningful as well as comparisons to collider-mode data

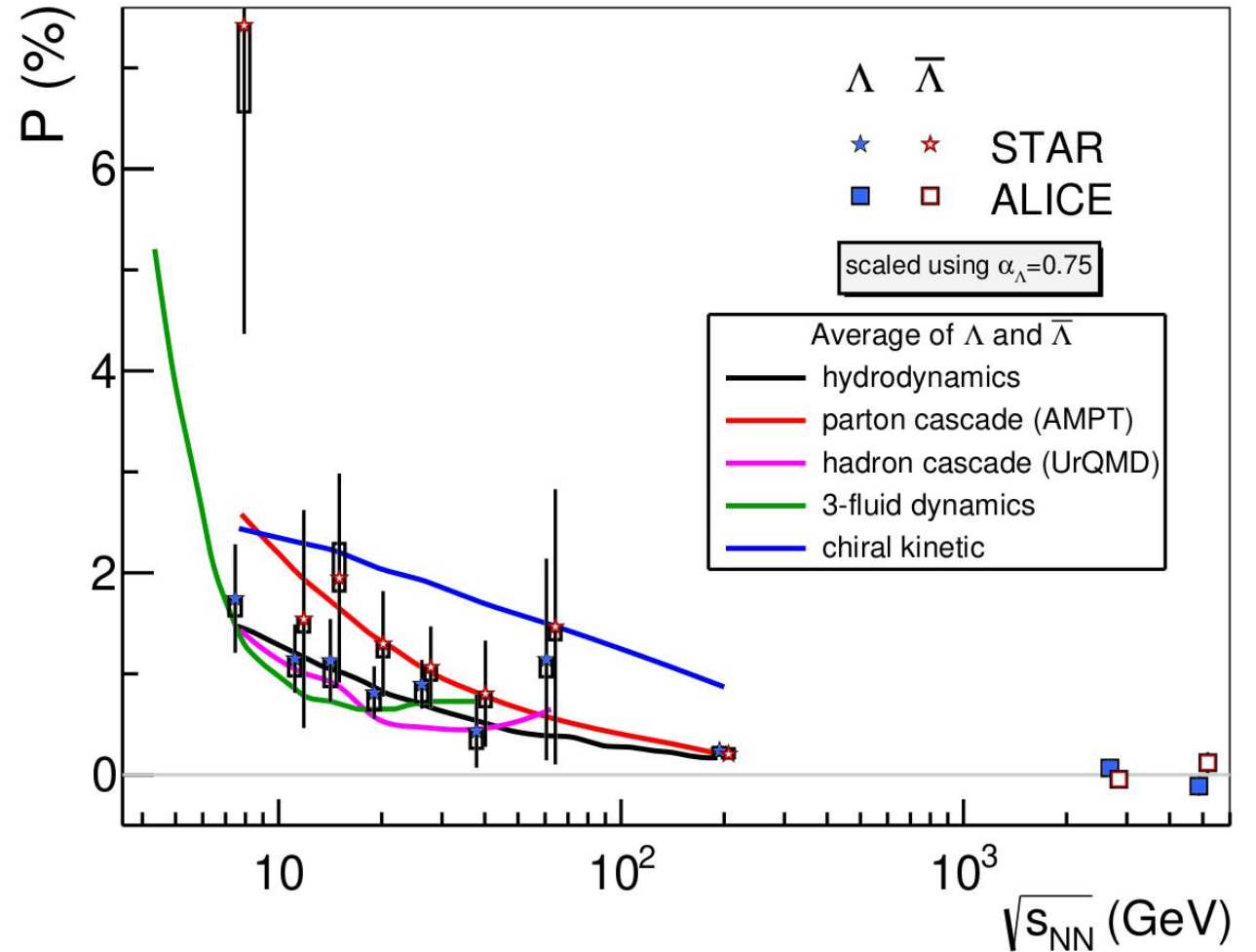
Systematic uncertainties

- We have contributions from the following:
 - Uncertainty on the corrective efficiency term A_0 (*)
 - Statistical uncertainty on the corrective decay parameter α_Λ
 - Statistical uncertainty on the corrective Ψ_1 resolution term $R_{EP}^{(1)}$
 - Uncertainty of the dependence of $\bar{P}_\Lambda^{\text{bgd.}}$ on $m_{\text{inv.}}$
- We add the differences between the \bar{P}_Λ measurements using the “standard” correction values and the adjusted correction values in quadrature, with respect to each differential variable
- We searched extensively for systematic mistakes, and adjusted the method when required

(*) B. I. Abelev *et al.* (STAR), Phys. Rev. C **76**, 024915 (2007), [Erratum: Phys.Rev.C 95, 039906 (2017)], arXiv:0705.1691 [nucl-ex].

Model predictions

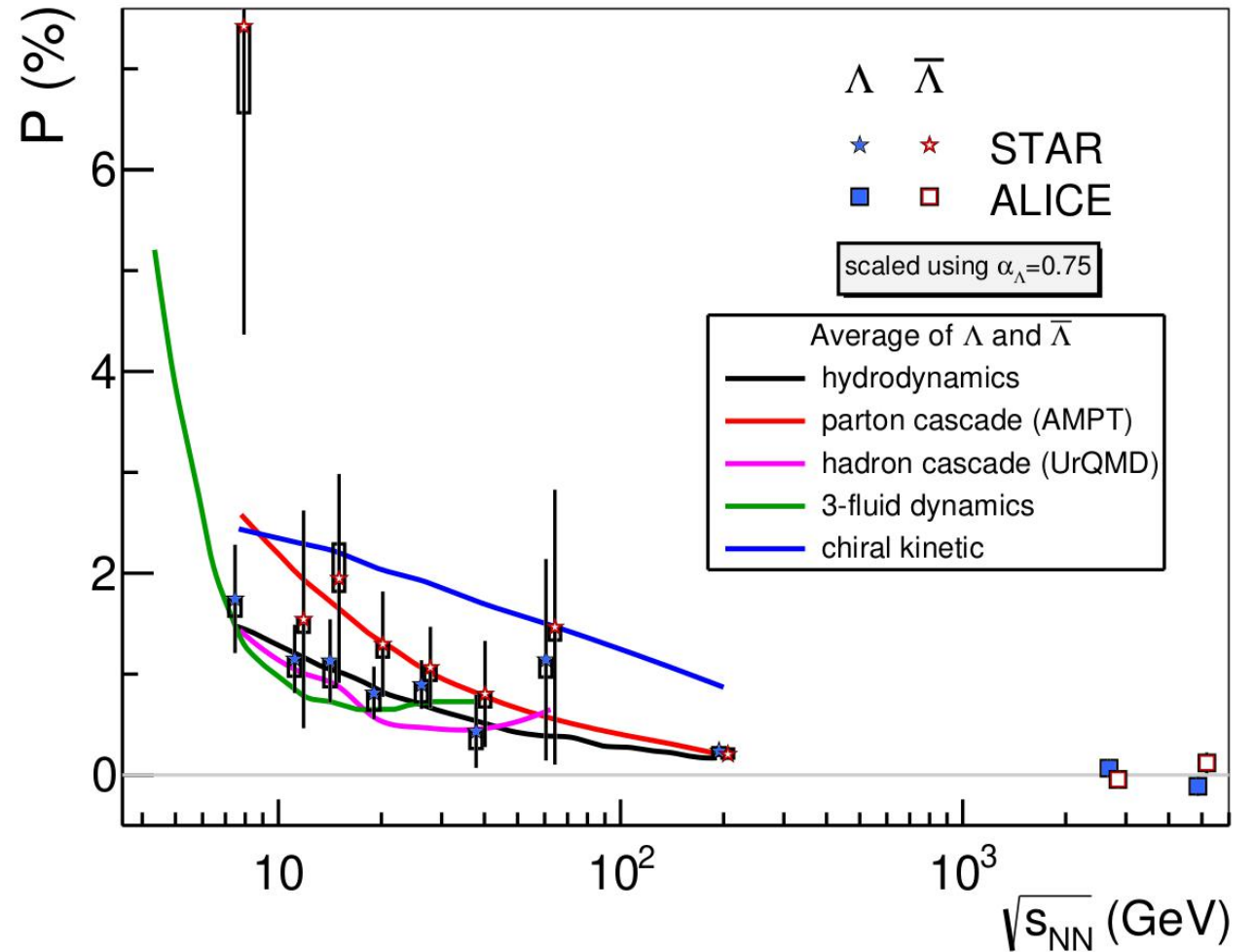
- In general, previous results have been reproduced well by a number of models with differing underlying assumptions



F. Becattini and M. A. Lisa, Ann. Rev. Nucl. Part. Sci. **70**, 395 (2020), arXiv:2003.03640 [nucl-ex].

Model predictions

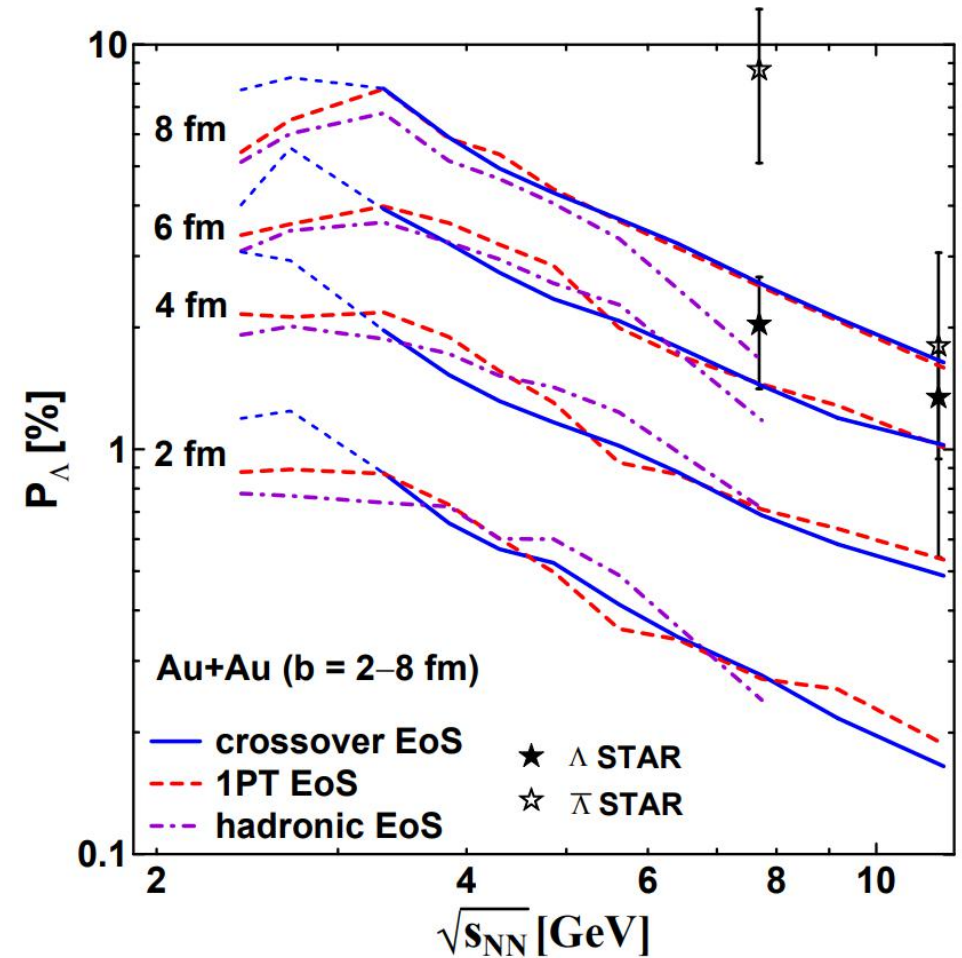
- In general, previous results have been reproduced well by a number of models with differing underlying assumptions
- Several new papers study \bar{P}_Λ at low $\sqrt{s_{NN}}$



F. Becattini and M. A. Lisa, *Ann. Rev. Nucl. Part. Sci.* **70**, 395 (2020), arXiv:2003.03640 [nucl-ex].

Model predictions

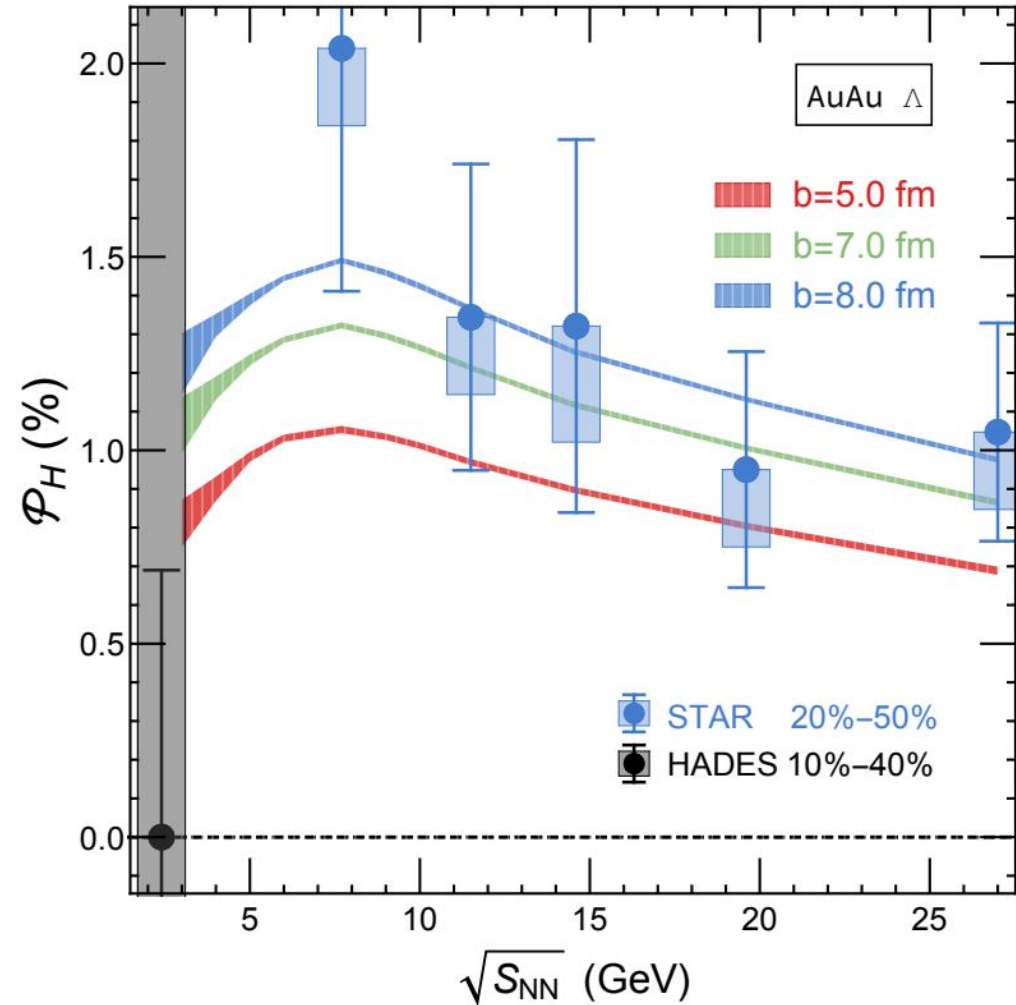
- In general, previous results have been reproduced well by a number of models with differing underlying assumptions
- Several new papers study \overline{P}_Λ at low $\sqrt{s_{NN}}$
 - 3-Fluid Dynamics



Y. B. Ivanov, Phys. Rev. C **103**, L031903 (2021),
arXiv:2012.07597 [nucl-th].

Model predictions

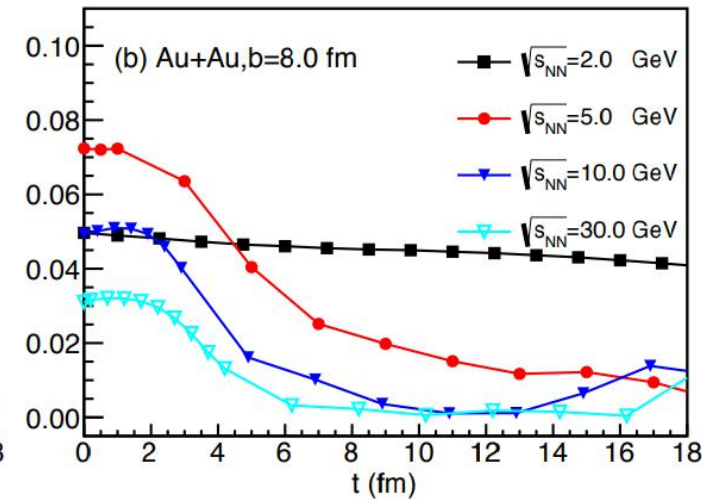
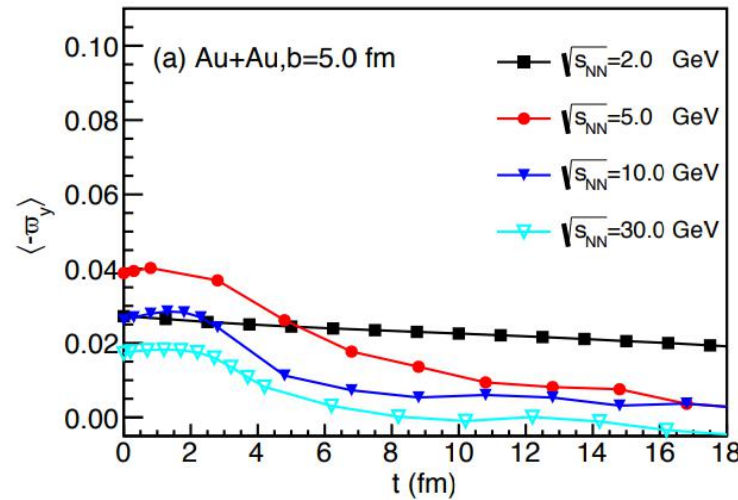
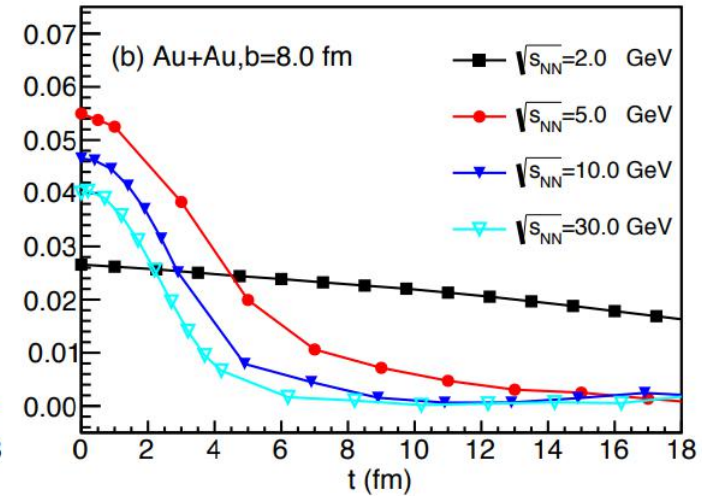
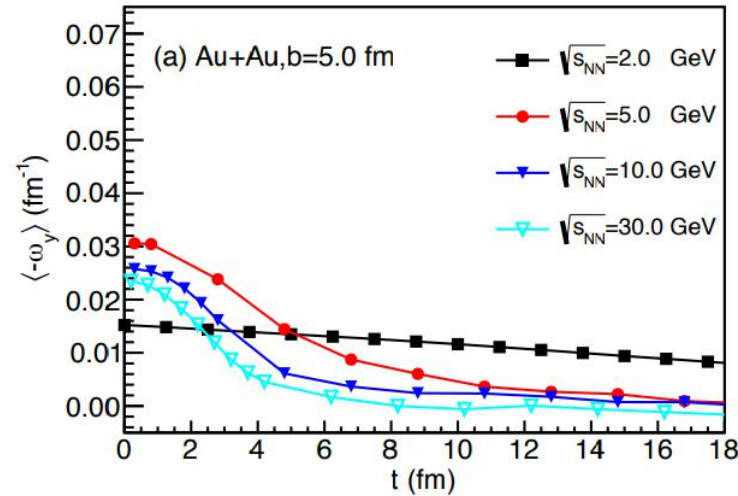
- In general, previous results have been reproduced well by a number of models with differing underlying assumptions
- Several new papers study \overline{P}_Λ at low $\sqrt{s_{NN}}$
 - 3-Fluid Dynamics
 - AMPT



Y. Guo, J. Liao, E. Wang, H. Xing, and H. Zhang, Locating the most vortical fluid in nuclear collisions with beam energy scan (2021), arXiv:2105.13481 [nucl-th].

Model predictions

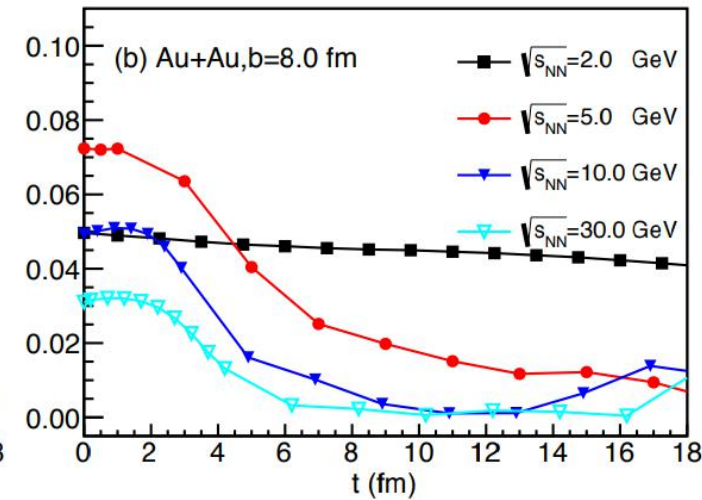
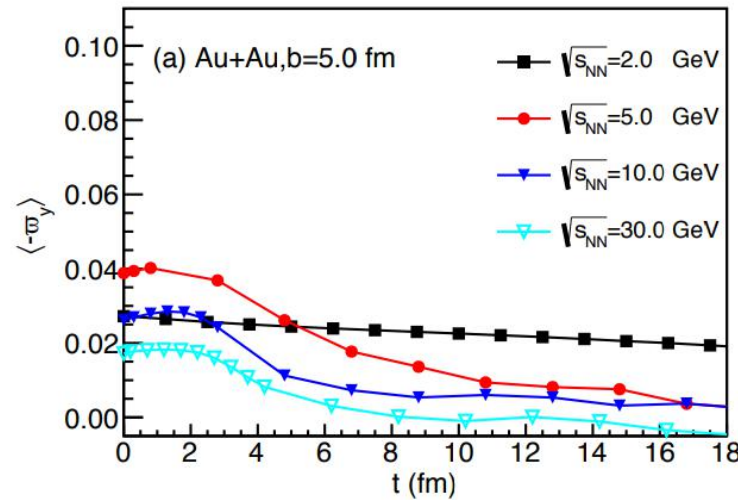
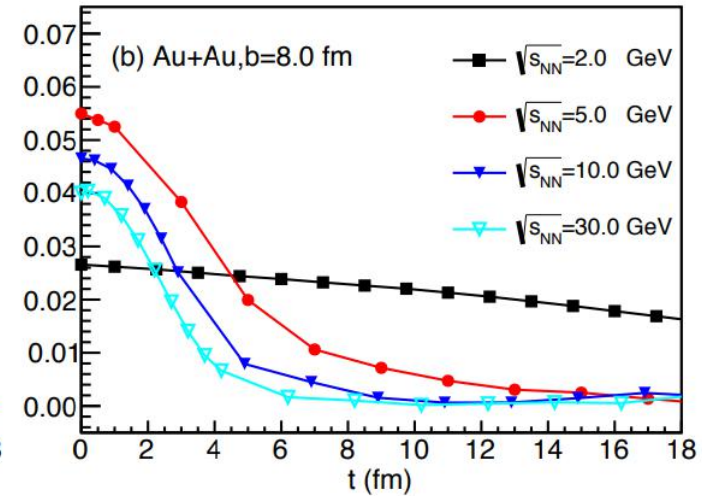
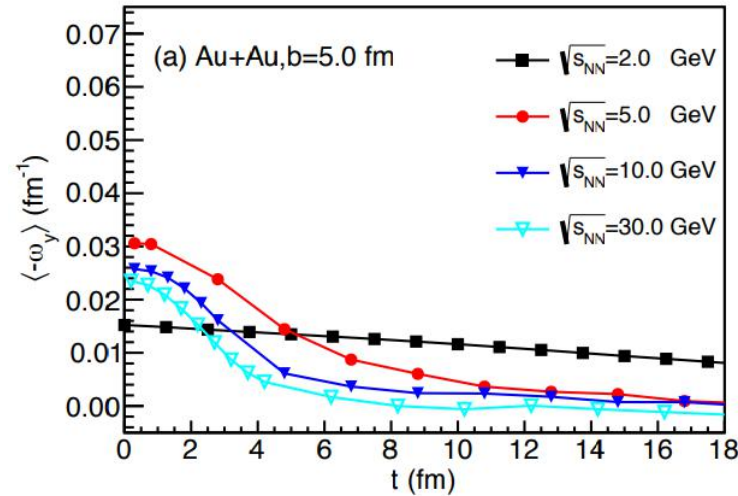
- In general, previous results have been reproduced well by a number of models with differing underlying assumptions
- Several new papers study \bar{P}_Λ at low $\sqrt{s_{NN}}$
 - 3-Fluid Dynamics
 - AMPT
 - UrQMD
 - Prediction of \bar{P}_Λ unclear



X.-G. Deng, X.-G. Huang, Y.-G. Ma, and S. Zhang, Phys. Rev. C **101**, 064908 (2020), arXiv:2001.01371 [nucl-th].

Model predictions

- In general, previous results have been reproduced well by a number of models with differing underlying assumptions
- Several new papers study \bar{P}_Λ at low $\sqrt{s_{NN}}$
 - 3-Fluid Dynamics
 - AMPT
 - UrQMD
 - Prediction of \bar{P}_Λ unclear
- Each predict a peak \bar{P}_Λ in the vicinity of $\sqrt{s_{NN}} = 3$ GeV

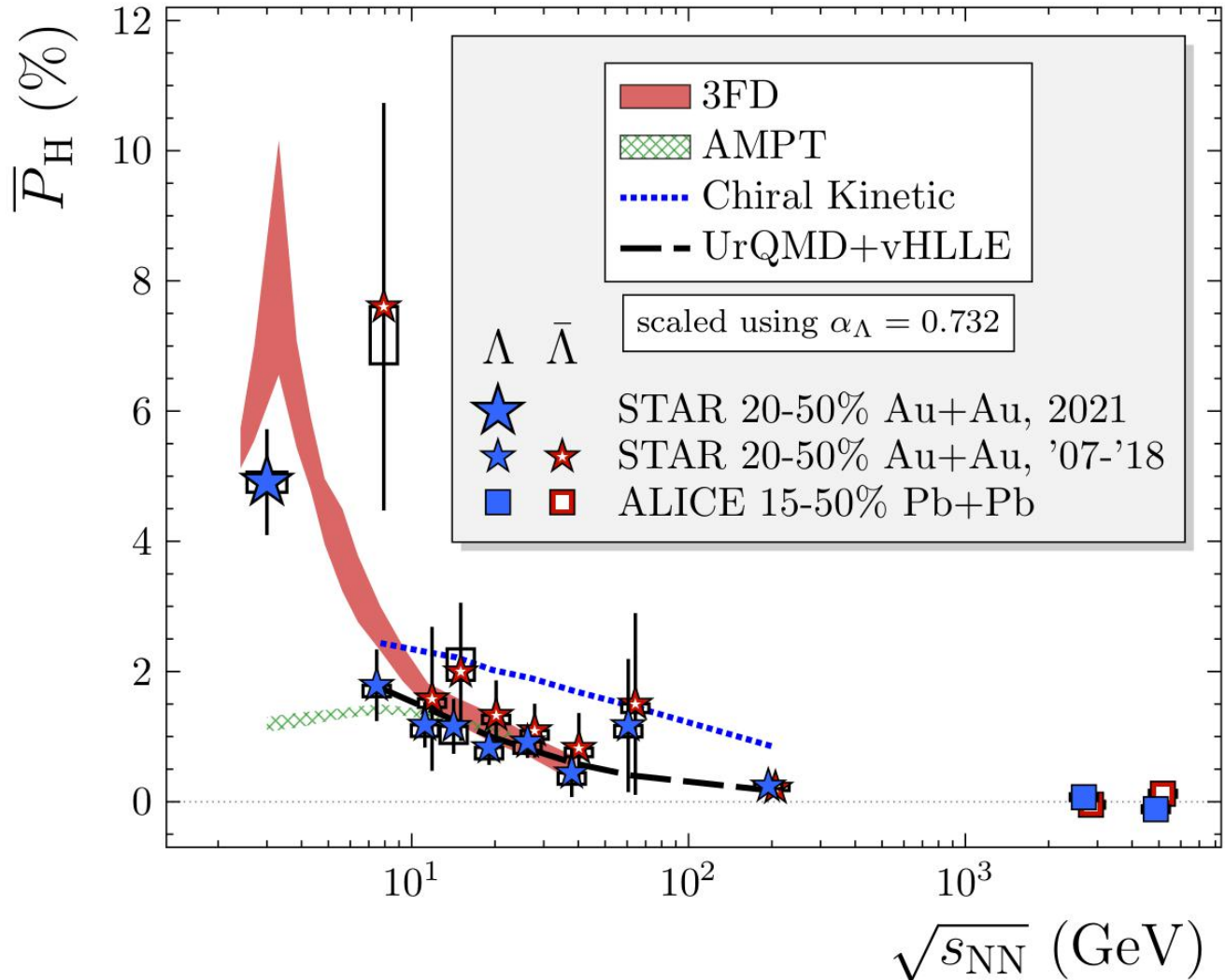


X.-G. Deng, X.-G. Huang, Y.-G. Ma, and S. Zhang, Phys. Rev. C **101**, 064908 (2020), arXiv:2001.01371 [nucl-th].

STAR's measurement

\bar{P}_Λ alongside previous publications demonstrates extended trend of falling \bar{P}_Λ w.r.t $\sqrt{s_{NN}}$

- \bar{P}_Λ at $\sqrt{s_{NN}} = 3$ GeV is the largest yet observed, with significance 6σ
 - Huge ω is present in heavy-ion collisions
- AMPT underestimates the data at low energy, while rough agreement with 3FD is shown
 - Suggests ω is affected strongly by the state of the system, which is a hadron gas at lower energies and fluid-like at higher energies; both support ω

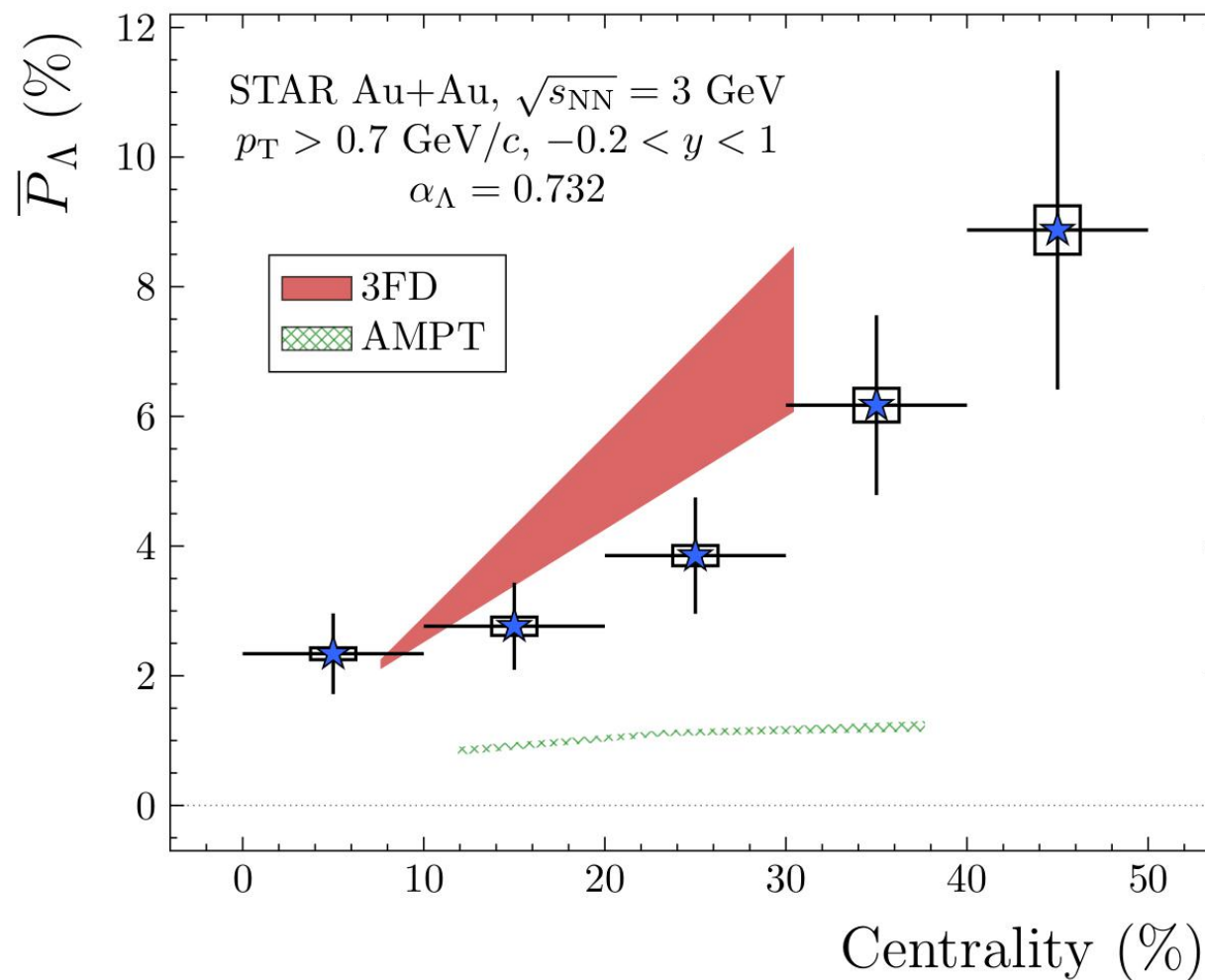


M. S. Abdallah et al. Global Λ -hyperon polarization in Au+Au collisions at $\sqrt{s_{NN}} = 3$ GeV. 7 2021.

arXiv:2108.00044 [nucl-ex]

Centrality dependence

- 3FD and AMPT each predict rising \bar{P}_Λ with collision centrality
- Observation consistent with phenomenon driven by angular momentum

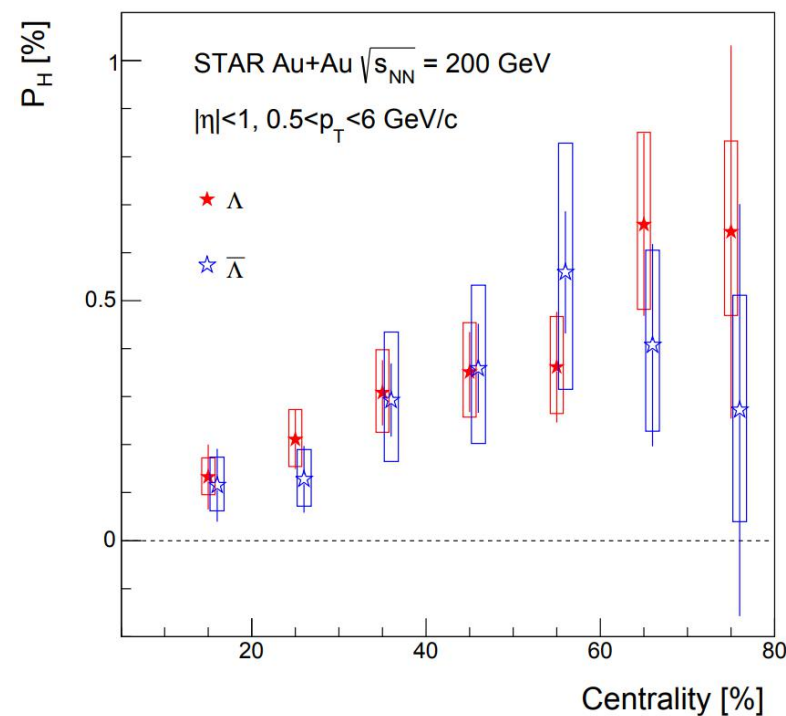
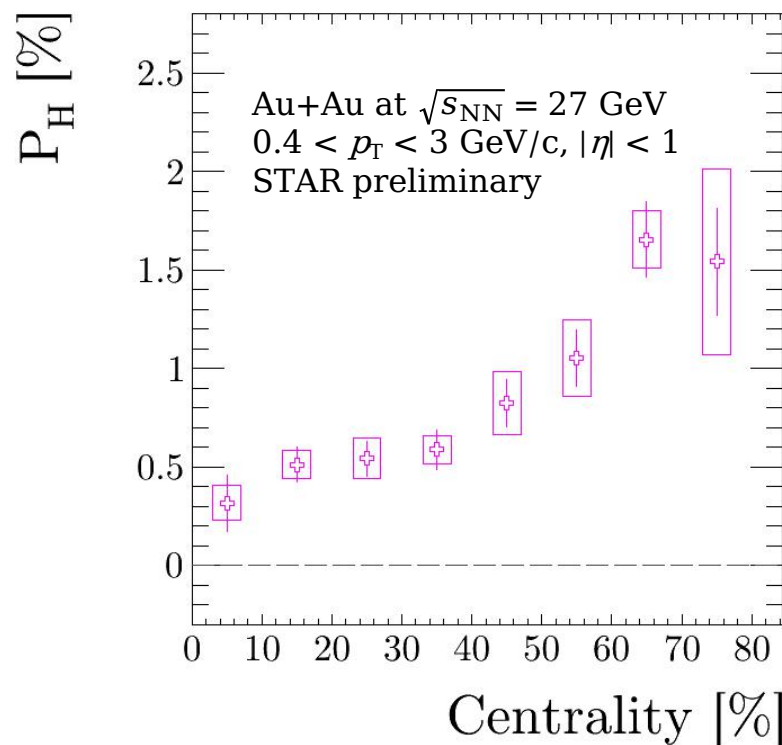


M. S. Abdallah et al. Global Λ -hyperon polarization in Au+Au collisions at $\sqrt{s_{NN}} = 3$ GeV. 7 2021.

arXiv:2108.00044 [nucl-ex]

Centrality dependence

- 3FD and AMPT each predict rising \bar{P}_Λ with collision centrality
- Observation consistent with phenomenon driven by angular momentum
- Such dependence also seen in previous studies

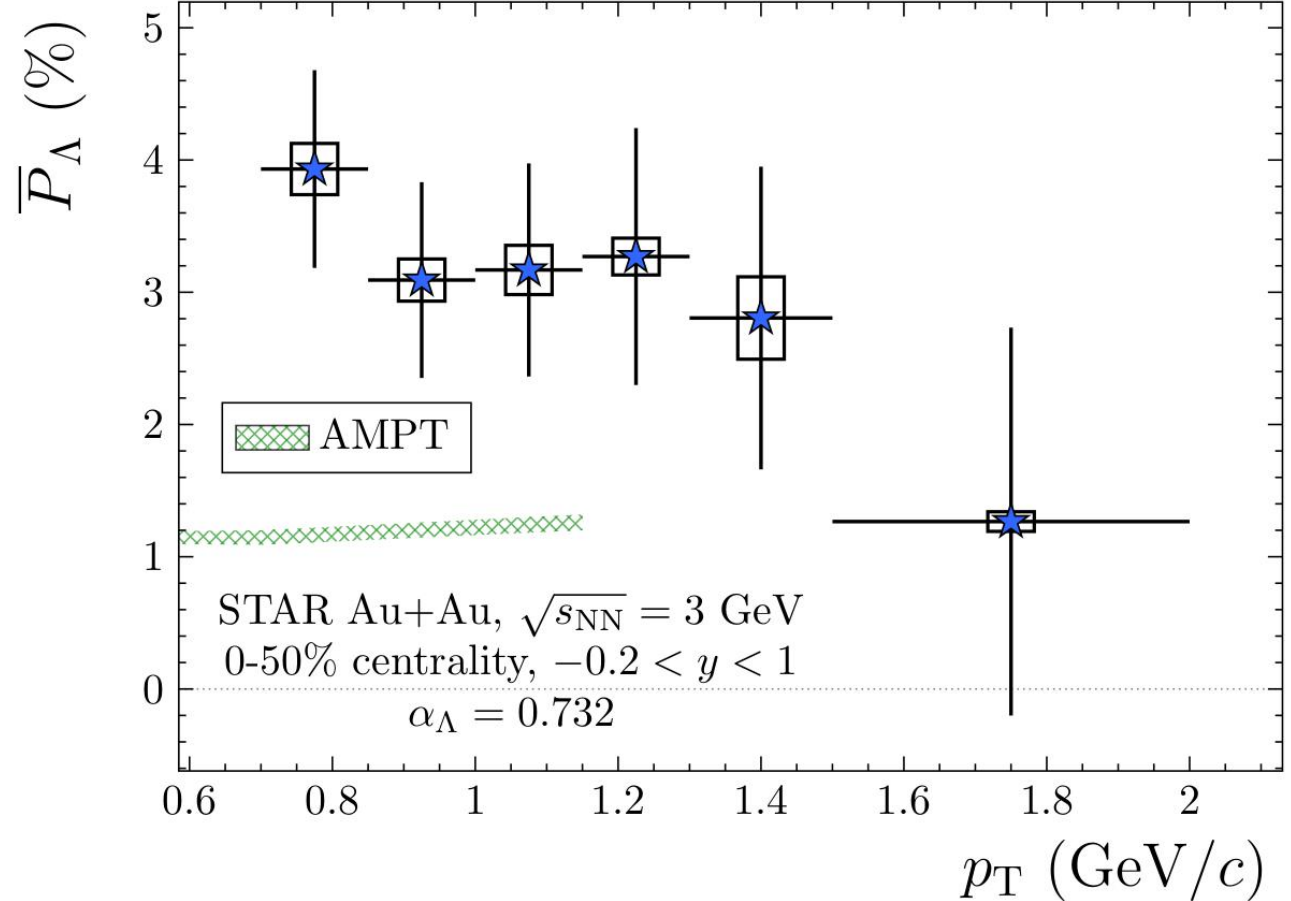


Joseph R. Adams. Differential measurements of lambda polarization in au+au collisions and a search for the magnetic field by star. *Nuclear Physics A*, 1005:121864, 2021.

Jaroslav Adam et al. Global polarization of Λ hyperons in Au+Au collisions at $\sqrt{s_{NN}} = 200$ GeV. *Phys. Rev. C*, 98:014910, 2018. arXiv:1805.04400 [nucl-ex]

p_T dependence

- AMPT predicts weak dependence on transverse momentum p_T
- No observed p_T dependence at $\sqrt{s_{NN}} = 3$ GeV
 - At higher p_T than what is statistically accessible, one might expect a suppression of \overline{P}_Λ due to hard processes

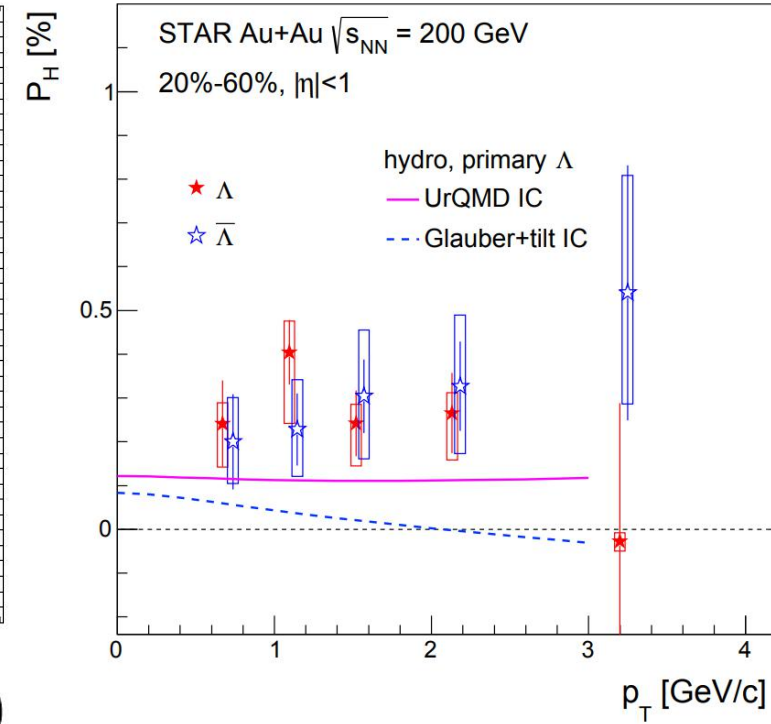
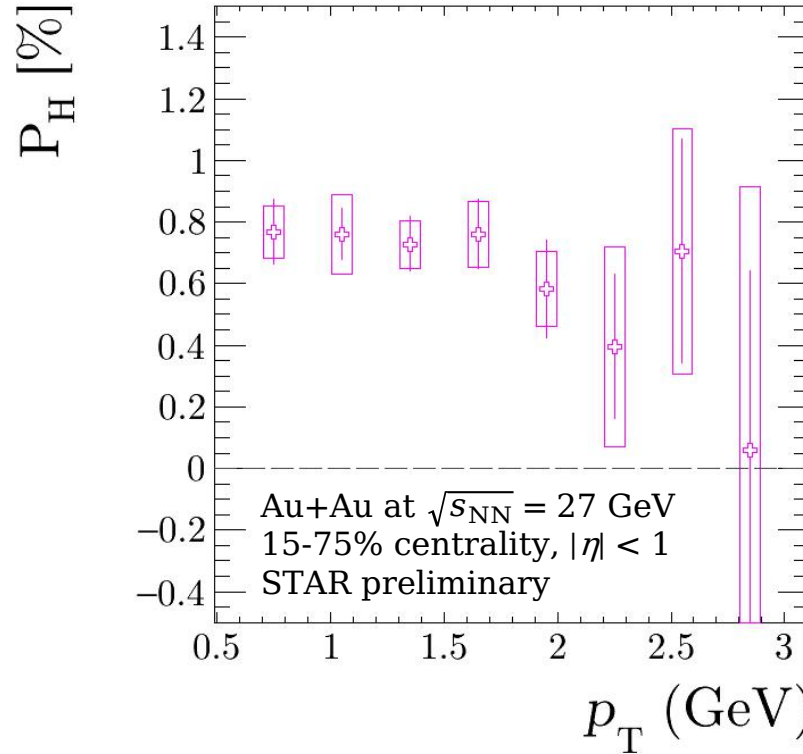


M. S. Abdallah et al. Global Λ -hyperon polarization in Au+Au collisions at $\sqrt{s_{NN}} = 3$ GeV. 7 2021.

arXiv:2108.00044 [nucl-ex]

p_T dependence

- AMPT predicts weak dependence on transverse momentum p_T
- No observed p_T dependence at $\sqrt{s_{NN}} = 3$ GeV
 - At higher p_T than what is statistically accessible, one might expect a suppression of \overline{P}_Λ due to hard processes
- Such lack of dependence again seen in previous studies



Joseph R. Adams. Differential measurements of lambda polarization in au+au collisions and a search for the magnetic field by star. *Nuclear Physics A*, 1005:121864, 2021.

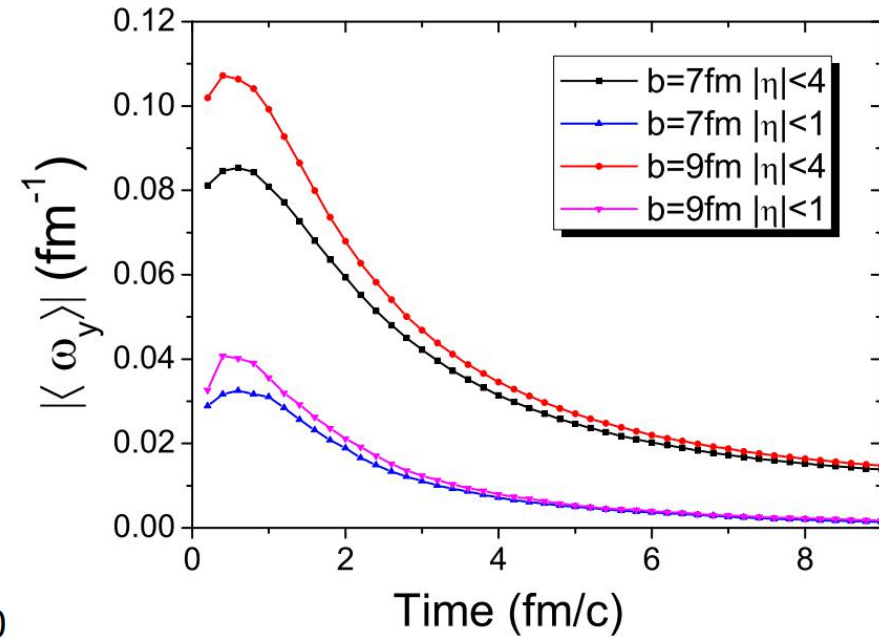
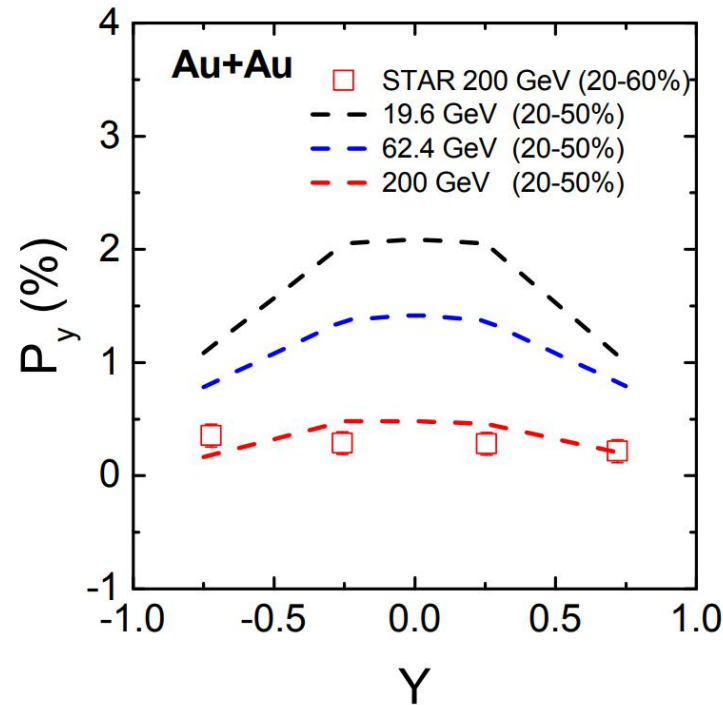
Jaroslav Adam et al. Global polarization of Λ hyperons in Au+Au collisions at $\sqrt{s_{NN}} = 200$ GeV. *Phys. Rev. C*, 98:014910, 2018. arXiv:1805.04400 [nucl-ex]

y dependence

- Many models predict strong dependence on rapidity y

y dependence

- Many models predict strong dependence on rapidity y
 - AMPT

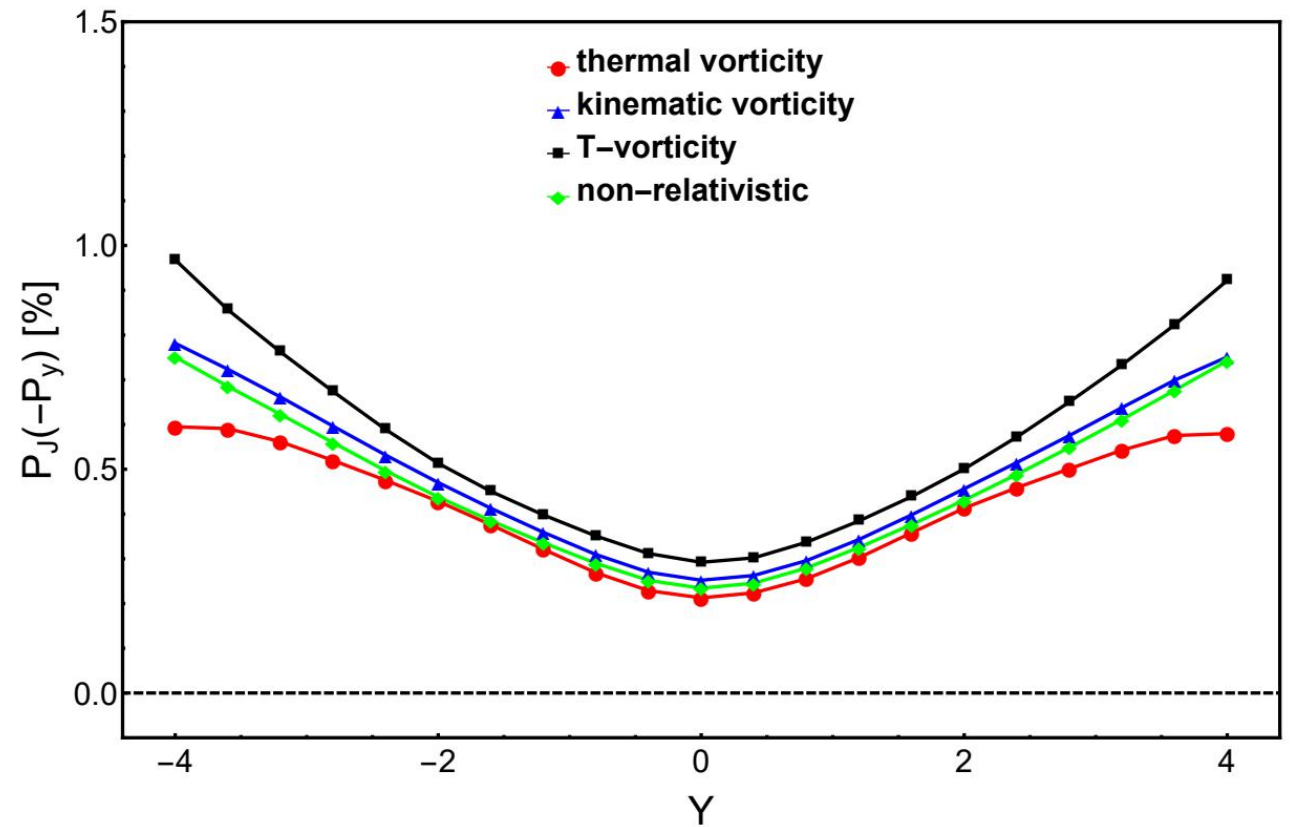


D.-X. Wei, W.-T. Deng, and X.-G. Huang, Phys. Rev. C **99**, 014905 (2019), arXiv:1810.00151 [nucl-th].

Y. Jiang, Z.-W. Lin, and J. Liao, Phys. Rev. C **94**, 044910 (2016), [Erratum: Phys.Rev.C 95, 049904(E) (2017)], arXiv:1602.06580 [hep-ph].

y dependence

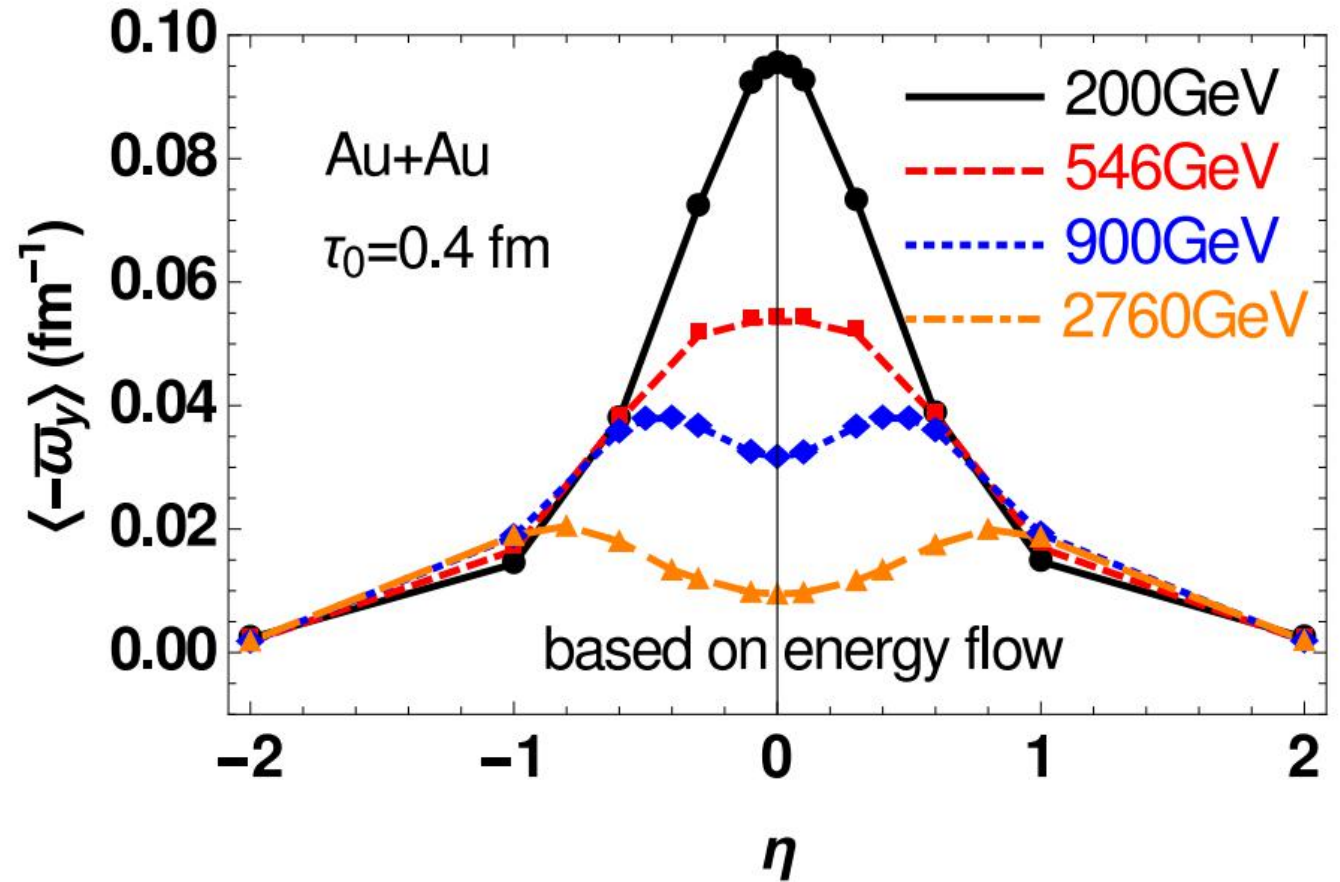
- Many models predict strong dependence on rapidity y
 - AMPT
 - Viscous hydro



H.-Z. Wu, L.-G. Pang, X.-G. Huang, and Q. Wang, Phys. Rev. Research. **1**, 033058 (2019), arXiv:1906.09385 [nucl-th].

y dependence

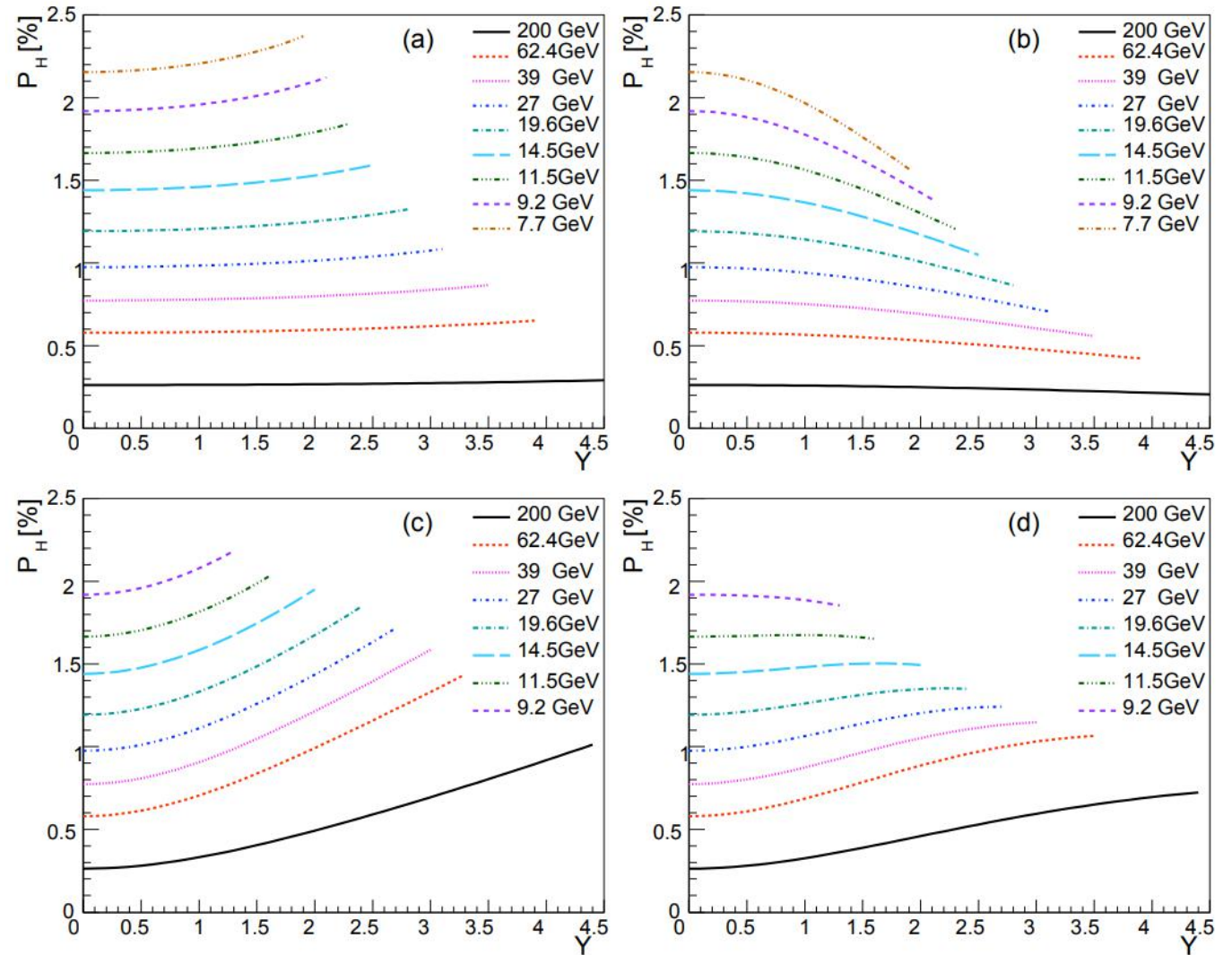
- Many models predict strong dependence on rapidity y
 - AMPT
 - Viscous hydro
 - HIJING



W.-T. Deng and X.-G. Huang, Phys. Rev. C **93**, 064907 (2016), arXiv:1603.06117 [nucl-th].

y dependence

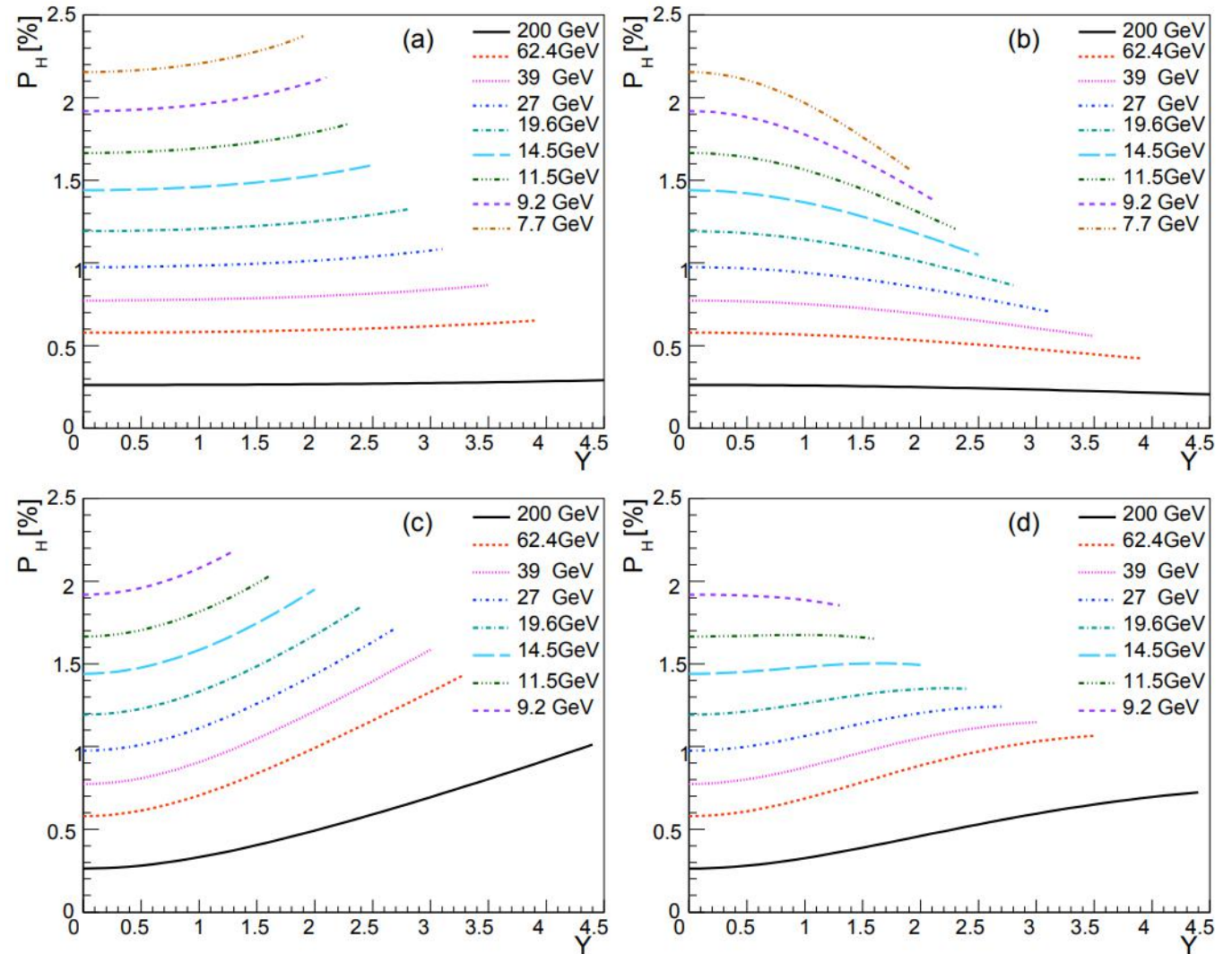
- Many models predict strong dependence on rapidity y
 - AMPT
 - Viscous hydro
 - HIJING
 - Geometric with different assumptions



Z.-T. Liang, J. Song, I. Upsal, Q. Wang, and Z.-B. Xu, Chin. Phys. C **45**, 014102 (2021), arXiv:1912.10223 [nucl-th].

y dependence

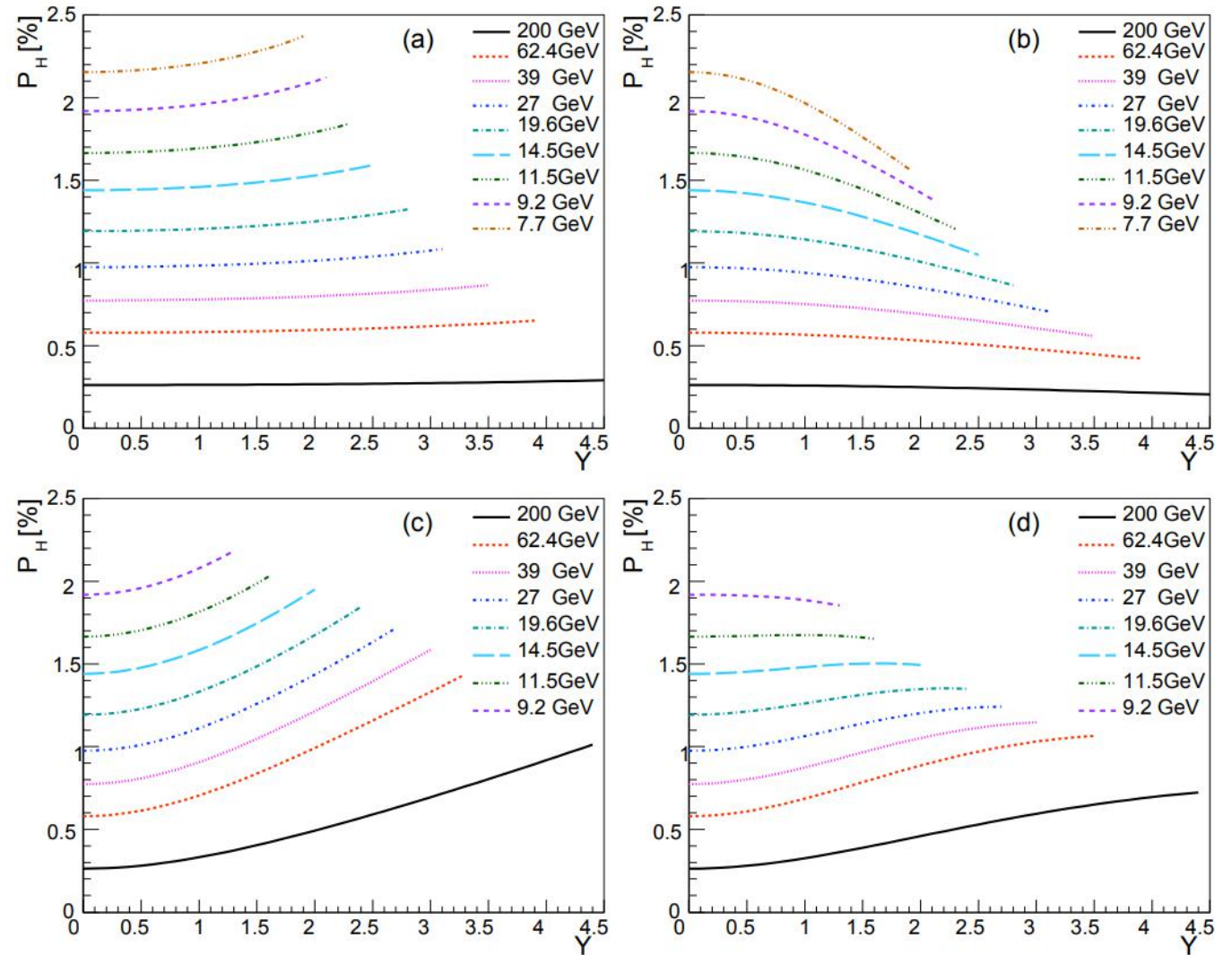
- Many models predict strong dependence on rapidity y
 - AMPT
 - Viscous hydro
 - HIJING
 - Geometric with different assumptions
 - And more!



Z.-T. Liang, J. Song, I. Upsal, Q. Wang, and Z.-B. Xu, Chin. Phys. C **45**, 014102 (2021), arXiv:1912.10223 [nucl-th].

y dependence

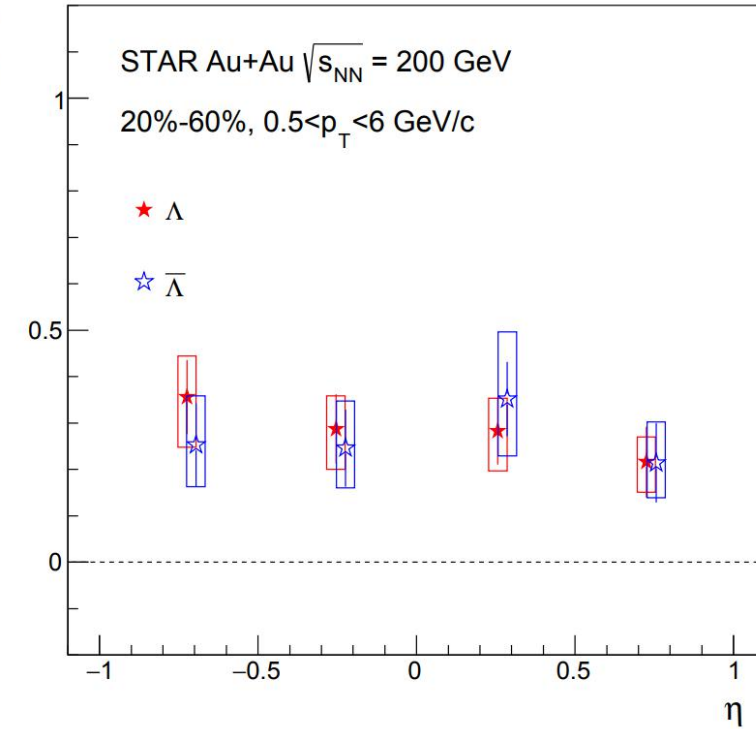
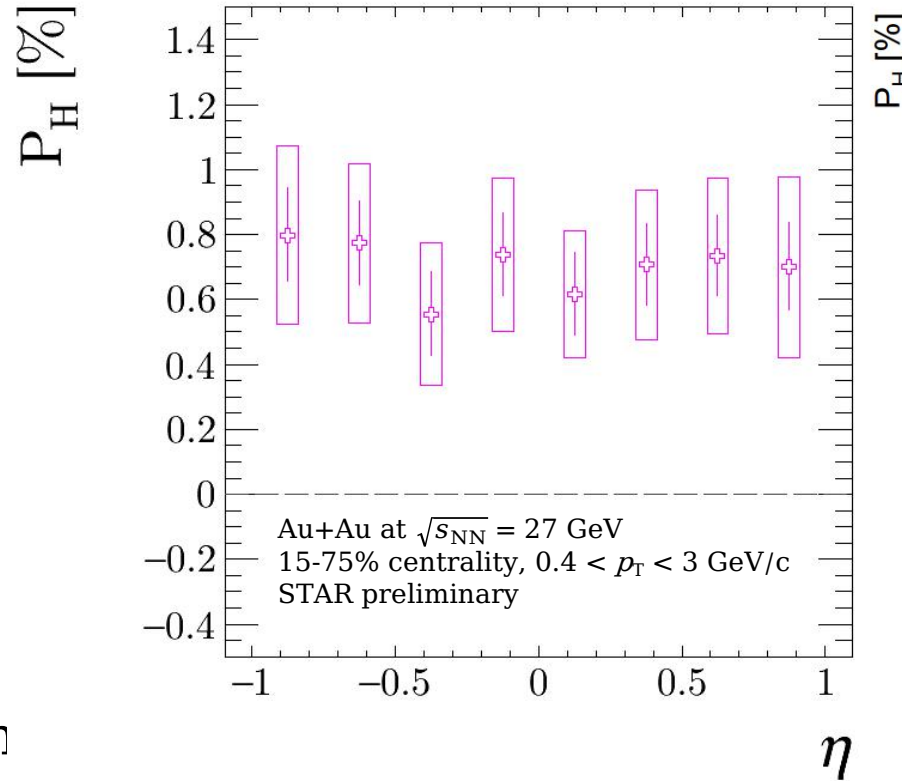
- Many models predict strong dependence on rapidity y
 - AMPT
 - Viscous hydro
 - HIJING
 - Geometric with different assumptions
 - And more!
- Most models predict more dramatic behavior at lower $\sqrt{s_{NN}}$



Z.-T. Liang, J. Song, I. Upsal, Q. Wang, and Z.-B. Xu, Chin. Phys. C **45**, 014102 (2021), arXiv:1912.10223 [nucl-th].

y dependence

- Many models predict strong dependence on rapidity y
 - AMPT
 - Viscous hydro
 - HIJING
 - Geometric with different assumptions
 - And more!
- Most models predict more dramatic behavior at lower $\sqrt{s_{NN}}$
- Previous studies saw no such dependence

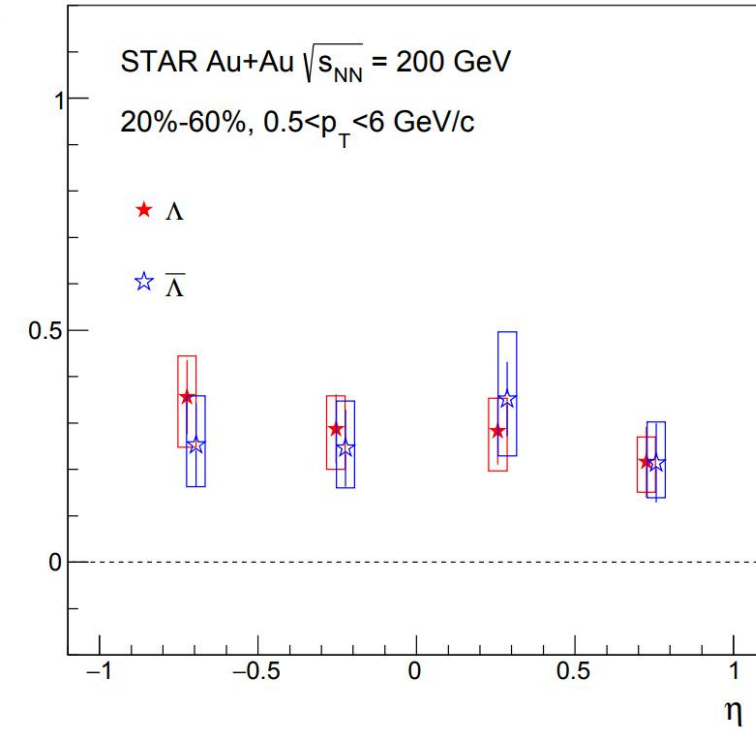
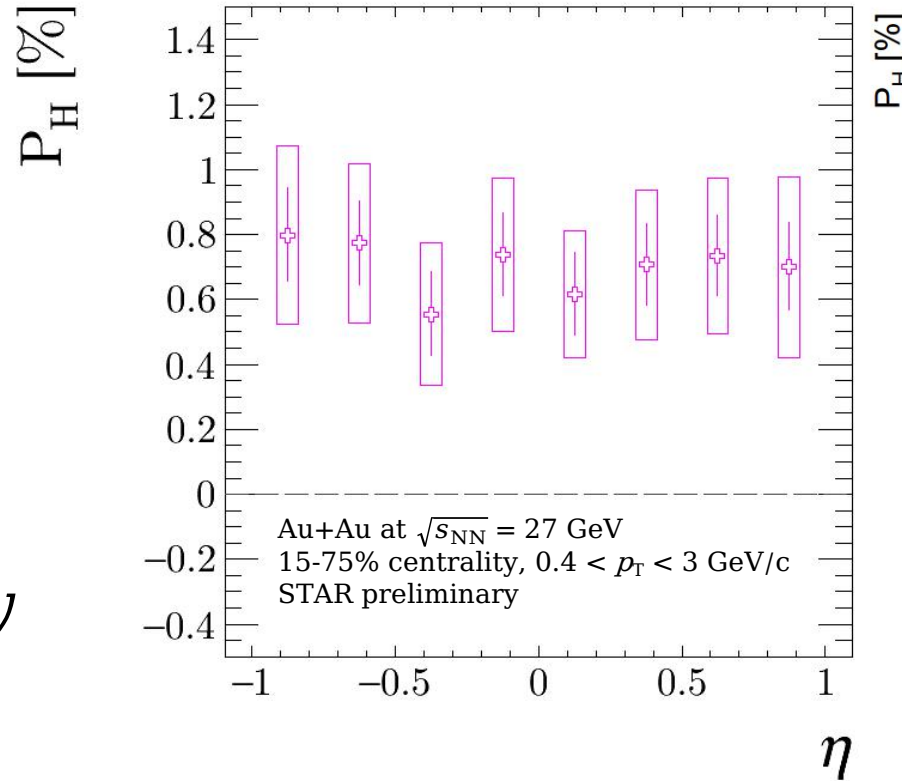


Joseph R. Adams. Differential measurements of lambda polarization in au+au collisions and a search for the magnetic field by star. *Nuclear Physics A*, 1005:121864, 2021.

Jaroslav Adam et al. Global polarization of Λ hyperons in Au+Au collisions at $\sqrt{s_{NN}} = 200$ GeV. *Phys. Rev. C*, 98:014910, 2018. arXiv:1805.04400 [nucl-ex]

y dependence

- Previous studies were limited by acceptance
 - Λ s at $|y| \approx |\eta| > 1$ inaccessible
- At $\sqrt{s_{NN}} = 3$ GeV the y distribution is narrow enough that even the most forward Λ s are reconstructed

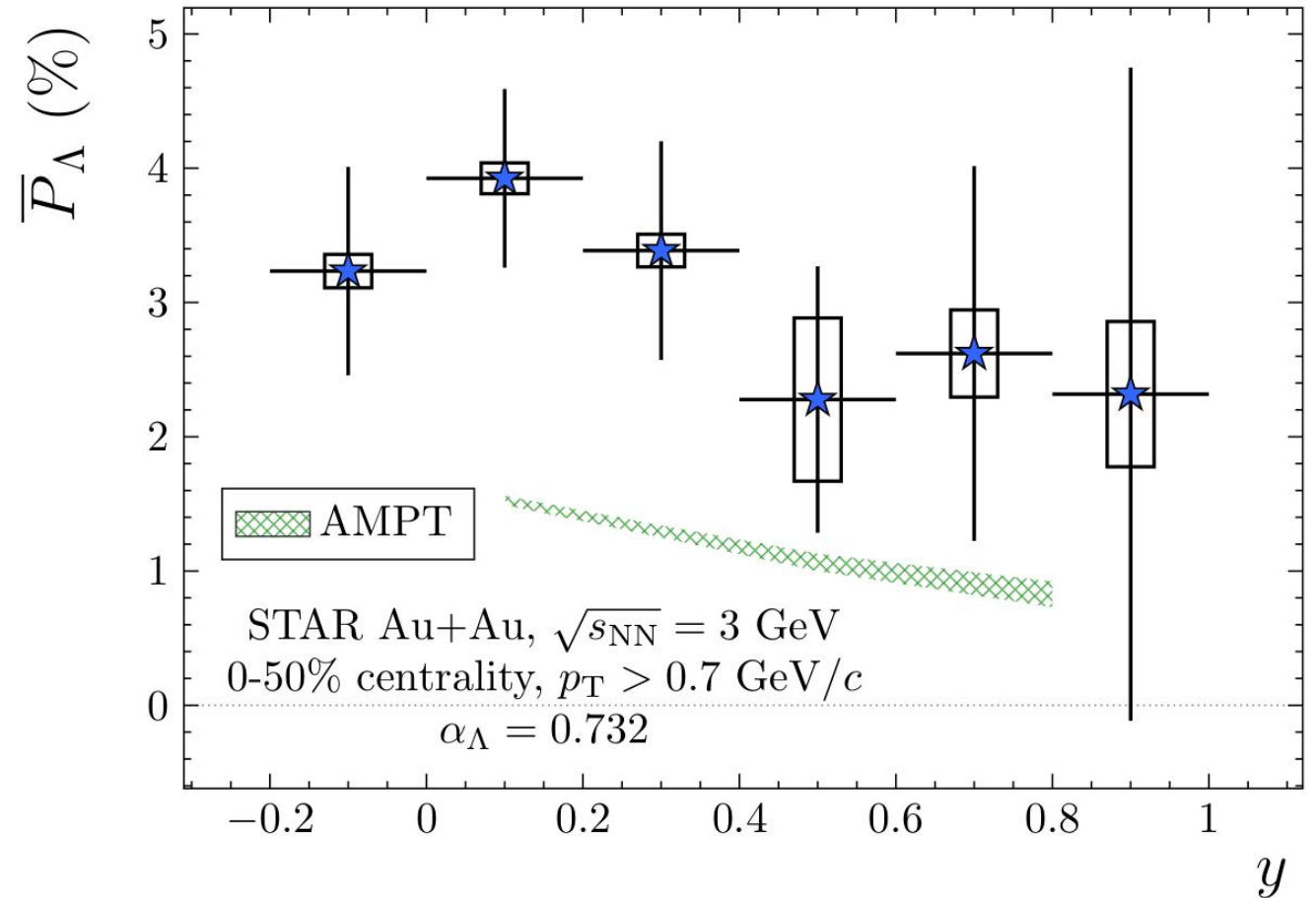


Joseph R. Adams. Differential measurements of lambda polarization in au+au collisions and a search for the magnetic field by star. *Nuclear Physics A*, 1005:121864, 2021.

Jaroslav Adam et al. Global polarization of Λ hyperons in Au+Au collisions at $\sqrt{s_{NN}} = 200$ GeV. *Phys. Rev. C*, 98:014910, 2018.

y dependence

- Previous studies were limited by acceptance
 - Λ s at $|y| \approx |\eta| > 1$ inaccessible
- At $\sqrt{s_{NN}} = 3$ GeV the y distribution is narrow enough that even the most forward Λ s are reconstructed
- Still, no observed dependence on y
 - The STAR forward upgrade will provide valuable supplemental studies



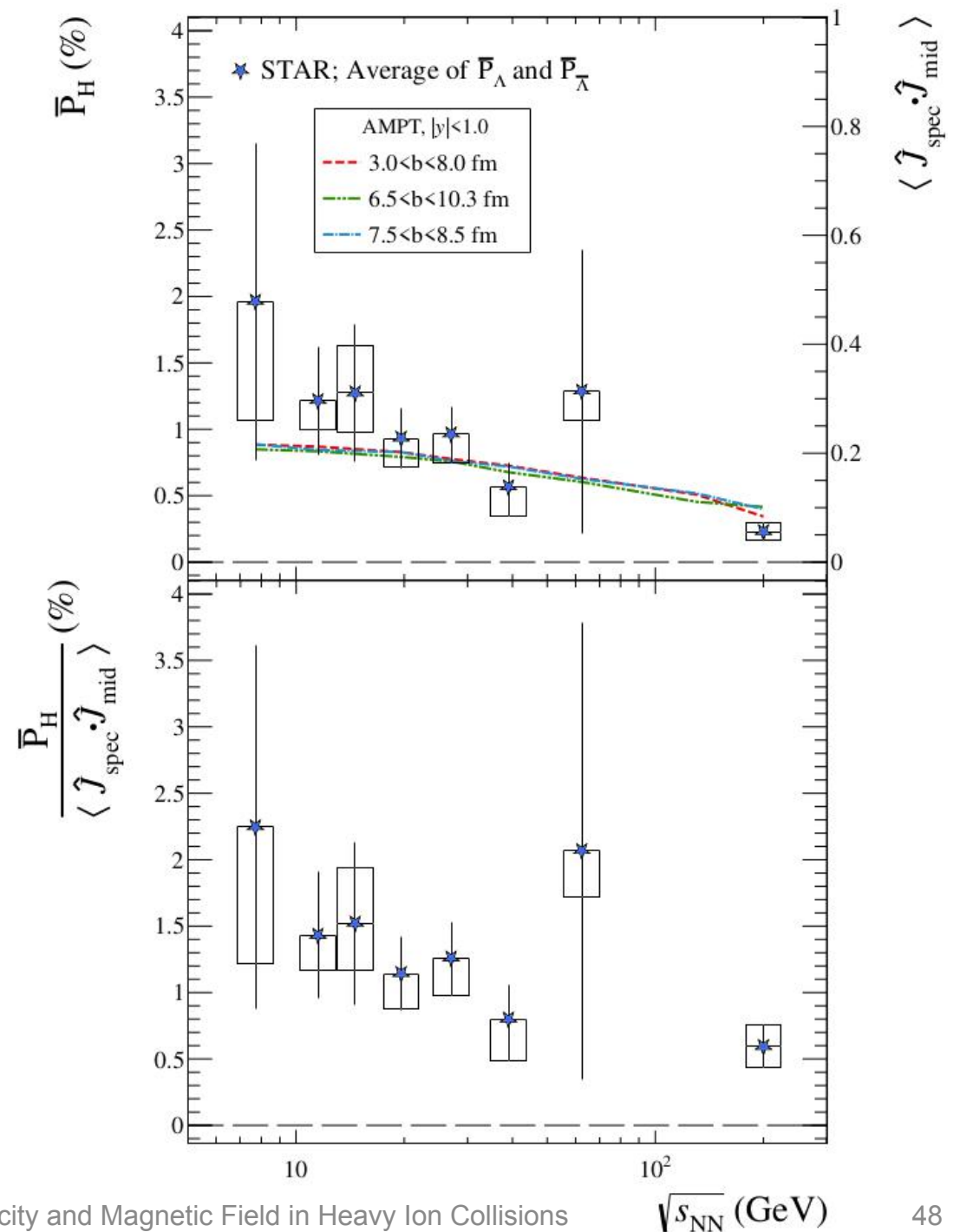
M. S. Abdallah et al. Global Λ -hyperon polarization in Au+Au collisions at $\sqrt{s_{NN}} = 3$ GeV. 7 2021.

arXiv:2108.00044 [nucl-ex]

y dependence

- Presumed y dependence sometimes used as an explanation for the dependence of \overline{P}_Λ on $\sqrt{s_{NN}}$
 - After all, system angular momentum increases with $\sqrt{s_{NN}}$ and therefore so should \overline{P}_Λ
- Very recent study shows such dependence due at least in part to initial-state fluctuations

Joseph R. Adams and Michael A. Lisa. Decorrelation of participant and spectator angular momenta in heavy-ion collisions. 9 2021. arXiv:2109.14726.



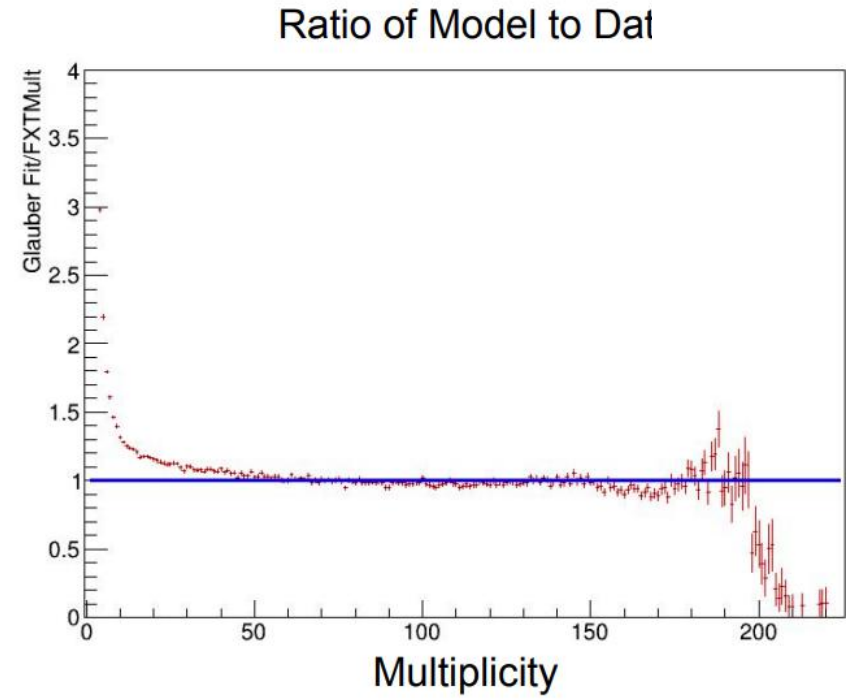
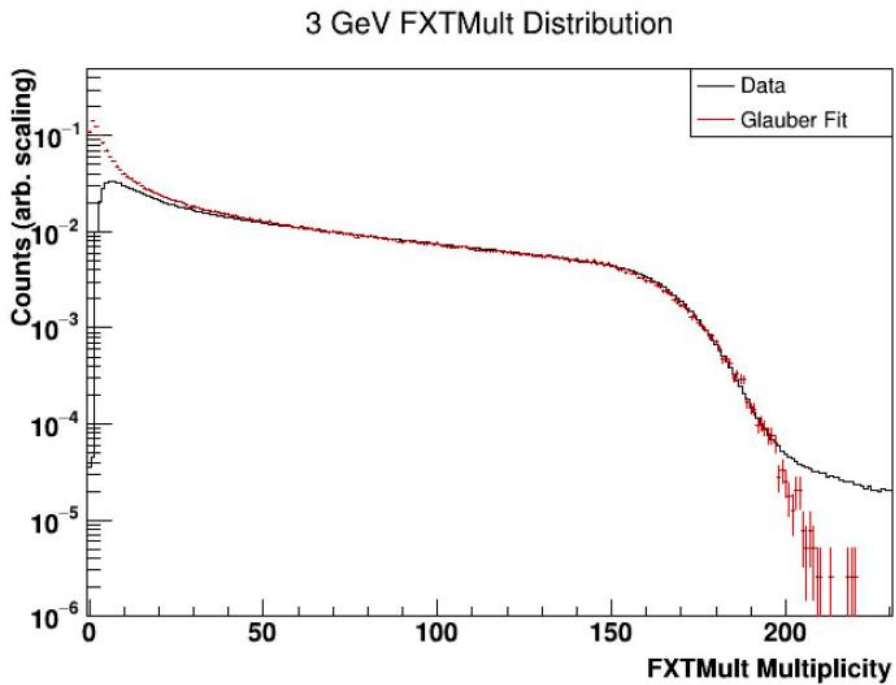
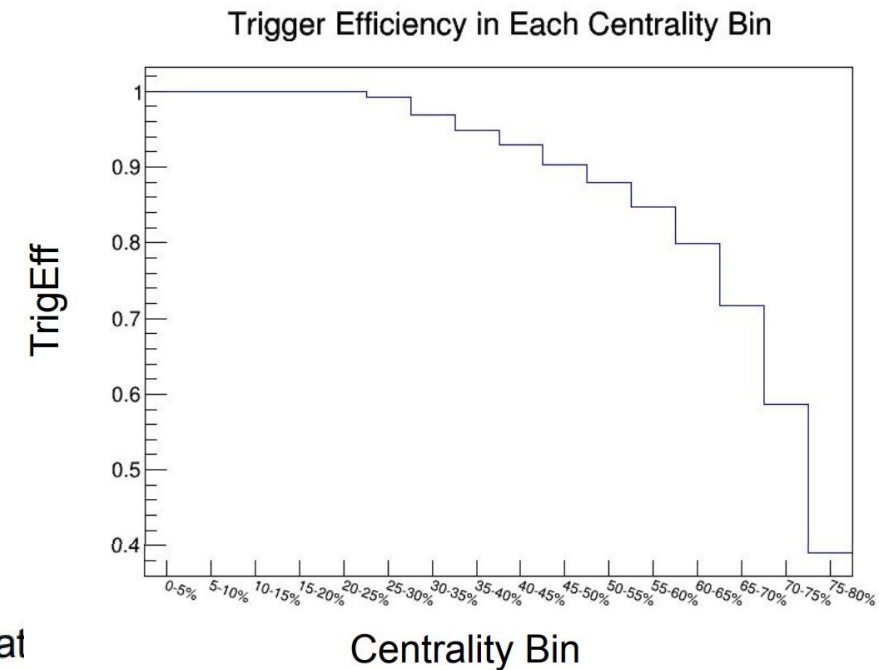
Summary

- A generalized invariant-mass method is introduced which is essential for STAR's fixed-target measurements of \bar{P}_Λ
 - This does not invalidate previous studies in collider mode where ν_1 is small and acceptance is symmetric in rapidity
- Measurement of \bar{P}_Λ at $\sqrt{s_{\text{NN}}} = 3$ GeV is largest and most-significant yet observed
- Measurement of \bar{P}_Λ vs. p_T and centrality are consistent with models, expectations, and previous measurements
- Measurement of \bar{P}_Λ vs. y is valuable at this collision energy due to acceptance of most-forward Λ
 - *No dependence seen, despite predictions from a wide variety of models!*
 - *STAR forward upgrade will provide crucial follow-up studies!*

BACKUP

Trigger efficiency corr.

- Zachary Sweger's study at https://drupal.star.bnl.gov/STAR/system/files/Sweger_3p0GeV_StandardNewest_fcv_2020Nov11.pdf



A_0 correction

- Recall the polarization definition
- Which, upon integration, yields
- Assuming a perfect detector, we get
- Without that assumption, we have

$$\frac{dN}{d \cos \theta^*} \sim 1 + \alpha_H P_H \cos \theta^* , \quad (1)$$

$$P_H = \frac{3}{\alpha_H} \langle \cos \theta^* \rangle . \quad (2)$$

$$P_H = \frac{8}{\pi \alpha_H} \langle \sin (\phi_p^* - \Psi_{\text{RP}}) \rangle . \quad (3)$$

$$\begin{aligned} \frac{8}{\pi \alpha_H} \langle \sin (\phi_p^* - \Psi_{\text{RP}}) \rangle &= \frac{4}{\pi} \overline{\sin \theta_p^*} P_H (p_t^H, \eta^H) - \frac{2}{\pi} \overline{\sin \theta_p^* \cos [2(\phi_H - \phi_p^*)]} P_H^{(2)} (p_t^H, \eta^H) \\ &= A_0(p_t^H, \eta^H) P_H (p_t^H, \eta^H) - A_2(p_t^H, \eta^H) P_H^{(2)} (p_t^H, \eta^H), \end{aligned} \quad (9)$$

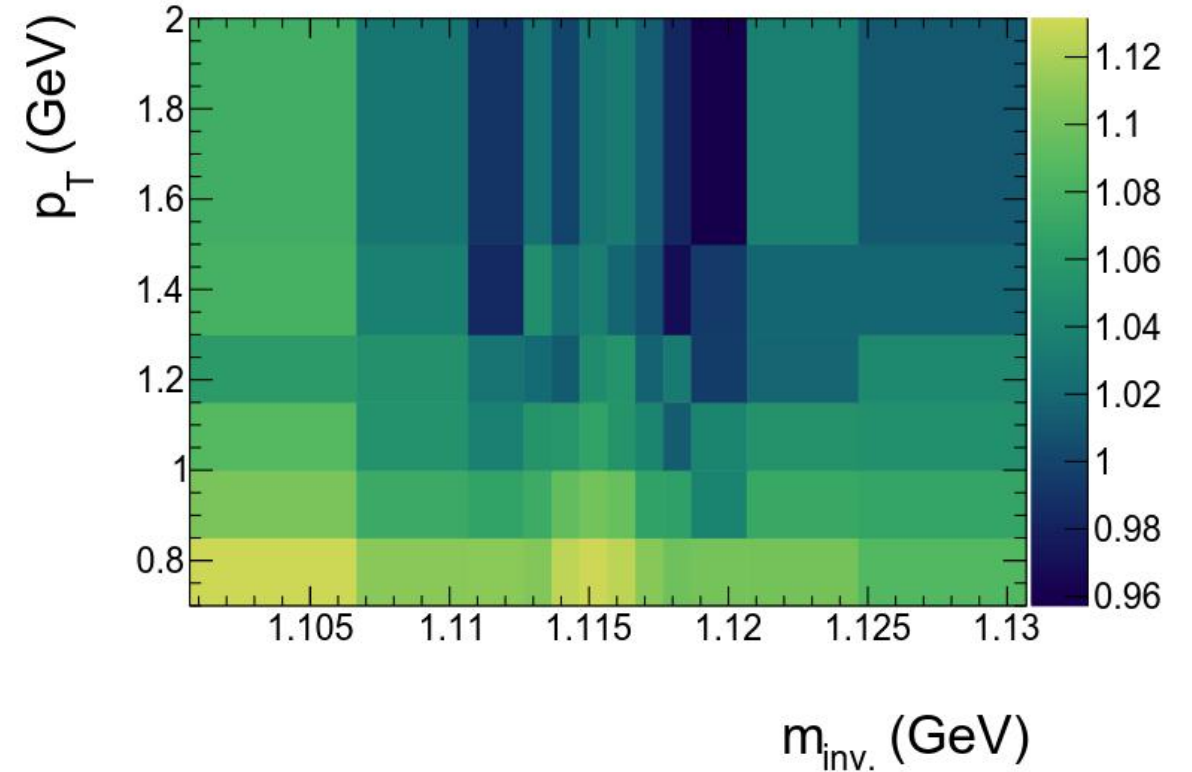
where functions $A_0(p_t^H, \eta^H)$ and $A_2(p_t^H, \eta^H)$ are defined by the average of $\sin \theta_p^*$ and $\sin \theta_p^* \cos [2(\phi_H - \phi_p^*)]$ over detector acceptance according to equations:

$$A_0(p_t^H, \eta^H) = \frac{4}{\pi} \overline{\sin \theta_p^*} \equiv \frac{4}{\pi} \int \frac{d\Omega_p^*}{4\pi} \frac{d\phi_H}{2\pi} A(\mathbf{p}_H, \mathbf{p}_p^*) \sin \theta_p^* . \quad (10)$$

$$A_2(p_t^H, \eta^H) = \frac{2}{\pi} \overline{\sin \theta_p^* \cos [2(\phi_H - \phi_p^*)]} \equiv \frac{2}{\pi} \int \frac{d\Omega_p^*}{4\pi} \frac{d\phi_H}{2\pi} A(\mathbf{p}_H, \mathbf{p}_p^*) \sin \theta_p^* \cos [2(\phi_H - \phi_p^*)] . \quad (11)$$

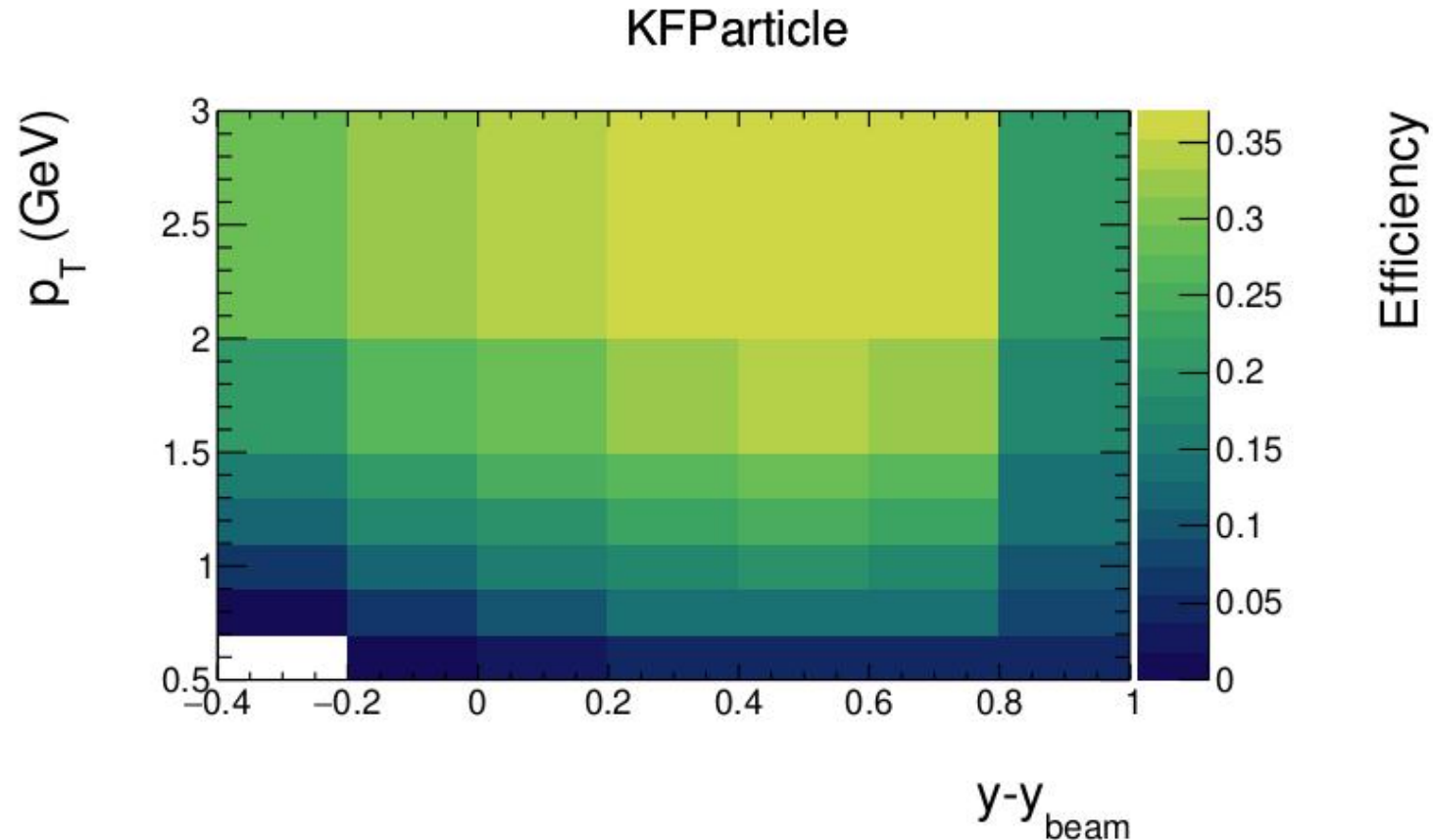
A_0 correction

- A_0 depends on $m_{inv.}$ as well as each differential variable, and we correct accordingly



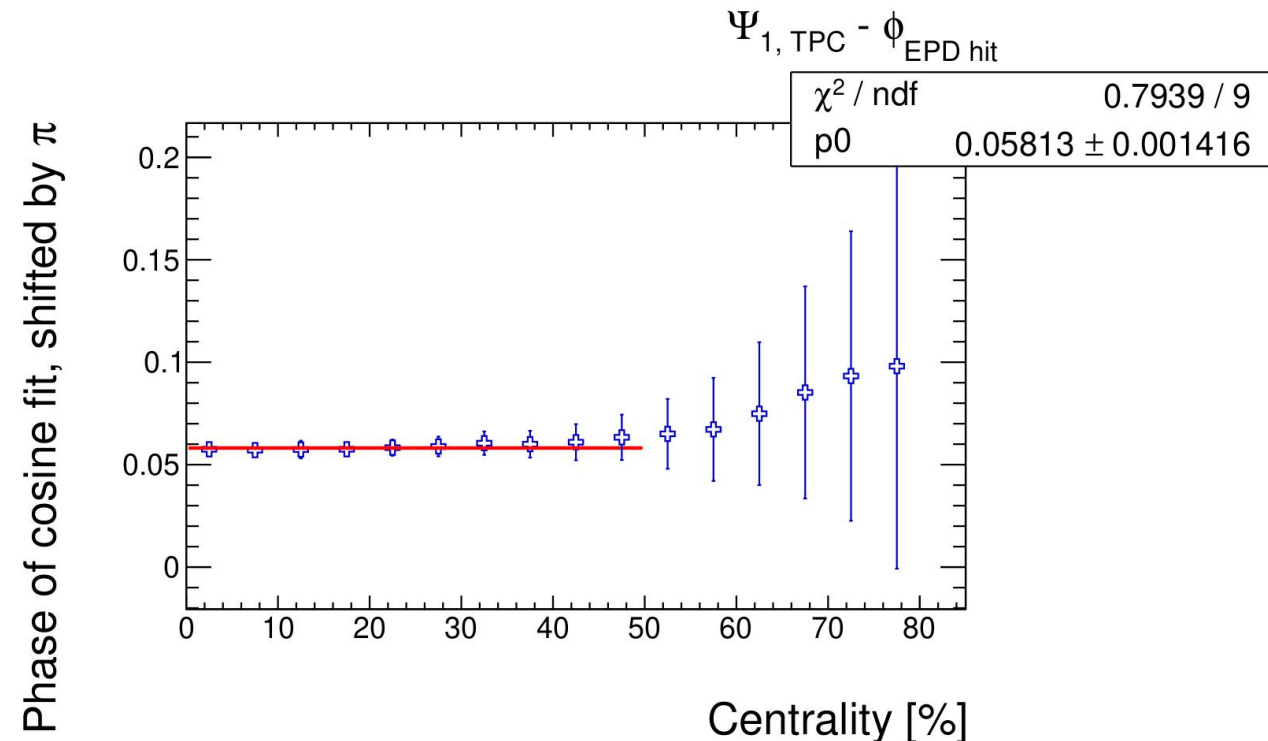
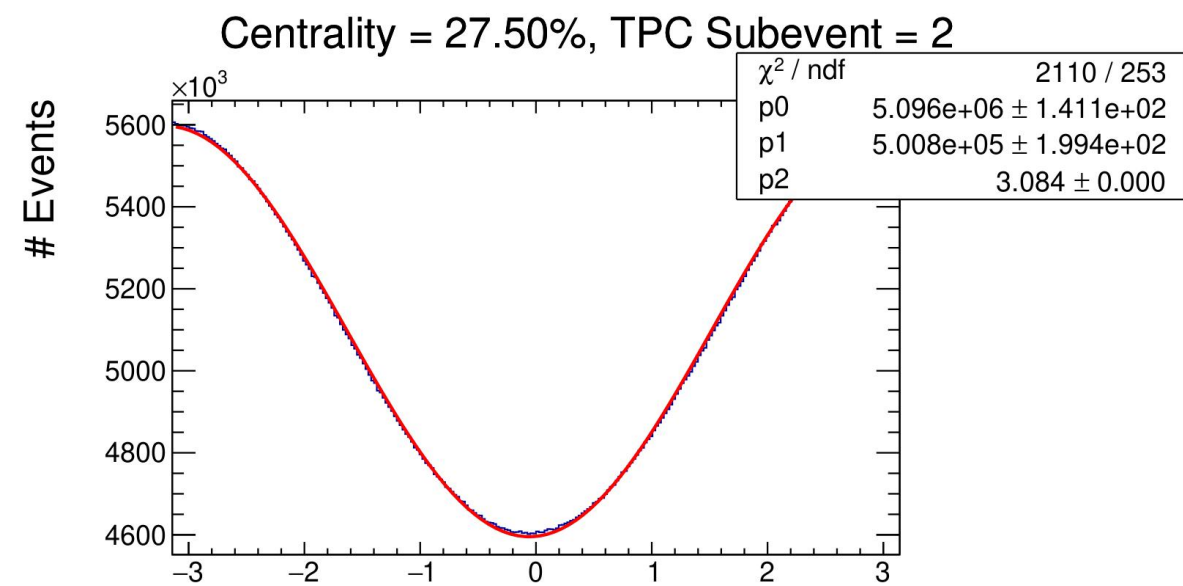
ε correction

- Using 1M embedded Λ s, we extract $\varepsilon(p_T, y)$
 - Embedding sample provided by Yue-Hang Leung
- $\varepsilon^{-1}(p_T, y)$ is used as a weight when filling \overline{P}_Λ profile histograms
- This needs to be calculated separately for every method when searching for systematic mistakes with $\Delta\overline{P}_\Lambda$



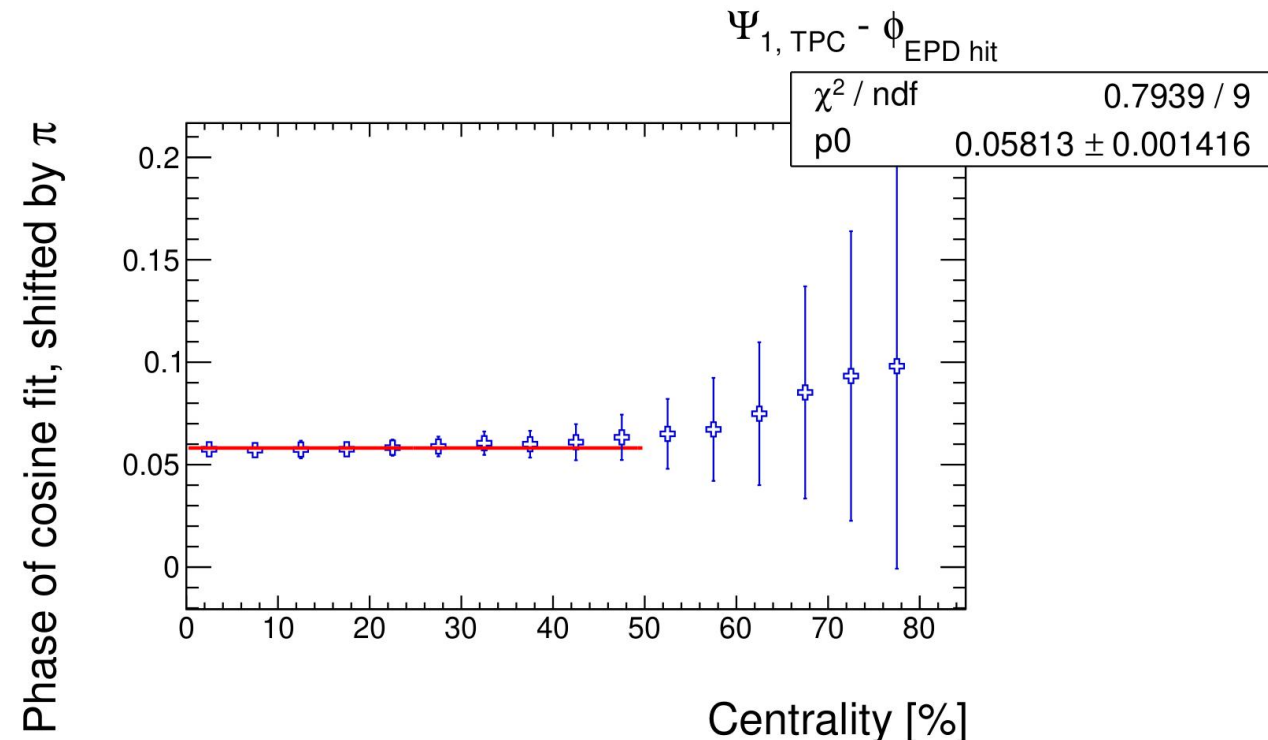
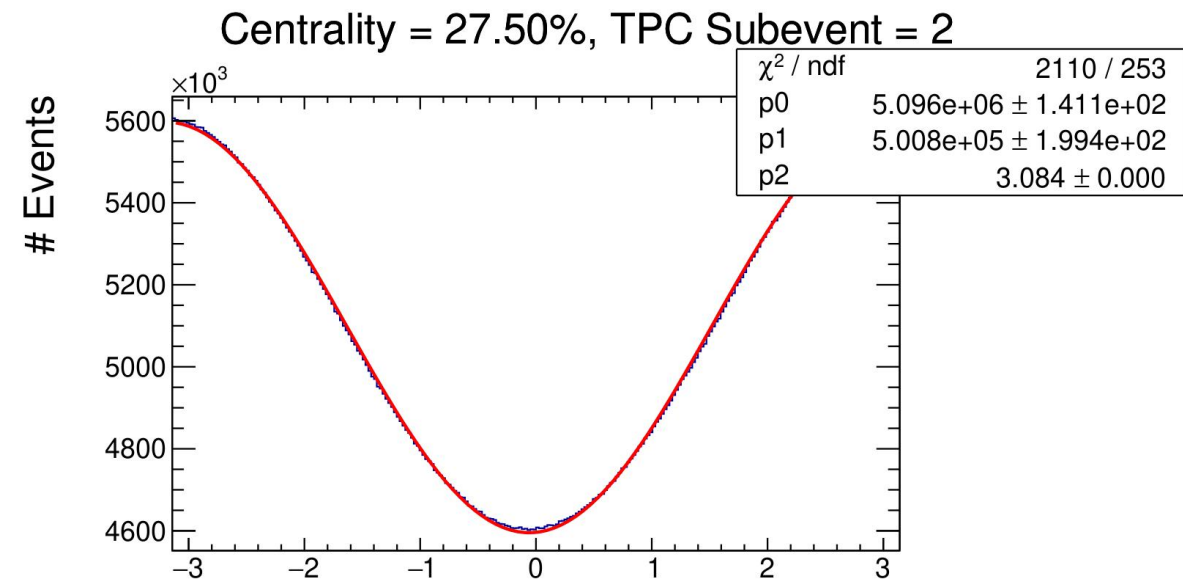
$\Delta\Psi_1$, EPD, \vec{B}_{STAR} correc.

- \vec{B}_{STAR} causes charged-track rotation, an effect for which the TPC can correct when calculating Ψ_1 through tracking
- The EPD cannot know φ_{DCA} and therefore suffers a rotation $\Delta\Psi_1$; this is especially pronounced at low energies where produced particles are mostly positively charged
- When calculating $\Psi_{1, \text{EPD}}$, we must correct for this effect



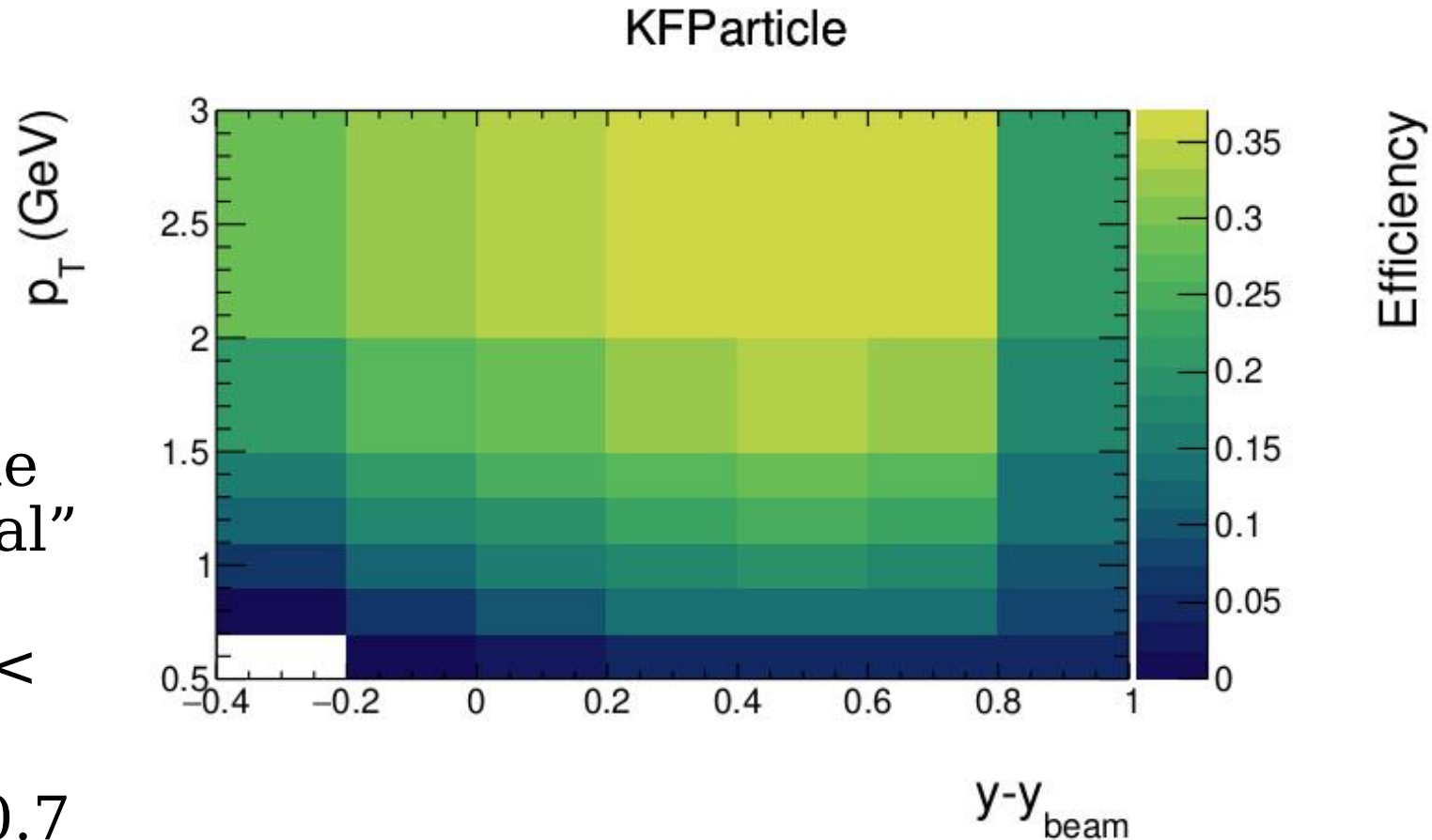
New centrality cut

- When correcting for this effect, we see a dependence of the correction on centrality, and this becomes stronger above 50% centrality
- Furthermore, when checking for stability in $R_{EP}^{(1)}$ while changing TPC reference subevents, we noticed instability above 50% centrality
- Lambda yield is anyways very low above 50% centrality, so we simply tighten the centrality cut
 - Previously was 60% for diff. meas.



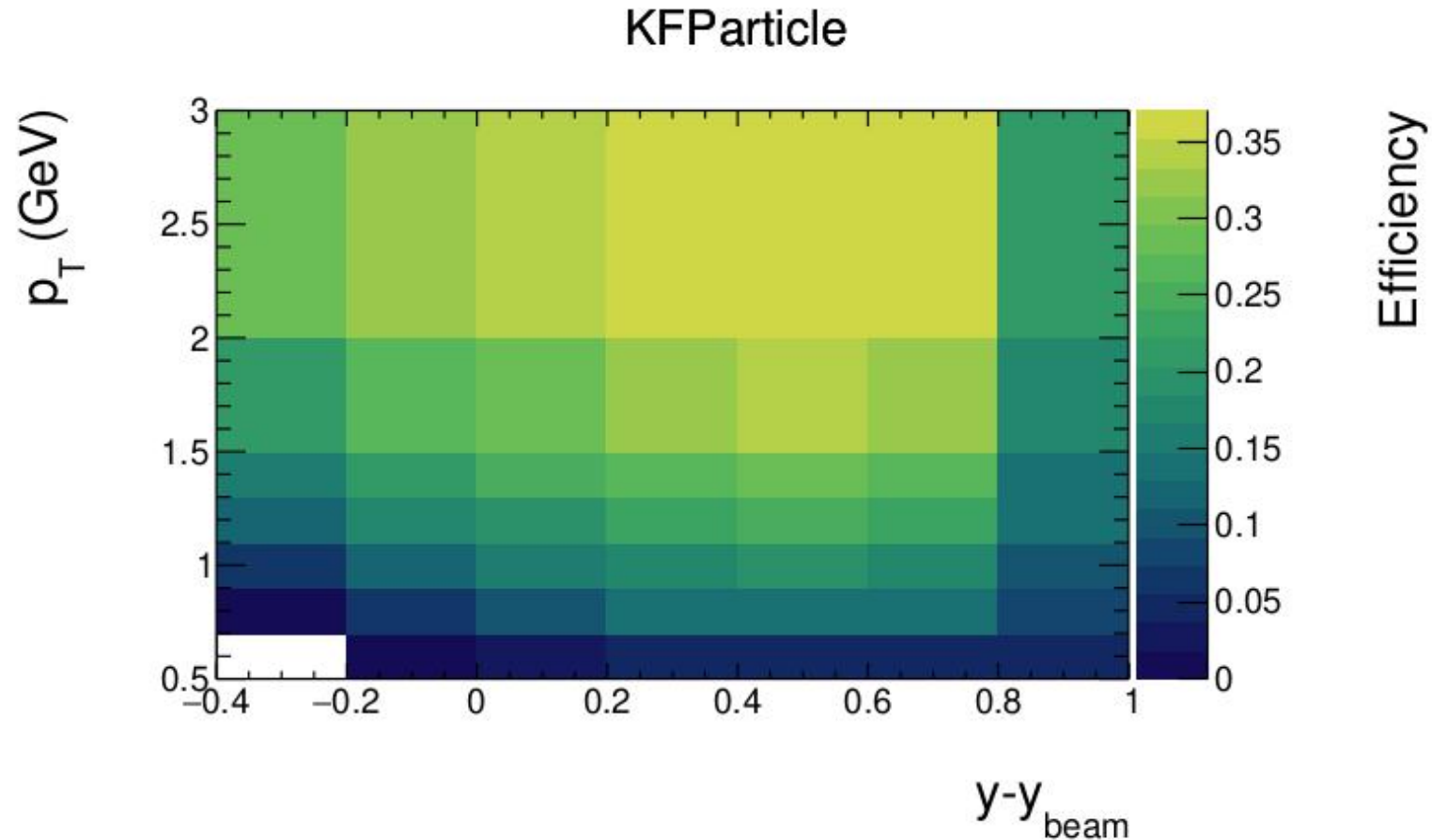
New p_T cut

- Efficiency corrections for $p_T < 0.7$ GeV become very large (order of magnitude larger than the average)
- More importantly, when checking for systematic mistakes through varying the Λ -finding algorithm (“manual” vs. KFParticle, varying topological cuts), \bar{P}_Λ at $p_T < 0.7$ GeV was unstable
- We therefore require $p_T > 0.7$ GeV
 - Previously no cut, dominated by $p_T > 0.4$ GeV



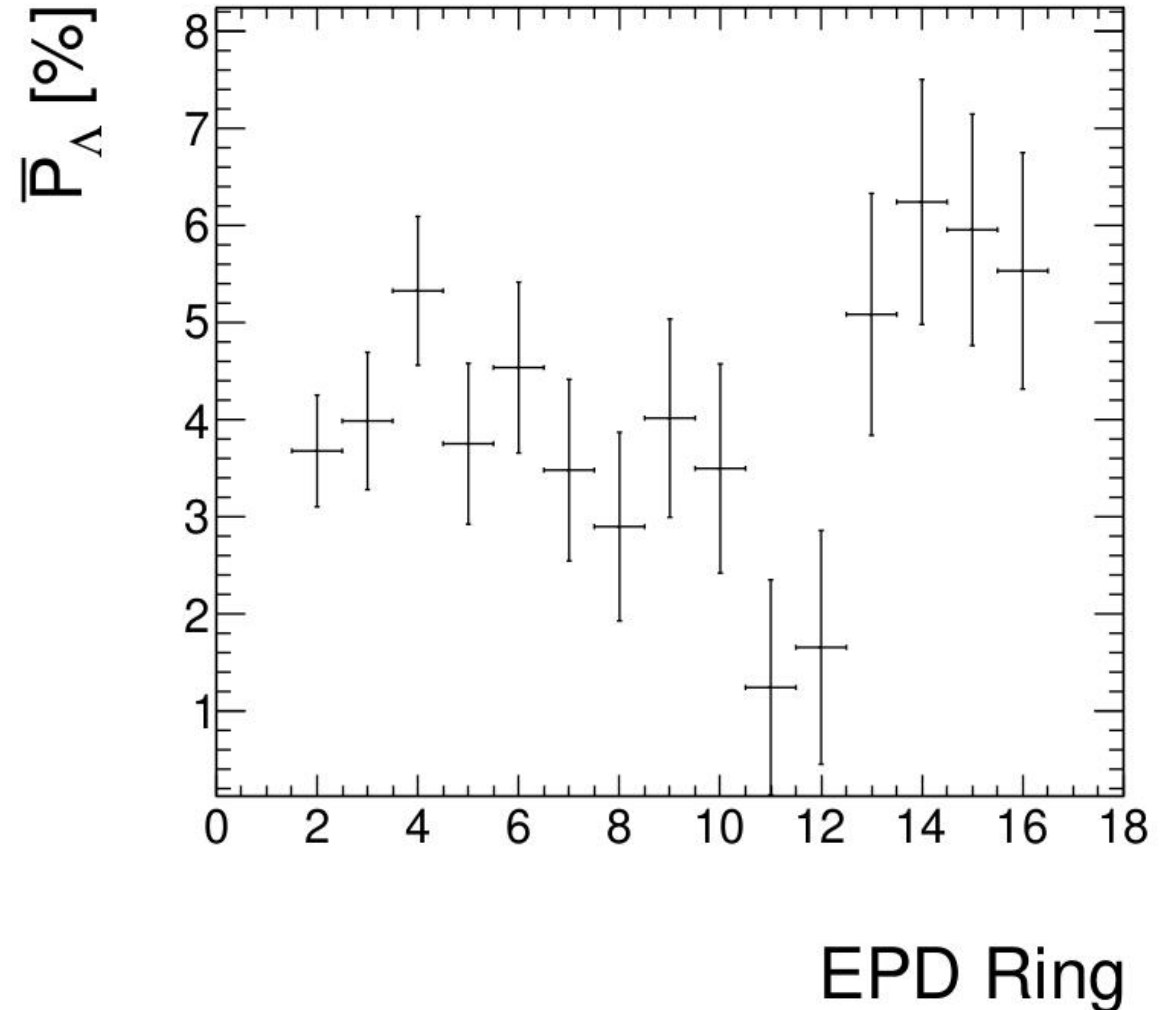
New y cut

- Efficiency corrections for $y < 0.2$ are large at low p_T
- More importantly, comparing integrated 0-50% centrality \overline{P}_Λ to the average obtained by fitting differential measurements with a pol0, or such pol0 fits to each other, there was a discrepancy when including the region $y < -0.2$
- We therefore require $y > -0.2$
 - Previously used $y > -0.4$



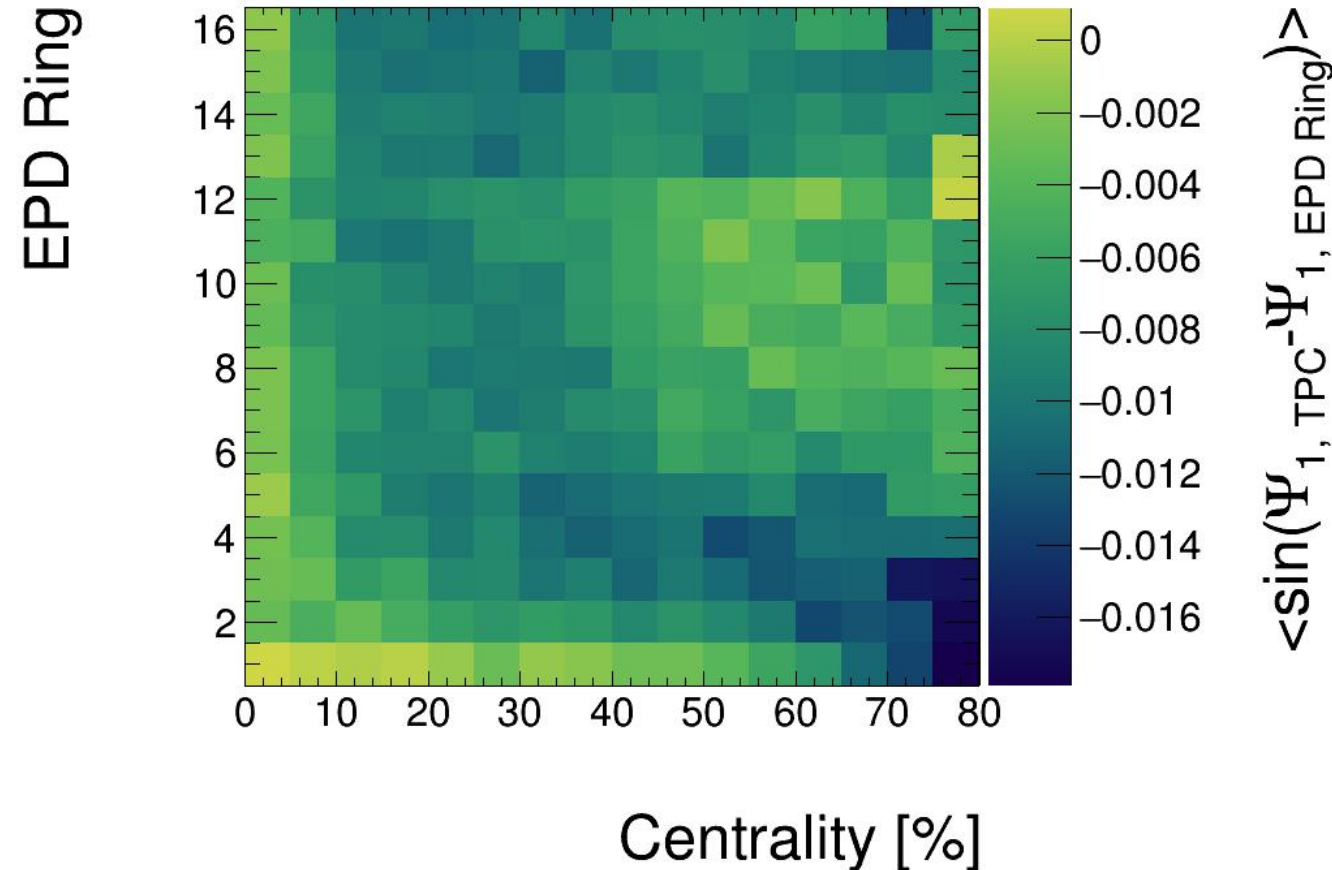
New EPD subevent

- When checking for systematic mistakes, we found a significant dependence of polarization on EPD ring in contrast to our expectations
- When looking at Ψ_1 correlations between EPD Rings and the TPC, we found a jump between rings 12 and 13, and a strange centrality dependence for rings below 13



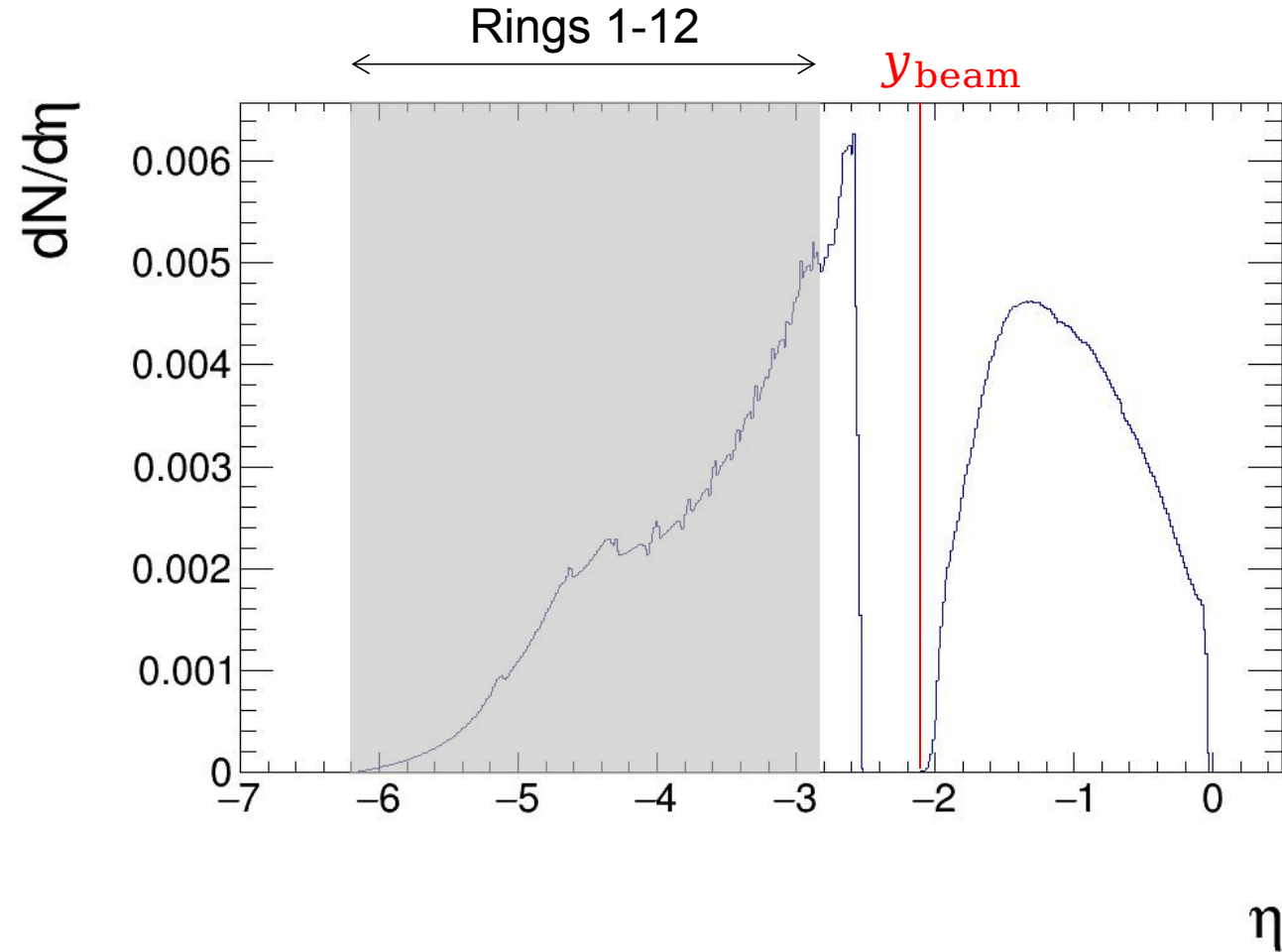
New EPD subevent

- When checking for systematic mistakes, we found a significant dependence of polarization on EPD ring in contrast to our expectations
- When looking at Ψ_1 correlations between EPD Rings and the TPC, we found a jump between rings 12 and 13, and a strange centrality dependence for rings below 13



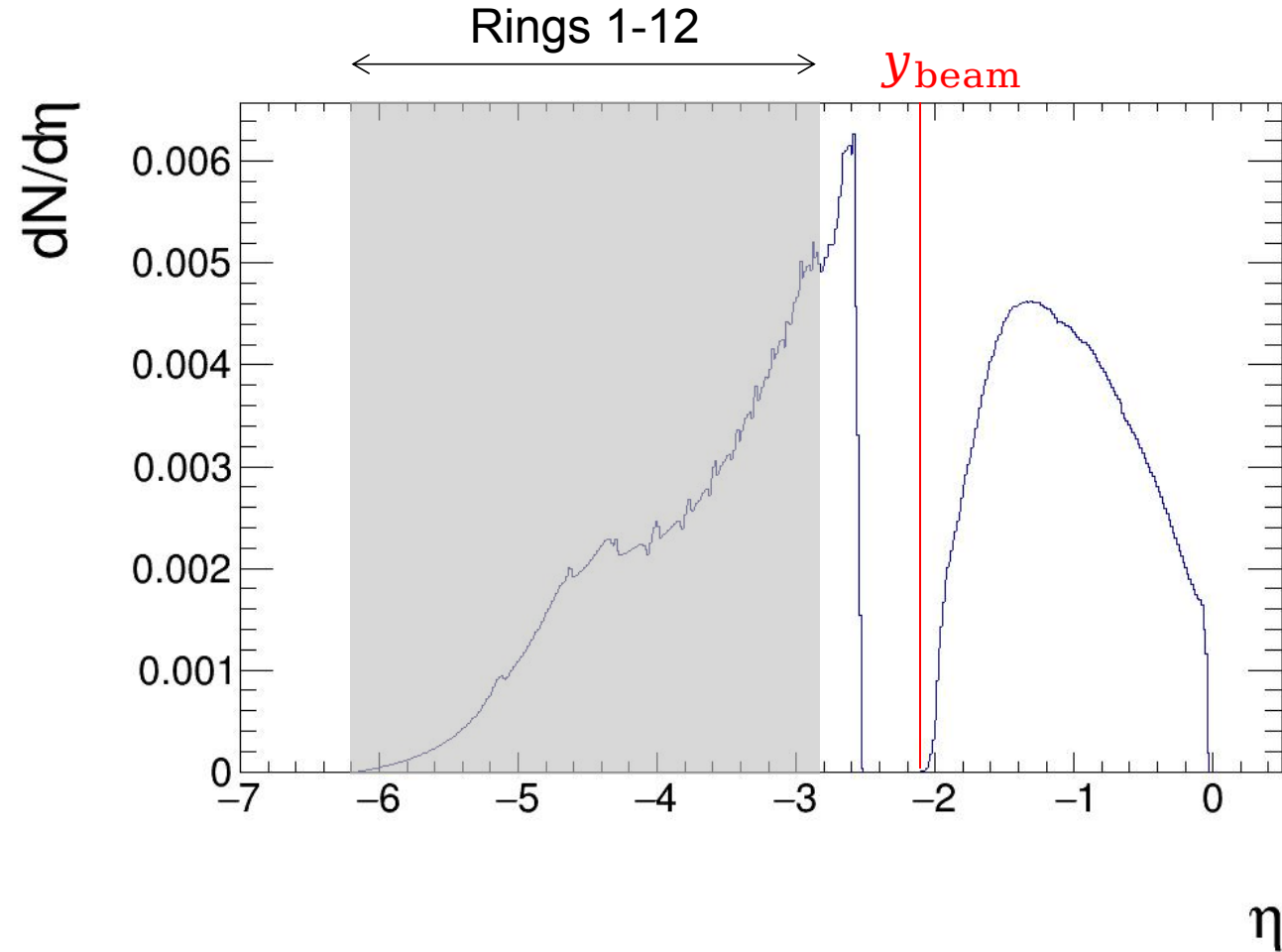
New EPD subevent

- Additionally, when checking for consistency in $R_{EP}^{(1)}$ while switching TPC subevents, rings 12 and below were unstable
- There is also anomalous behavior in $dN/d\eta$ at Ring 12
- Ultimately this behavior is not understood, but particles so far forward of y_{beam} may be questionable to begin with



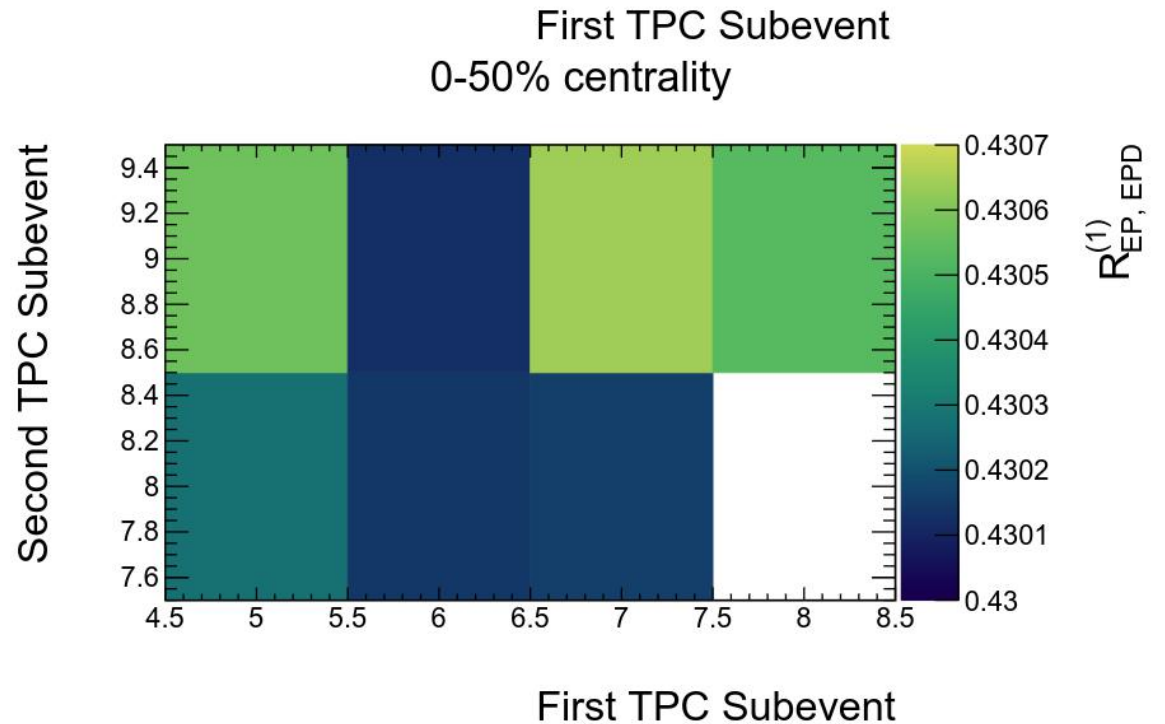
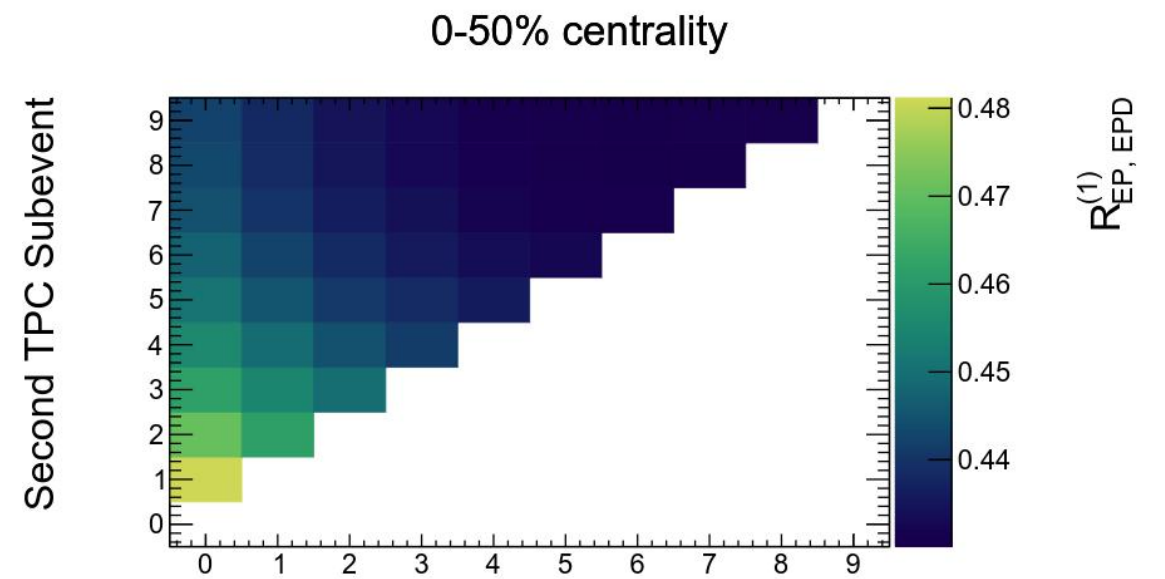
New EPD subevent

- For these reasons (and anyways because we want a smaller subevent to avoid momentum-conservation effects) we restrict ourselves to Rings 13-16
 - Previously used $-2.9 < \eta < -2.6$



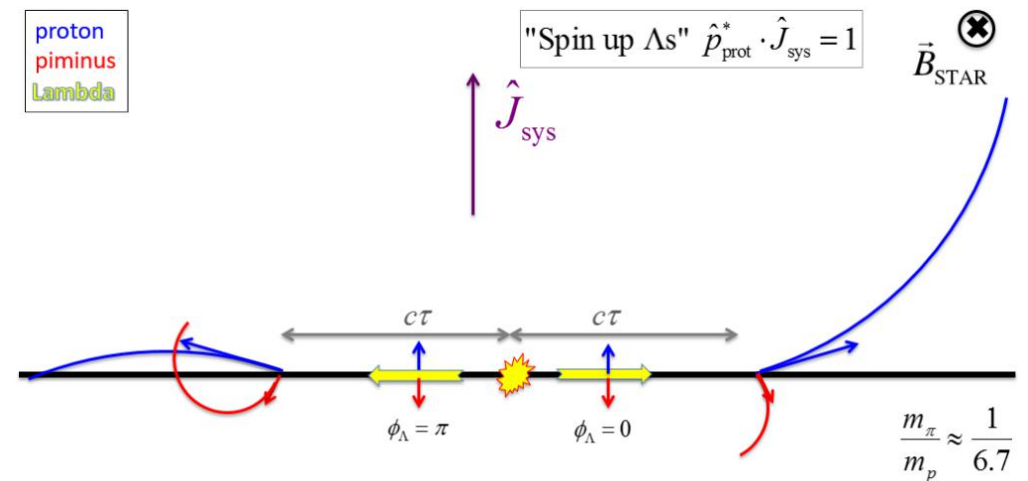
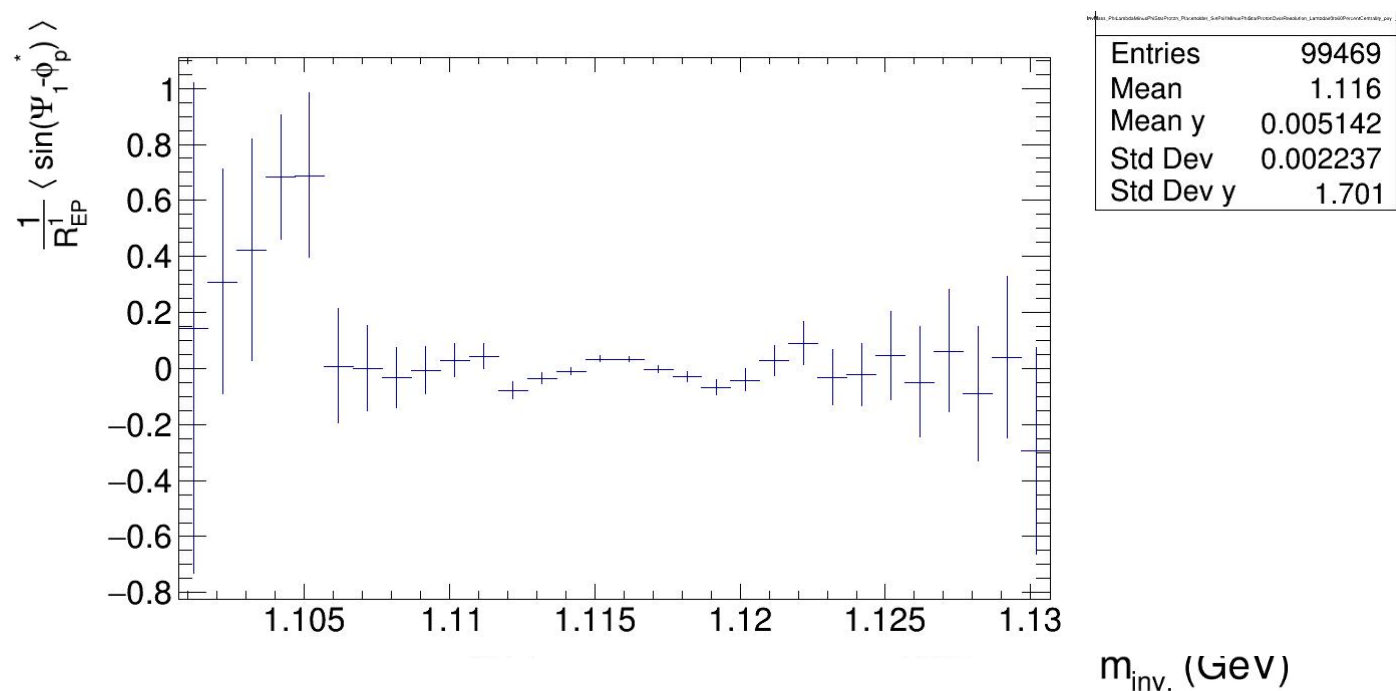
New TPC subevents

- When choosing TPC subevents, we want to avoid non-flow correlations
- Absent non-flow correlations, $R_{EP}^{(1)}$ should not depend on the choice of reference subevents
- In the region shown below, $R_{EP}^{(1)}$ is stable and the choice is therefore arbitrary; we choose reference subevents 5 and 8, corresponding to $-0.5 < \eta < -0.4$ and $-0.2 < \eta < -0.1$
 - Previously used EPD $-3.9 < \eta < -3.3$ and TPC $-0.7 < \eta < -0.4$



Further comments on the AEE

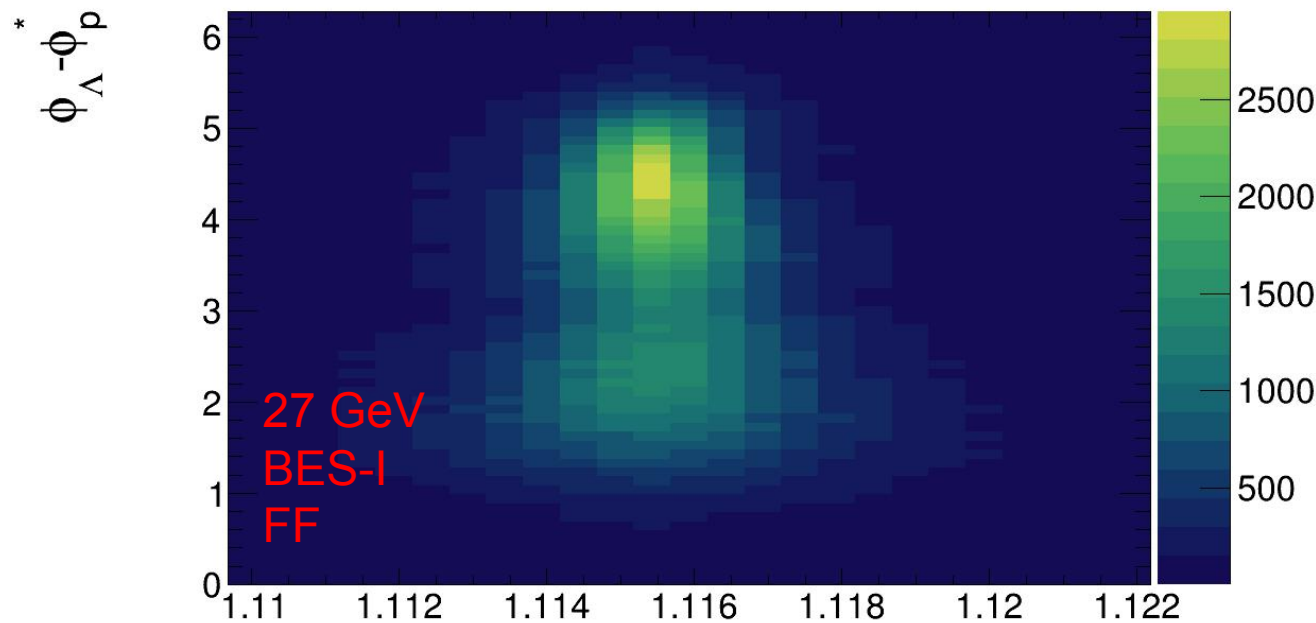
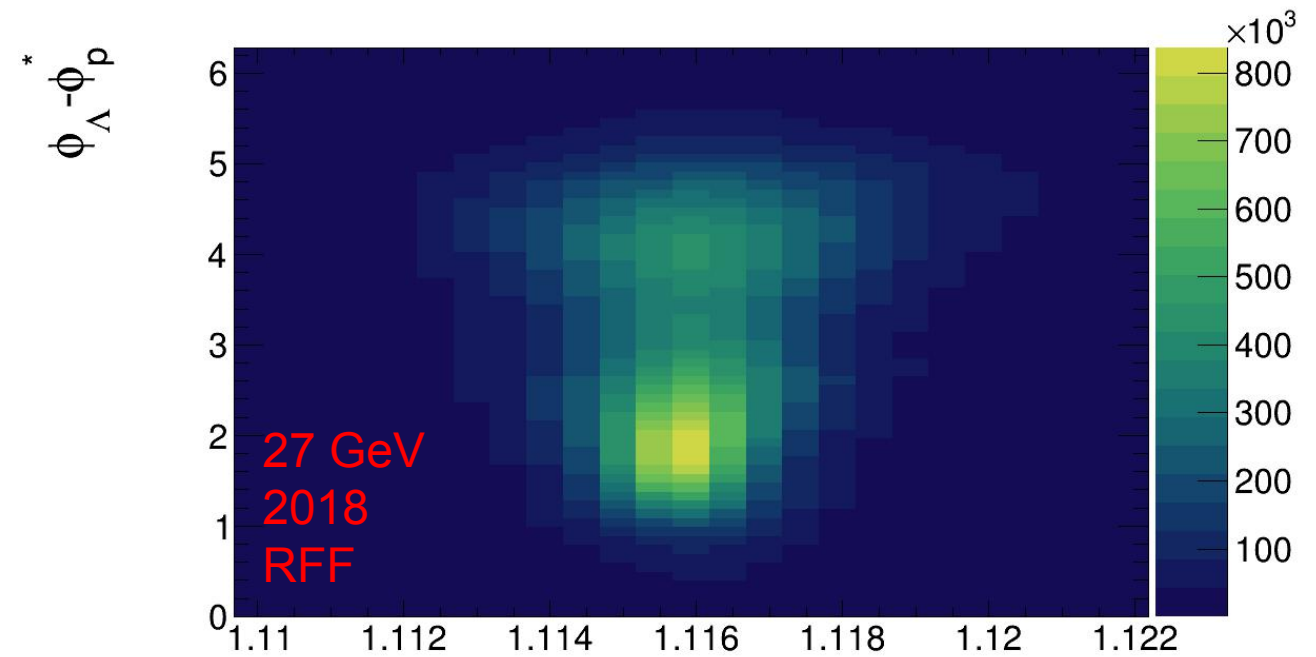
- Not only do we have broader invariant mass distributions for $\varphi_\Lambda - \varphi_p^* > \pi$, we also measure fewer Lambdas
- Since embedded Lambdas have no background, we can take a simple average of \bar{P}_Λ over $m_{inv.}$ for all Lambdas without doing the invariant-mass method. This can potentially explain why that average is non-zero
- This can potentially be explained by the “spin efficiency”



The “efficiency” of measuring a “spin-up Lambda” at $\phi=0$ is different than that at $\phi=\pi$.
 * due to cuts

Further comments on the AEE

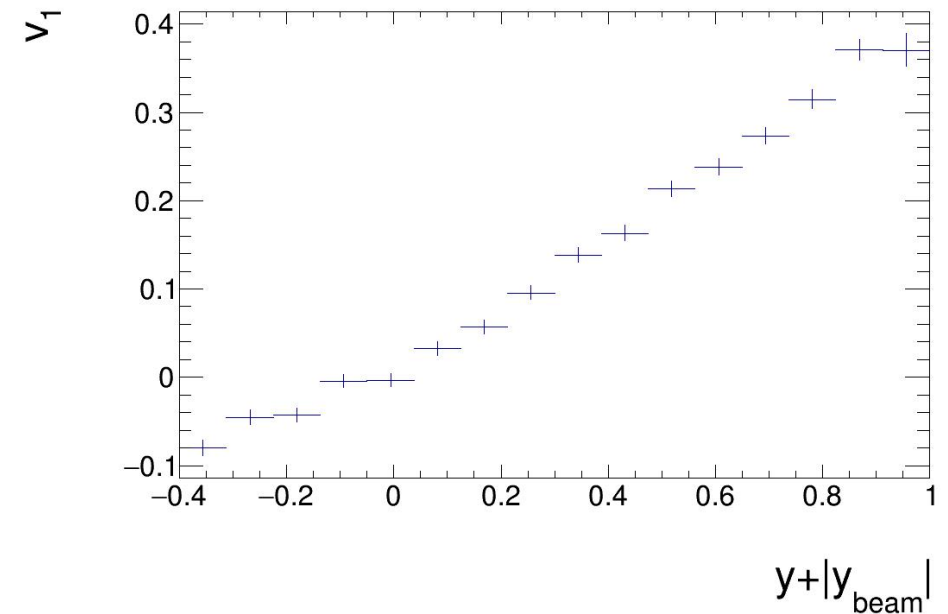
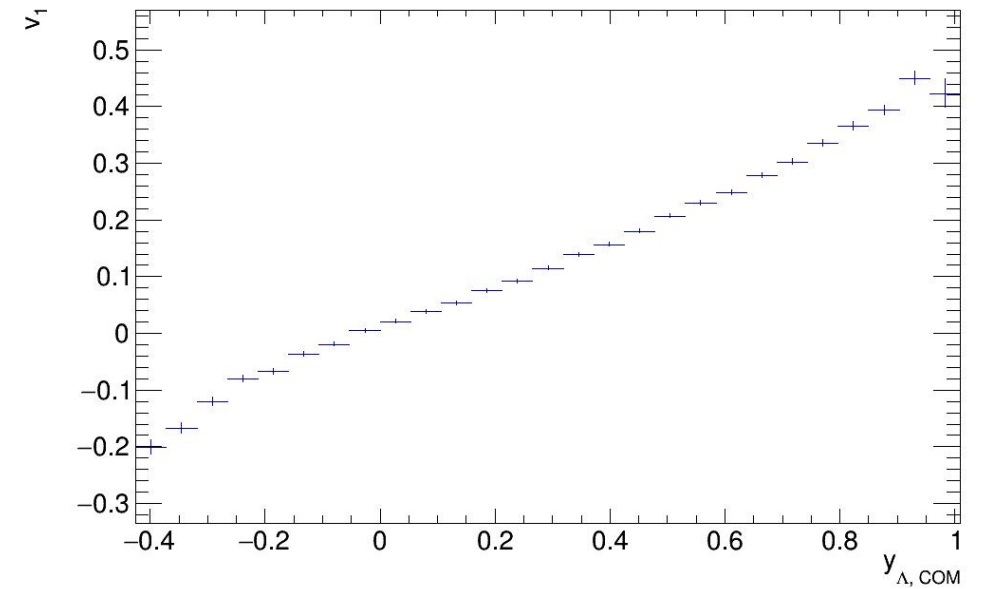
- We know that this is related to the magnetic field
 - The effect is exactly reversed when looking at the two magnetic field orientations at 27 GeV
- The sharper/brighter distributions correspond to daughter tracks crossing



Further comments on the AEE

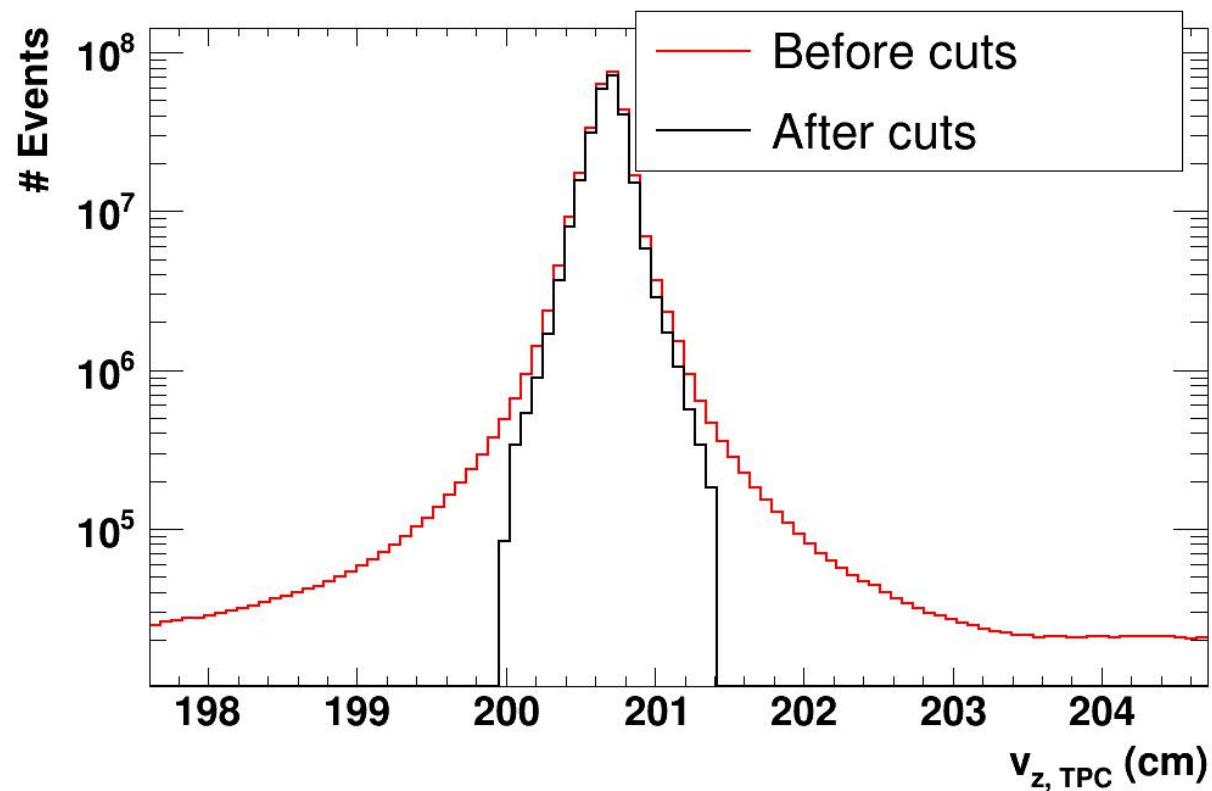
- STAR cannot measure production-plane polarization without doing careful corrections using embedding or other methods are developed
 - The AEE is measured using the same observable as the production-plane polarization; not only does the invariant mass distribution depend on emission angle, but so does the Lambda yield

- Embedded Lambdas are given a v_1 that approximately matches the real data



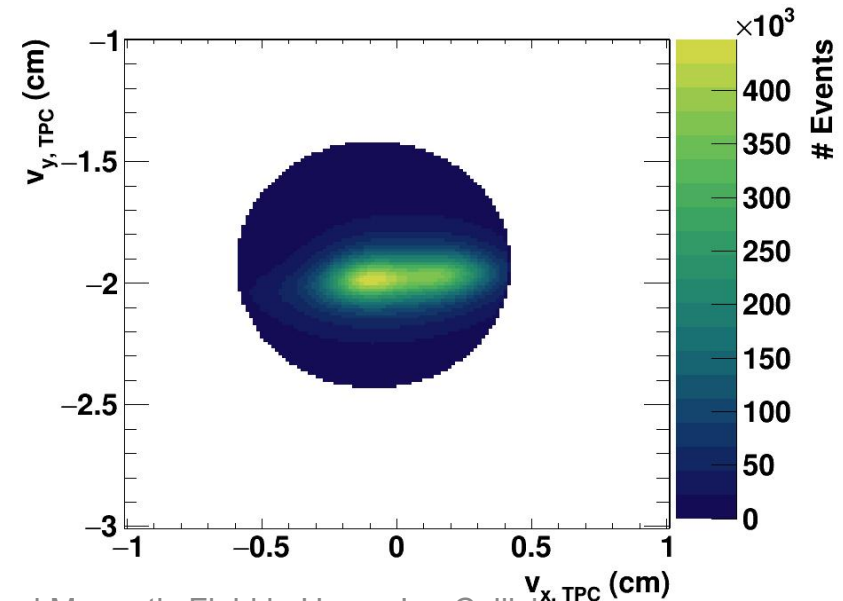
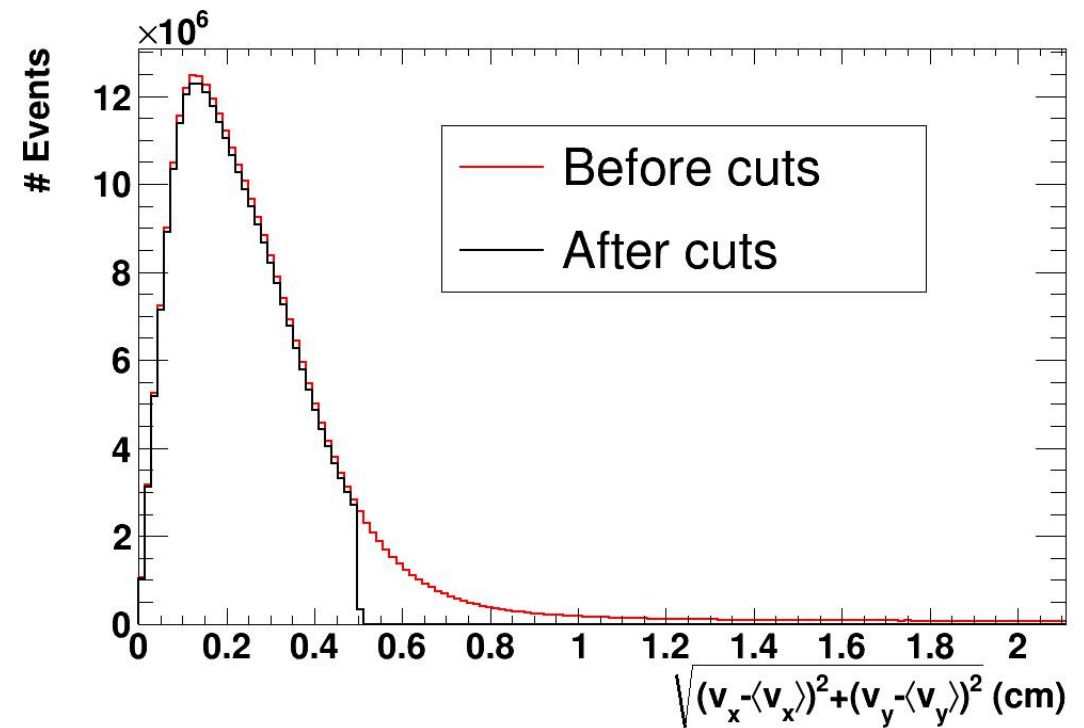
Event cuts

- The v_z distribution is sharply peaked about $\langle v_z \rangle = 100.7$ cm. We impose a cut of ± 0.7 cm.



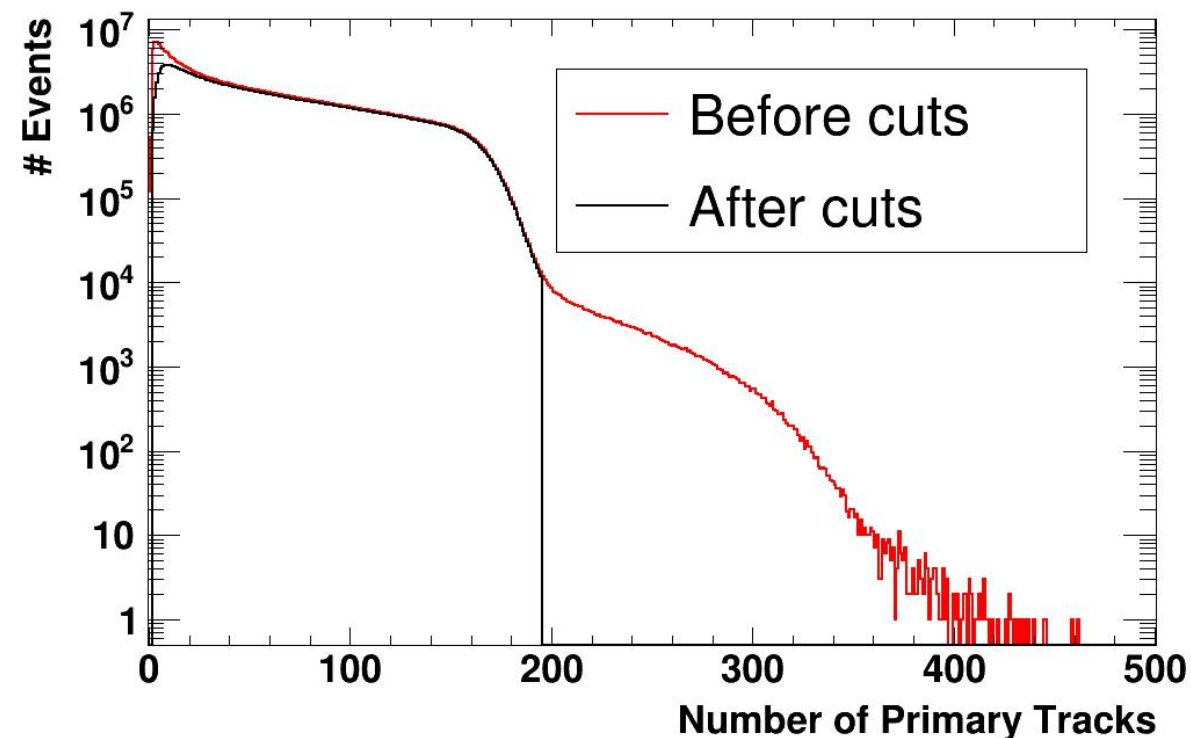
Event cuts

- The beam is steered away from (0,0) in order to hit the gold foil; we therefore impose a cut on $\nu_T - \langle \nu_T \rangle$ (instead of ν_T) of 0.5 cm



Event cuts

- The pileup cut and centrality definitions were determined by the UC Davis group



Event cuts

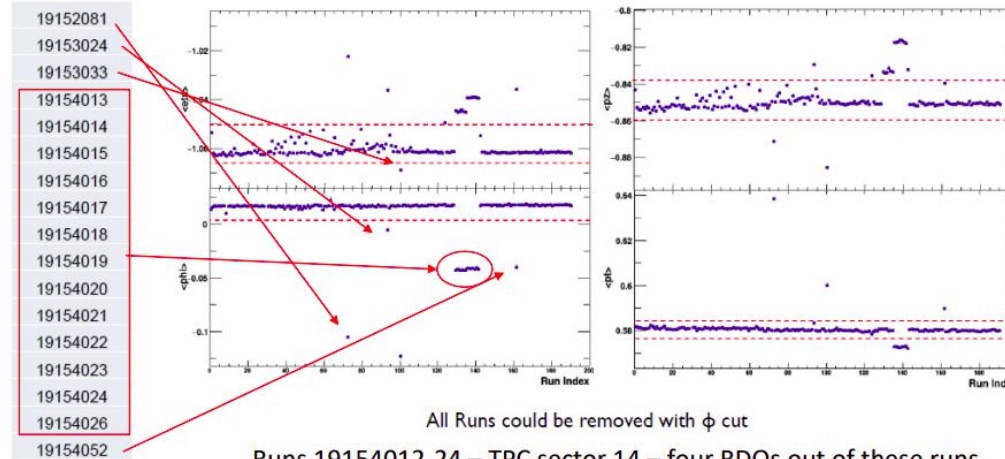
- UC Davis group also leading QA study on this data set
 - Nearly finalized
- We implement this bad-run rejection

QA – Sam Heppelmann

Sam looked at four QA indicators: $\langle\eta\rangle$, $\langle\phi\rangle$, $\langle p_z\rangle$, and $\langle p_T\rangle$
 → Sam concluded and only $\langle\phi\rangle$ was important

Run Selection

Removed Runs



SAMUEL HEPPELMANN | UC DAVIS | STAR COLLABORATION MEETING LBNL

3/13/2020

10

Bad Run List for All analyses:

Run Number	Run Count	Bad	bbce_tofmult	hlt_Good	Ratio	Reason to Reject
19151029	1	Bad	352741	181933	0.515769	This was the first run for the FXT program. It was run
19152001	30	Bad	1	0	0	only 1 event
19152078	73	bad	105205	75162	0.714434	1 minute run , not in the log book
19153023	94	bad	57532	41655	0.724032	3.5 minute run , getting almost no rate, asked MC
19153032	101	bad	22251	17574	0.789807	35 second run , run stopped with TPC trips
19153065	124	bad	46626	36463	0.782031	35 second run, two inner TPC tripped
19154012	130	bad	3659275	3120438	0.852748	TPX 14 (4 RDOs) out
19154013	131	bad	3648387	3088966	0.846666	TPX 14 (4 RDOs) out
19154014	132	bad	3341251	2831904	0.847558	TPX 14 (4 RDOs) out
19154015	133	bad	1372269	1145009	0.834391	TPX 14 (4 RDOs) out
19154016	134	bad	2031168	1726407	0.849958	TPX 14 (4 RDOs) out
19154017	135	bad	2456321	2085858	0.84918	TPX 14 (4 RDOs) out
19154018	136	bad	2121499	1797981	0.847505	TPX 14 (4 RDOs) out
19154019	137	bad	3981715	3363315	0.84469	TPX 14 (4 RDOs) out
19154020	138	bad	3473212	2931558	0.844048	TPX 14 (4 RDOs) out
19154021	139	bad	3728863	3158431	0.847023	TPX 14 (4 RDOs) out
19154022	140	bad	2354219	1996394	0.848007	TPX 14 (4 RDOs) out
19154023	141	bad	1090521	931044	0.853761	TPX 14 (4 RDOs) out
19154024	142	bad	820024	696414	0.849261	TPX 14 (4 RDOs) out
19154026	143	bad	2276626	1962781	0.862145	No BTOW
19154051	162	bad	24158	17507	0.728525	30 second run, TPC inners all tripped

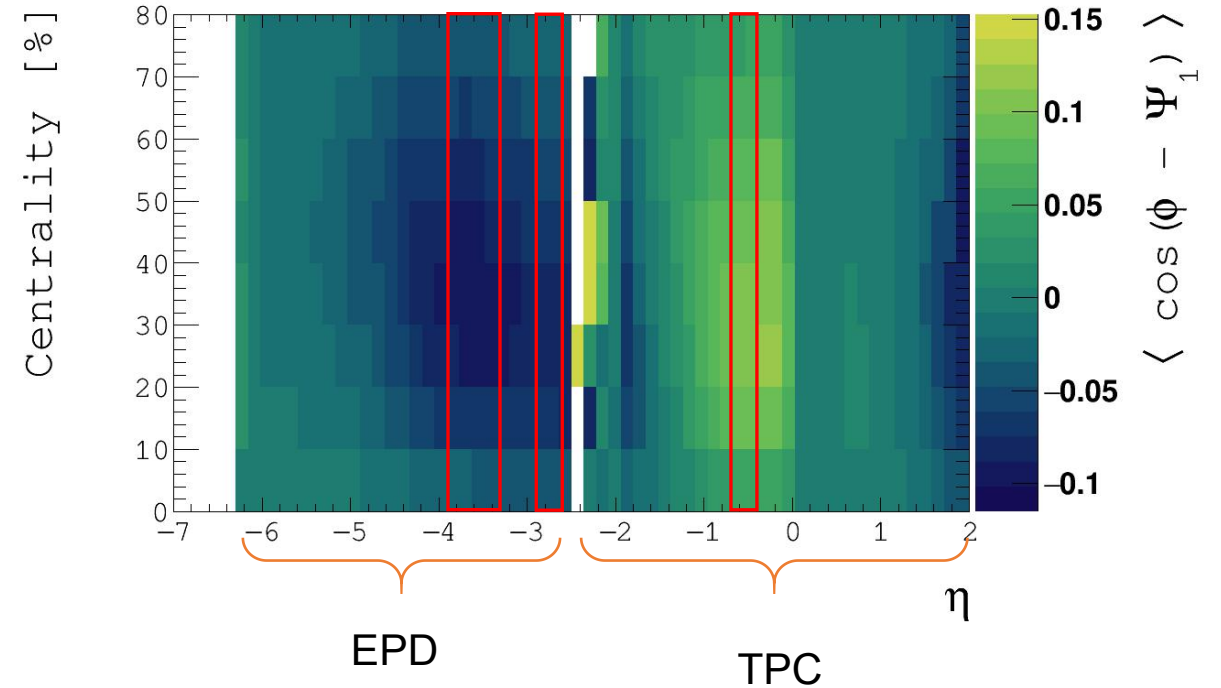
Event cuts

- We use events triggered on BBC East and TOF (trigger ID 620052)
- 308M readable events, 240M used for analysis (after cuts)

Ψ_1 determination

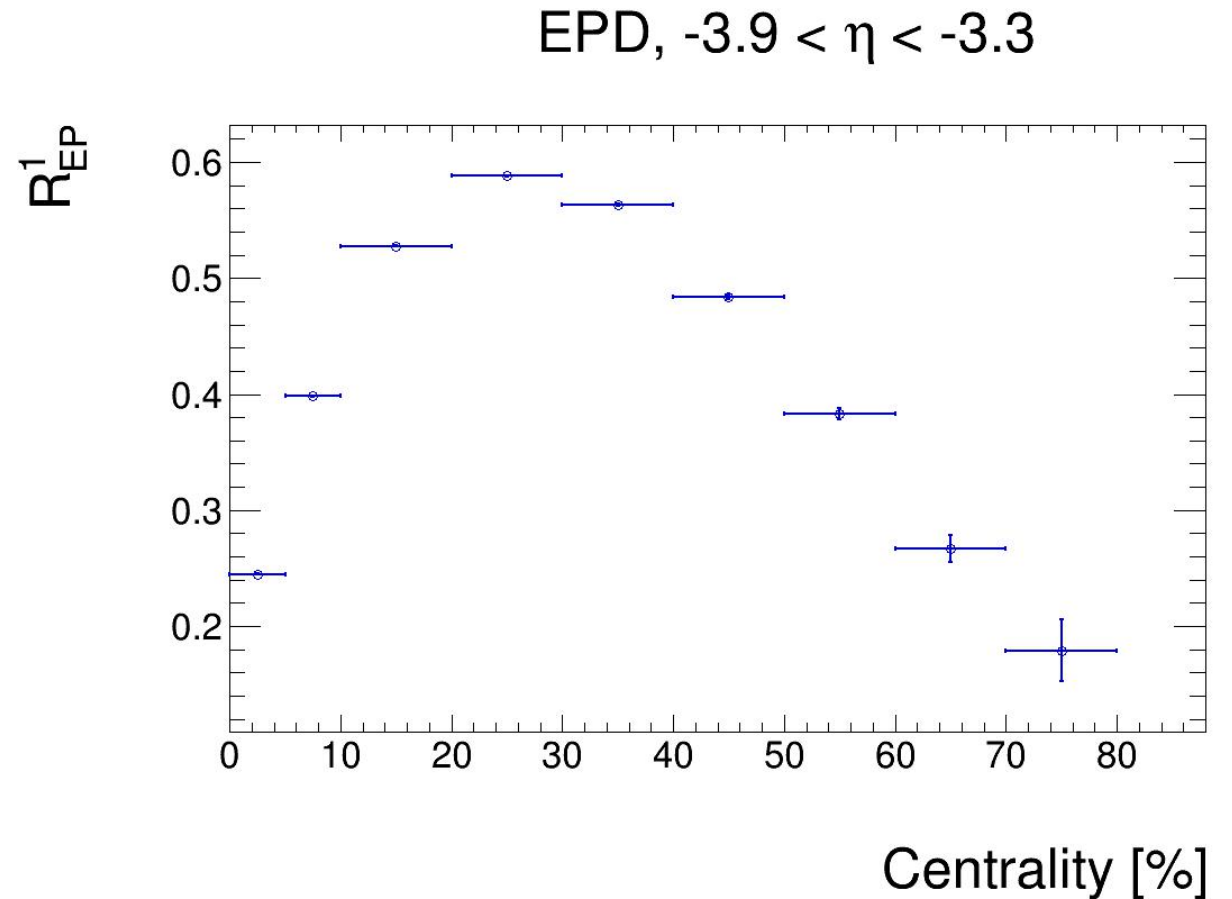
- We reduce the effects of momentum conservation on $R_{EP}^{(1)}$ by choosing subevents with small rapidity widths
 - $R_{EP}^{(1)}$ is reduced in order to more accurately describe it

$$R_{1, EPD} = \sqrt{\frac{\langle \cos(\psi_{1, EPD SE1} - \psi_{1, TPC}) \rangle \langle \cos(\psi_{1, EPD SE2} - \psi_{1, TPC}) \rangle}{\langle \cos(\psi_{1, TPC} - \psi_{1, EPD SE2}) \rangle}}$$



Ψ_1 determination

- We reduce the effects of momentum conservation on $R_{\text{EP}}^{(1)}$ by choosing subevents with small rapidity widths
 - $R_{\text{EP}}^{(1)}$ is reduced in order to more accurately describe it
- We still have good $R_{\text{EP}}^{(1)}$ by choosing a region in the EPD with large ν_1

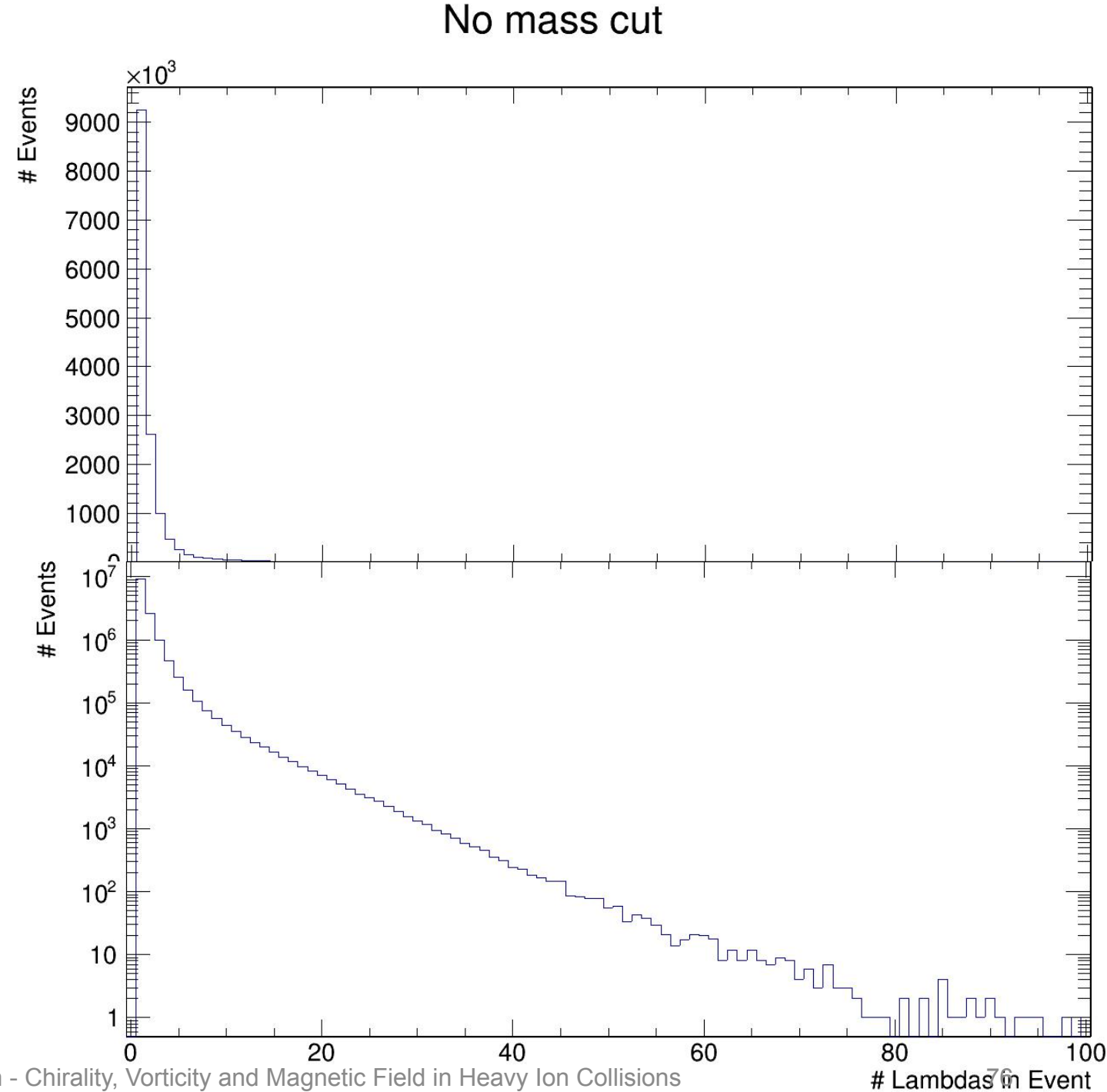


Finding Lambdas

- We use the KFParticle package to identify Lambdas, with few modifications
 - `StKFParticleInterface::instance()->CleanLowPVTrackEvents();`
 - `StKFParticleInterface::instance()->SetChiPrimaryCut(10);`
 - Λ DCA to PV < 1 cm (we want primary Lambdas)
 - Enforce one Lambda per event (“Thunderdome”)

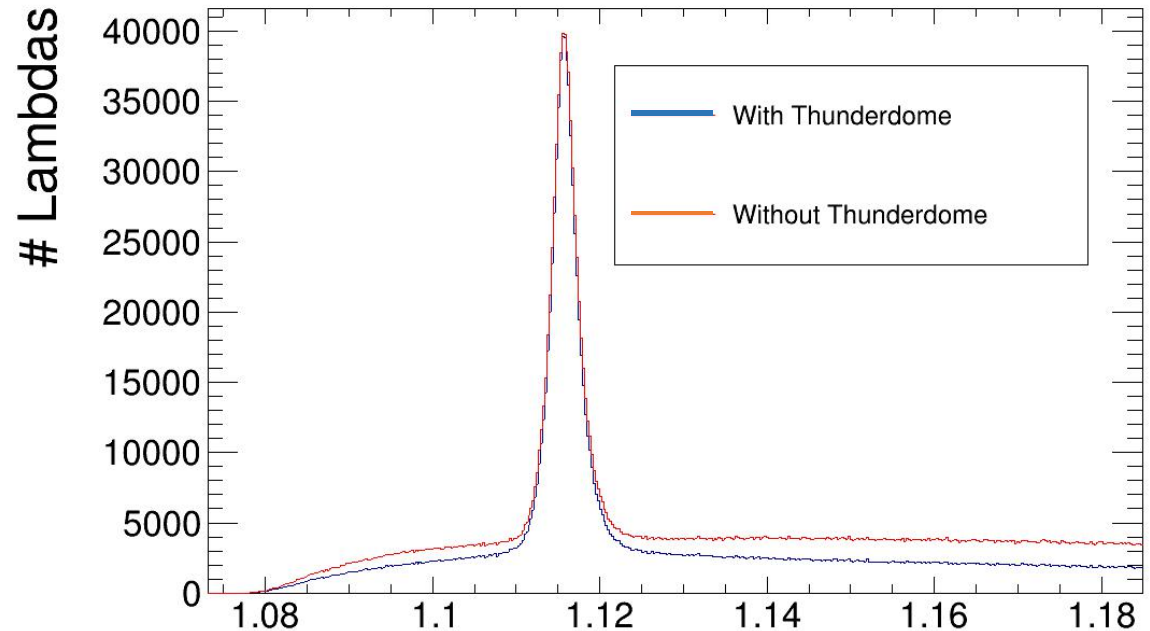
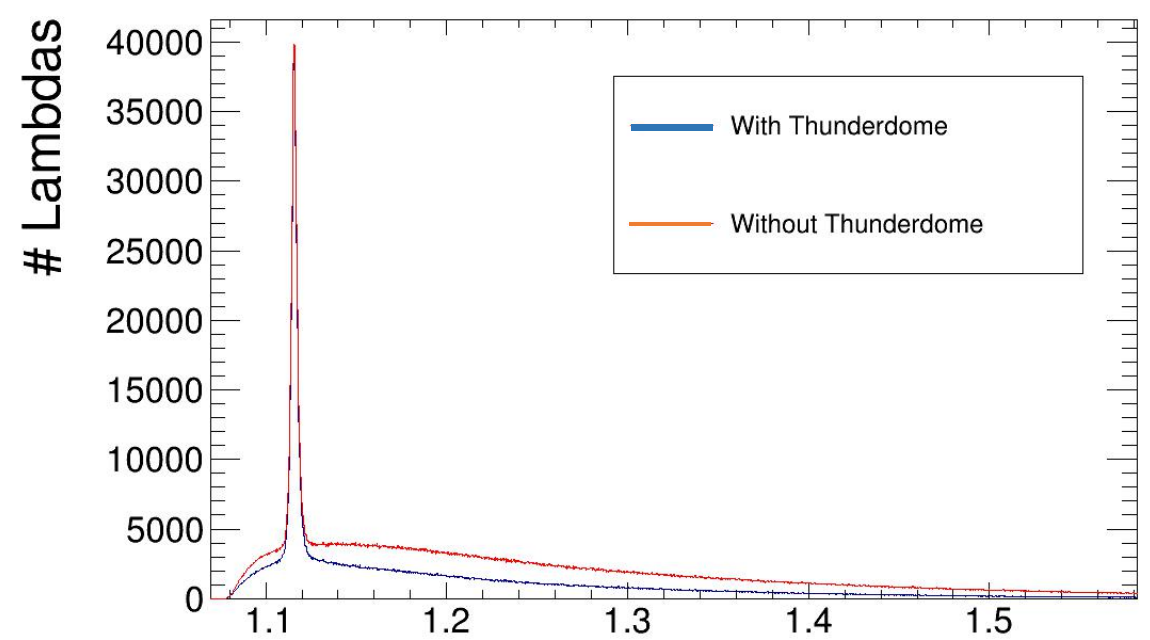
Thunderdome

- Some events have many, many Lambdas
 - Pions are being paired up with more than one proton in an event
 - For events with more than one Lambda, need to choose best
 - Look at all matches and take the one with the smallest $|m_{\text{inv}} - m_{\Lambda}|$



Thunderdome

- Some events have many, many Lambdas
 - Pions are being paired up with more than one proton in an event
 - For events with more than one Lambda, need to choose best
 - Look at all matches and take the one with the smallest $|m_{\text{inv}} - m_{\Lambda}|$
- We can see the effects on the invariant mass distribution and purity



Correcting for momentum conservation

- Methods for correcting for momentum conservation effects on flow and event-plane resolution are known [1]
 - But they require the knowledge of particle p_T

$$f \equiv \frac{\langle wp_T \rangle}{\sqrt{\langle w^2 \rangle \langle p_T^2 \rangle}}$$
$$= \langle wp_T \rangle_Q \sqrt{\frac{M}{\langle w^2 \rangle_Q N \langle p_T^2 \rangle}}$$

- There's no way to get this from the EPD
 - Can't get around it with anything clever, like $p_T \leftrightarrow \langle p_T \rangle|_\eta$

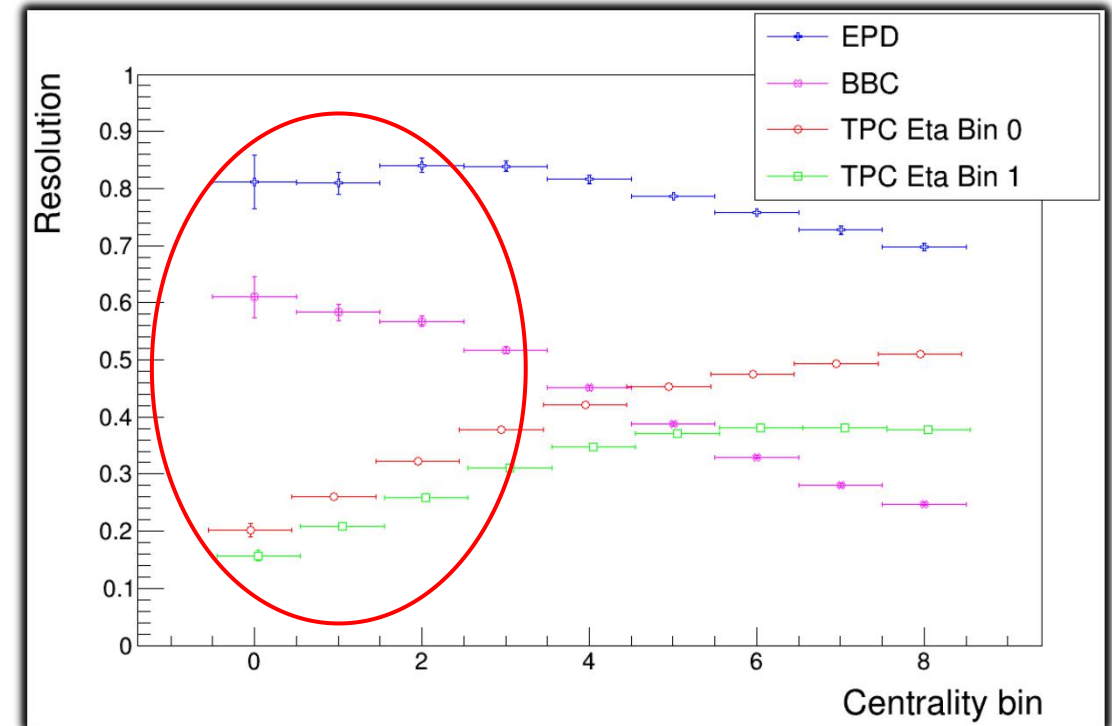
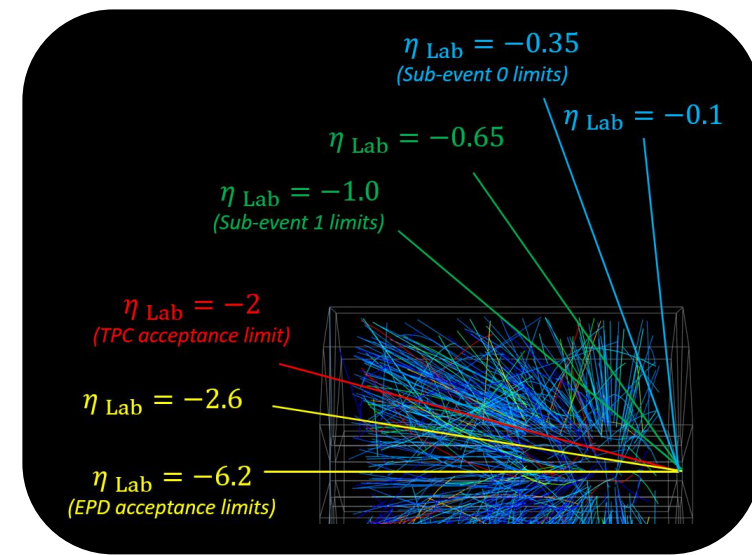
[1] N. Borghini, et al. "Effects of momentum conservation on the analysis of anisotropic flow". <https://arxiv.org/pdf/nucl-th/0202013.pdf>

Using full EPD

- When using fast offline picoDsts:
 - A three-detector method is used for the calculation of the event-plane resolution

$$R_{1, \text{EPD}} = \sqrt{\frac{\langle \cos(\psi_{1, \text{EPD}} - \psi_{1, \text{TPC SE1}}) \rangle \langle \cos(\psi_{1, \text{EPD}} - \psi_{1, \text{TPC SE2}}) \rangle}{\langle \cos(\psi_{1, \text{TPC SE1}} - \psi_{1, \text{TPC SE2}}) \rangle}}$$

• Momentum conservation decreases correlation between TPC subevents and increases correlation between TPC and EPD/BBC



- Lambda yield is influenced by the missing iTPC sector

